

Characterization of Sirt2 using conditional RNAi in mice

Inaugural-Dissertation

zur

Erlangung des Doktorgrades

der Mathematisch-Naturwissenschaftlichen Fakultät

der Universität zu Köln

vorgelegt von

Martina Reiss

aus Friedrichshafen

Köln 2011

Berichterstatter: Prof. Dr. Jens C. Brüning
Prof. Dr. Peter Kloppenburg

Tag der mündlichen Prüfung: 11.01.2011

“Enjoying with your science is that it never stops being exciting.”

- Oliver Smithies, 2007 Nobel Laureates in Medicine

Table of contents

<i>Table of contents</i>	4
<i>Figure index</i>	7
<i>Table index</i>	8
<i>Abbreviations</i>	9
<i>1 Introduction</i>	12
1.1 RNA interference	12
1.2 shRNA/siRNA based RNAi in mammalian cells	14
1.3 RNAi in transgenic animals	15
1.3.1 Tissue specific RNAi in transgenes using the Cre/loxP system	16
1.3.2 Inducible RNAi in transgenes using the tet-system	17
1.4 Tissue specific and inducible RNAi in mice	18
1.5 The mammalian sirtuins	18
1.6 Regulatory functions of the sirtuins	21
1.6.1 Sirt1	21
1.6.2 Sirt2.....	22
1.6.3 Sirt3, 4 and 5	23
1.6.4 Sirt6 and Sirt7	24
1.7 Objectives	25
<i>2 Material and Methods</i>	26
2.1 Chemicals	26
2.2 Molecular biology	28
2.2.1 Cloning of promoter fragments or genes	28
2.2.2 Cloning plasmid constructs 1, 2 and 6	28
2.2.3 Cloning plasmid constructs 3, 4, 5 and 7	31
2.2.4 Isolation of Genomic DNA	34
2.2.5 Polymerase Chain Reaction (PCR)	34
2.2.6 Southern Blot	36
2.2.7 RNA Extraction and Quantitative Realtime-PCR (qPCR)	37
2.2.8 DNA sequencing.....	38

2.2.9 Quantification of DNA and RNA	39
2.2.10 Protein extraction	39
2.2.11 Western Blot	39
2.2.12 Enzyme-linked Immunosorbent Assay (ELISA)	40
2.3 Histological analysis	40
2.4 Cell culture	40
2.4.1 Embryonic stem cell lines	41
2.4.2 Embryonic stem cell culture	42
2.4.3 Transfection of ES cells with the exchange vector	42
2.4.4 Doxycycline (dox) treatment of ES cells	43
2.4.5 Analysis of doxycycline content in mouse serum	43
2.4.6 β -Galactosidase assay	43
2.5 Mouse experiments	44
2.5.1 Animal care	44
2.5.2 Mice	45
2.5.3 Body weight, blood collection and blood glucose levels	45
2.5.4 Glucose and insulin tolerance test	46
2.5.5 Food intake and indirect calorimetry	46
2.5.6 Behavioral analysis	46
2.5.7 MPTP treatment	47
3 Results	48
3.1 Generation of Cre-mediated spatially and temporally regulated shRNA expression system	48
3.1.1 The effect of a single loxP site on promoter activity <i>in vitro</i>	48
3.1.2 Spatially and temporally activated RNAi of LacZ in mice by the hybrid Pol III system	53
3.1.3 Spatially and temporally activated RNAi of Sirt2 in mice by the hybrid Pol III system	56
3.2 Phenotypical analysis of inducible Sirt2-knockdown mice	58
3.2.1 Knockdown efficiency demonstrated by two individual shRNAs against Sirt2	58
3.2.2 The effect of Sirt2 knockdown on energy homeostasis control	62
3.2.3 Effect of Sirt2 knockdown focused on glucose metabolism	64
3.2.4 The effect of Sirt2 knockdown during embryogenesis	70
3.2.5 The effect of Sirt2 knockdown in neurodegenerative disease	72
4 Discussion	75
4.1 Spatially and temporally controlled RNAi	75
4.2. Phenotypical analysis of Sirt2 knockdown in mice	77
4.2.2 The role of Sirt2 knockdown during embryogenesis	78

4.2.2 The effect of Sirt2 knockdown on glucose and energy homeostasis	79
4.2.3 Effect of Sirt2 knockdown in a mouse model of Parkinson Disease	81
5 Summary	84
6 Zusammenfassung.....	85
7 References.....	87
8 Acknowledgements	100
9 Erklärung.....	101
10 Curriculum vitae.....	102

Figure index

Figure 1: The small-interfering RNA (siRNA) pathway	14
Figure 2: Deacetylation and ADP-ribosylation activity by mammalian sirtuins	20
Figure 3: Overview of Infusion cloning method.....	32
Figure 4: Schematic overview of promoter configurations after Cre-mediated recombination	49
Figure 5: Analysis of seven configurations at the <i>rosa26</i> locus in mouse ES cells.....	52
Figure 6: Schematic overview illustrating the activation of H1/U6 hybrid mediated gene silencing (A) and its analysis in vivo (B, C).....	55
Figure 7: Knockdown level of Sirt2 <i>in vitro</i> and <i>in vivo</i> using the inducible hybrid H1/U6 system	58
Figure 8: Two specific shRNAs against Sirt2 results each to an efficient Sirt2 knockdown <i>in vivo</i>	59
Figure 9: Sirt2 knockdown in mice exposed to a NCD or HFD.....	61
Figure 10: Knockdown of Sirt2 does not affect metabolic control on normal diet	63
Figure 11: Knockdown of Sirt2 does not affect metabolic control on high fat diet	64
Figure 12: Unchanged glucose metabolism in Sirt2 knockdown mice on normal diet	66
Figure 13: Unchanged glucose metabolism and energy balance in Sirt2 knockdown mice on high fat diet	67
Figure 14: Effect of Sirt2 KD on adipocyte size and PPAR γ mRNA expression in EWAT.....	69
Figure 15: Sirt1 mRNA expression in Sirt2 knockdown animals fed on HFD	70
Figure 16: Possible role of Sirt2 in regulatory networks controlling embryonic processes	71
Figure 17: Rotarod analysis and knockdown efficiency of Sirt2 knockdown and wt control mice treated either with MPTP or saline.....	74

Table index

Table 1: Main characteristics of mammalian situins	21
Table 2: Chemicals	27
Table 3: Fusion PCR-synthetic1.1, -synthetic2.1 and –synthetic6.1	30
Table 4: Primers used for fusion PCR-synthetic1.1, -synthetic2.1 and -synthetic6.1	31
Table 5: Primers used for cloning of construct 3, 4, 5 and 7	34
Table 6: Primers used for genotyping.....	35
Table 7: Probes for Southern Blot generated by digestion of vector DNA	36
Table 8: Probes for Southern Blot generated by PCR	37
Table 9: Real-Time analysis probes.....	38
Table 10: Custom Real-Time analysis probes	38
Table 11: Custom Real-Time analysis probes for small RNA	38
Table 12: Antibodies used for western blot analysis	40
Table 13: Embryonic stem cell lines at TaconicArtemis GmbH	41
Table 14: Animal food.....	45

Abbreviations

°C	degrees Celsius
μ	micro
3'	three prime end of DNA sequences
5'	five prime end of DNA sequences
A	adenosine
AceCS2	acetyl coenzyme A synthetase 2
ADP	adenosine diphosphate
ADPR	ADP ribose
AKT	proteinkinase B
as	antisense
ATP	adenosine triphosphate
C	cytosine
Caggs	chicken β-actin-promoter with CMV enhancer
cDNA	complementary DNA
CMV	cytomegalovirus
CNS	central nervous system
CPS1	carbomyl phosphate synthetase 1
CR	caloric restriction
Cre	site specific recombinase from phage P1 (causes <u>re</u> combination)
Ct	cycle treshold
Da	Dalton
ddH ₂ O	double distilled water
DMSO	dimethylsulfoxide
DNA	desoxyribonucleic acid
DNase	desoxyribonuclease
dNTP	desoxyribonucleotide-triphosphate
Dox	doxycycline
DSE	distal sequence element
dsRNA	double stranded RNA
DTT	Dithiothreitol
E.coli	<i>Escherichia coli</i>
e.g.	exempli gratia
ECL	enhanced chemiluminescence
EDTA	ethylendiamine tetraacetate
ELISA	enzyme-linked immunosorbent assay
EtBr	ethidium bromide
EtOH	ethanol
EWAT	epigonadal white adipose tissue
floxed	loxP flanked
Flp	flippase
Fluc	firefly luciferase
FOXO1	forkhead-O transcription factor 1
FRT	flip-recombinase targets

g	gram
G	guanine
G418	geneticin
GAPDH	glyceraldehyd-3-phosphate dehydrogenase
GDH	glutamate dehydrogenase
GTT	glucose tolerance test
h	hour
H&E	hematoxylin/eosin
HCl	hydrochloric acid
HDAC	histone deacetylase
HEPES	N-2-hydroxyethylpiperazine-N'-2-ethansulfonic acid
HFD	high-fat diet
Hp1bp3	heterochromatin protein1 binding protein3
Hygro	hygromycin
Hz	Hertz
i.p.	intraperitoneal
IR	insulin receptor
itetR	codon optimized version of tetR
ITT	insulin tolerance test
k	kilo
kb	kilobase pairs
KCl	potassium chloride
kDa	kilodalton
l	liter
<i>lacZ</i>	gene encoding the enzyme beta-galactosidase
loxP	recognition sequence for Cre (<u>locus of x</u> -ing over phage <u>P1</u>)
m	milli
M	molar
mES cells	mouse embryonic stem cells
MgCl ₂	magnesium chloride
min	minute
miRNA	micro RNA
mRNA	messenger RNA
NaCl	sodium chloride
NAD	nicotinamide adenine dinucleotide
NADH	nicotinamide adenine dinucleotide reduced
NAM	nicotinamide
NaOH	sodium hydroxide
NCD	normal chow diet
Neo	neomycin
NMR	nuclear magnetic resonance
Nt	nucleotide
OD	optical density
ORF	open reading frame
PAGE	polyacrylamid gel electrophoresis
pAhGH	human growth hormone poly adenylation

PB	phosphate buffer
PBS	phosphate buffered saline
PCR	polymerase chain reaction
PGC-1 α	PPAR γ coactivator-1
PGK	phosphoglycerate kinase
PIE	promoter inhibitory element
Pol III	RNA polymerase III
PPAR γ	peroxisome proliferator-activated receptor gamma
PSE	proximal sequence element
Puro	puromycin
qRT-PCR	quantitative realtime PCR
rDNA	ribosomal DNA
RISC	recombinase mediated cassette exchange
Rluc	renilla luciferase
RMCE	recombinase mediated cassette exchange
RNA	ribonucleic acid
RNAi	RNA interference
RNAi	RNA interference
RNAi	RNA interference
RNase	ribonuclease
RT	room temperature
rtTA	reverse tetracycline transactivator
s	sense
SDS	sodiumdodecylsulfate
sec	second
SEM	standard error of the mean
SGK1	serum- and glucocorticoid regulated kinase 1
shRNA	short hairpin RNA
siRNA	short interfering RNA
SNP	single nucleotide polymorphism
T3	triiodothyronine
TAE	Tris-acetic acid-EDTA buffer
TBS	Tris buffered saline
tetO	tetracycline operator
tetR	tetracycline repressor
Tris	2-amino-2-(hydroxymethyl)-1,3-propanediol
tTA	tetracycline transactivator
U	units
UTR	un-translated region
V	Volt
v/v	volume per volume
VO ₂	volume of oxygen
VP	viral protein
w/v	weight per volume
ZsGreen	<i>Zoanthus sp.</i> green fluorescent protein

1 Introduction

1.1 RNA interference

RNA interference (RNAi) is a cellular mechanism to regulate gene expression by sequence-specific posttranscriptional gene silencing. First described in 1998 by Fire and Mello in the invertebrate nematode *Caenorhabditis elegans* (1), RNAi became more attention and it has since been studied in a wide range of eukaryotic organisms such as fungi, flies, plants and mammals (2). Originally, RNAi had probably evolved to an important defence mechanism in many organisms against viruses, inverted repeat transgenes, or transposable elements that include a double strand RNA (dsRNA) step in their replication cycle (3). When present within a cell, dsRNAs are recognized by the ribonuclease called Dicer and are further converted into smaller dsRNA molecules of 21 base pairs with a 2-nucleotide 3'-overhangs (4). These molecules are called short interfering RNAs (siRNAs) that direct RNAi (5-8). SiRNAs are then shuttled into an RNAi-specific protein complex to form the RNA-induced silencing complex (RISC) (Figure 1). This ribonucleoprotein complex might undergo activation in the presence of ATP so that the antisense component of the unwound siRNA becomes exposed and paired with the cognate mRNA (9, 10). Subsequently, the RISC complex recognize and cleaves homologous mRNA endonucleolytically, thereby decreasing the production of the corresponding protein (11, 12). Thus, any mRNA bearing a homologous sequence with an appropriate siRNA is degraded and its expression is knocked down to 10-40 % of its normal levels (13). The assembly of RISC is asymmetrical with a clear strand bias (14), meaning that only one strand of the duplex is preferentially loaded (15) while the other strand will be destroyed. The strand whose 5' end has lower internal stability is preferentially incorporated into RISC. Thus, antisense (guide) strand of chemically synthesized siRNAs should have lower internal stability of its 5' end and is an important parameter for siRNA design. This is further supported by Reynolds and colleagues, who found few sequence specific characteristics (16). Most of the rules for siRNA design were implemented in various software programs, whereas many of them incorporate the original Tuschl algorithm. Studies have revealed that siRNA specificity is not as stringent since pairing between the hexamer seed region of a siRNA guide strand (nucleotides 2-7) and complementary sequences in the 3'UTR of mature transcripts has

been implicated in off-target gene regulation and false positive phenotypes (17-19). In a minority of siRNA based experiments, unspecific effects due to immune stimulation or saturation of the RNAi machinery have been described (20, 21). Appropriate control experiments, such as transfection of different siRNAs directed against the target mRNA may anticipate off-target effects.

As longer dsRNAs provoke an interferon response in mammalian cells, leading to non-specific mRNA degradation and global inhibition of protein translation rather than the desired specific knockdown, the technology was initially restricted to organisms showing no interferon response, such as *Caenorhabditis elegans* and *Drosophila melanogaster* (5, 22). However, dsRNAs shorter than 30 bp were shown to circumvent interferon response in mammalian cells (5). Since efficient knockdown in transfected mammalian cells were first described with *in vitro* synthesized siRNAs (5, 6), RNAi techniques have become widely used an experimental tool to define the functional roles of individual genes, particularly in disease.

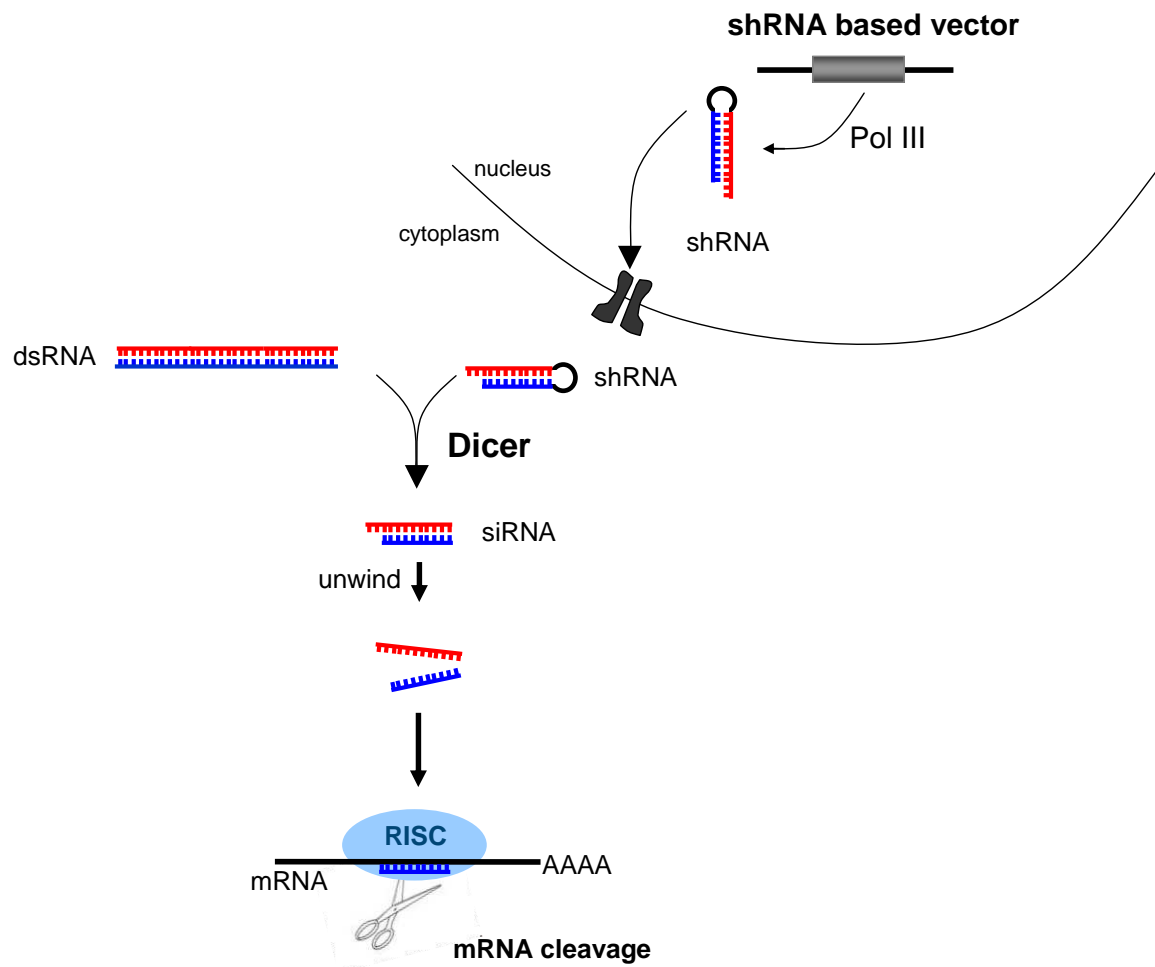


Figure 1: The small-interfering RNA (siRNA) pathway

DsRNAs or vector based shRNAs are processed into siRNAs by the ribonuclease called Dicer (4). SiRNAs are incorporated in the RNA-induced silencing complex (RISC) and ATP-dependent unwinding of siRNAs activates RISC (10). Active RISC is thus guided to degrade the specific target mRNAs (11, 12).

(abbreviations: dsRNA=double stranded RNA; shRNA=short hairpin RNA; siRNA=short interfering RNA; RISC=RNA induced silencing complex; mRNA=messenger RNA)

1.2 shRNA/siRNA based RNAi in mammalian cells

In mammalian cells, RNAi can be induced artificially by introducing chemically synthesized siRNAs (5). The design of effective siRNAs can be supported by several algorithms available (16, 23-25). Although siRNAs are easy to produce and their effects are transient in actively replicating cells, the duration of silencing is dependent of rate on cell division that can be 3-7 days in proliferating cells, but can persist for 3 weeks and more in

terminally differentiated cells, such as neurons (26). Subsequently, several large-scale RNAi screens have been conducted in mammalian tissue culture cells using synthetic siRNAs (27). These screens have identified genes involved in apoptosis, signalling, regulation of protein stability and the ultraviolet radiation damage response. On the other hand, RNAi based screening in mammalian cells have been limited to easily transfectable, rapidly dividing adherent cell types (28).

An alternative provides the expression of short hairpin RNAs (shRNAs) (29-31) resulting in intracellular production of siRNA molecules by recruiting the endogenous processing machinery (32, 33). While transient transfection is advantageous for fast analysis of shRNA mediated effects, stable transfection ensures long-term, reproducible as well as defined shRNA effects. ShRNA expression vectors have been engineered using both viral (including retroviral (34), adenoviral (35, 36) and lentiviral (37) vectors), and plasmid systems (32, 38, 39). Plasmids containing RNA polymerase III (pol III) dependent promoters, like those of the U6 and H1 genes are perfectly suited to produce double-stranded short hairpin RNAs (shRNAs) that are processed into siRNAs inside the cell (28) (Figure 1). The localization of the regulatory sequences immediately upstream of the Pol III transcription start site ensures expression of exact shRNA sequences without additional or unwanted nucleotides, a critical requirement for precise siRNA function (40). Promoters of this type are preferred as they naturally direct the synthesis small RNA transcripts with defined termination sequences consisting of 4–5 thymidines (the termination signal for RNA polymerase III) and have no requirement for downstream promoter elements (41-43). Further, pol III dependent promoters are constitutively expressed in all cell types and display a high level of activity (43). To increase their utility for cell culture studies, vectors that mediate inducible pol III dependent expression of siRNAs were developed (44-46).

1.3 RNAi in transgenic animals

Transgenic RNAi finds tremendous applicability in the creation of *in vivo* animal models mimicking gene knockout animals (47). The major advantage of shRNA transgenes is that they do not have to be bred into homozygosity to see the knockout effect as they behave like dominant-negative alleles (40). In addition, transgenic RNAi is less time consuming in

generation. The effect of RNAi in different cell types of mice have been demonstrated through injection of shRNA expression vectors into the tail vein (48, 49). Moreover, gene knockdown in multiple tissues of mice or rats can be achieved by random transgenesis including random ES cell transfection, pronucleus injection or lentiviral transduction (50-55). Since random transgenesis in these experiments demonstrated various shRNA expression patterns in each individual mouse line, predicted RNAi from a defined genomic locus has been shown efficiently and applicable (56).

However, vector mediated RNAi has limited germline transmission to only those shRNAs targeting genes whose knockdown is compatible with viability and fertility. Therefore, conditional RNAi approaches are an appropriate tool for the elucidation of gene function at varied levels of gene expression and generation of mice with mild phenotypes when gene knock-out is fatal. Today, shRNA expression can be either activated by temporal control (e.g. the tet-inducible systems) or in a tissue specific manner (e.g. the Cre/loxP system).

1.3.1 Tissue specific RNAi in transgenes using the Cre/loxP system

A number of important biological questions can be addressed simply by a knockdown of a gene of interest at a given tissue in the adult mouse. The Cre/loxP recombination system allows for this type of control and implicates a Cre recombinase derived from bacteriophage P1 and two 34 bp loxP (locus of crossover (x) in P1) sites (include two 13 bp palindrome sequences separated by a spacer fragment of 8 bp), recognized by Cre (57). Cre-mediated catalysis results in a reciprocal recombination between the two similarly oriented loxP sites, followed by an excision of the DNA segment between the loxP sites leaving a single loxP site behind. In contrast, recombination between inverted loxP sites causes inversion of the sequence placed between them. The U6 promoter is preferably used for the Cre/loxP based RNAi systems and consists of three tightly spaced elements. Distal and proximal sequence elements (DSE and PSE) are 5' of the TATA box that is located 26 bases downstream from transcriptions initiation. Several groups have developed strategies to activate RNAi upon Cre-excision (58-64). Tissue specific control of shRNA expression can be achieved by insertion of a loxP flanked stop cassette close to the TATA box of the pol III dependent promoter, thereby blocking transcription. Excision of the stop cassette through Cre mediated recombination

results in gene silencing in a given tissue (61, 63, 65). In another approach, the loxP flanked stop cassette was placed between the DSE and PSE regulatory elements of the U6 promoter. Since a single loxP site in the same position does not interfere with transcription, the system allows controllable RNAi through Cre mediated recombination of the stop cassette. A further strategy employed a loxP flanked stop cassette that is embedded in the loop of the shRNA (60-62). Upon Cre recombination, the single loxP site is part of shRNA transcript. A loss of RNAi potency has not been observed (61).

The Cre/loxP system has also been applied for temporal control of shRNA expression. Cre recombinase activity was regulated by using a tamoxifen controllable Cre-ER fusion protein (66-68). However, Cre mediated excision of a DNA fragment is a one-time and irreversible event thereby reducing its usefulness for many applications.

1.3.2 Inducible RNAi in transgenes using the tet-system

A well-defined regulatory system of *Escherichia coli* (*E.coli*) is the tet operon that can be used to direct temporal control of shRNA expression and inducible gene silencing (45, 69). The tet inducible based system uses the transposon 10 (Tn10) specified tetracycline-resistance (tet) operon of *E. coli* (70). Activity of the tet operon is regulated by the tet repressor (tetR) which binds to a DNA sequence termed an operator (tetO) in the absence of tetracycline, resulting in transcriptional repression. Tet inducible RNAi vectors have been created by inserting a tetO sequence in the pol III promoter between the TATA box and the transcription start without altering the position of the promoter elements relative to each other or with respect to the transcription start site (45, 69, 71). In the absence of the inducer doxycycline, the tetR binds on the tetO thereby sterically hinders binding of polymerase III to the modified H1 promoter whereas shRNA expression is “off”. Upon addition of dox which binds to the tetR, the tetR undergoes a conformational change that results in reduced binding to the tetO with a subsequent activation in shRNA production (72). Several approaches have been performed to apply this strategy for the temporary control of antisense or shRNA expression in cultured cell lines (44, 45, 71, 73) as well as in mice and rat (69, 74, 75). One main drawback of this system is the leaky expression *in vivo* in the un-induced state, which can be diminished by using of a codon optimized version of the tetR (itetR) (45, 69, 76).

First approaches implying the tet inducible shRNA expression system were performed on mouse xenograft tumormodels. Immunocompromised mice harboring the tet inducible RNAi system and implanted tumor cells, developed tumor growth as normal in the absence of dox and repressed promoter. As demonstrated on several studies, dox treatment initiated silencing of pro-cancerous genes that yielded in tumor regression. Thus, tet inducible RNAi served as a valuable tool for loss-of-function screens of genes, required for the proliferation and survival of cancer cells (77).

1.4 Tissue specific and inducible RNAi in mice

The temporal and spatial control of gene inactivation avoids embryonic lethality and permits to dissect gene function at high precision. However, these unique approaches do not fully exploit the major experimental advantage of RNAi: in principle, its effects can be simultaneously: tissue specific and inducible. In the following three concepts, different principles have been demonstrated for a transgenic RNAi technology that can be used for spatially, temporally and reversible regulated gene expression of any target gene. Yu and McMahon developed a strategy for Cre-mediated activation of shRNA transcription in mouse ES cells (68). In addition, these cells contained a Cre-ER fusion transgene whose recombinase activity was controlled by the inductor 4OH-tamoxifen. The system has been shown to be applicable *in vitro* as well as in chimeric embryos (68). In the approach of Dickens and his colleagues (78), transgenic mice with a tet-regulatable shRNA expression cassette were generated and crossed with a transgenic tet transactivator mouse line. These double-transgenic mice produced shRNAs in a tissue specific manner that can be regulated by doxycycline (78). A new strategy developed and focused within this work relied on the use of site-specific recombination by the Cre/loxP technology according to inducible shRNA transcription by the tetO/tetR system.

1.5 The mammalian sirtuins

The founding member of the sirtuin family of histone deacetylases (HDACs) was the silent information regulator 2 (Sir2) of the budding yeast *Saccharomyces cerevisiae* (79). In

yeast, Sir2 has been shown to mediate the effects of calorie restriction on the extension of life span, thus longevity is promoted by high levels of Sir2 activity (80, 81). In mammals, seven sirtuins (Sirt1-7) have been identified, each of them sharing a conserved 275-amino-acid catalytic core domain. Like their yeast homologs, the mammalian sirtuins (Sirt1-7) are class III HDACs and require nicotinamide adenine dinucleotide (NAD^+) as a cofactor (82) to deacetylate substrates ranging from histones to transcriptional regulators (83). The deacetylating enzymatic activity of sirtuins uses NAD^+ as a catalyst to transfer the acetyl group from proteins and peptides to the ADP-ribose (ADPR) moiety of NAD^+ , yielding the acetyl ester metabolites 2'-O- and 3'-O-acetyl-ADP-ribose (AADPR), nicotinamide (NAM) and the deacetylated protein (Figure 2). The nicotinamide ribosyl bond is cleaved and one net water molecule is added to nicotinamide ribose, a reaction unique to sirtuins (84). The deacetylation activity of the sirtuins is controlled by the cellular $[\text{NAD}^+]/[\text{NADH}]$ ratio and thus differs from other HDACs. NAD^+ thereby activates whereas nicotinamide and reduced nicotinamide adenine dinucleotide (NADH) inhibits the deacetylation process (85-89). Thus, depending on cellular $[\text{NAD}^+]/[\text{NADH}]$ ratios and NAM levels, sirtuins may facilitate the conversion of nutritional status into modulation of gene and protein function, leading ultimately to changes in cellular function (90). Two Sirtuins, Sirt4 and Sirt6 possess NAD^+ -dependent ADP-ribosyl transferase activity (Figure 2), the biological significance of which is less well understood (91-93). In addition, Sirt2 and Sirt6 have been shown to perform both the ADP-ribosyl transferase and deacetylation activity (93, 94).

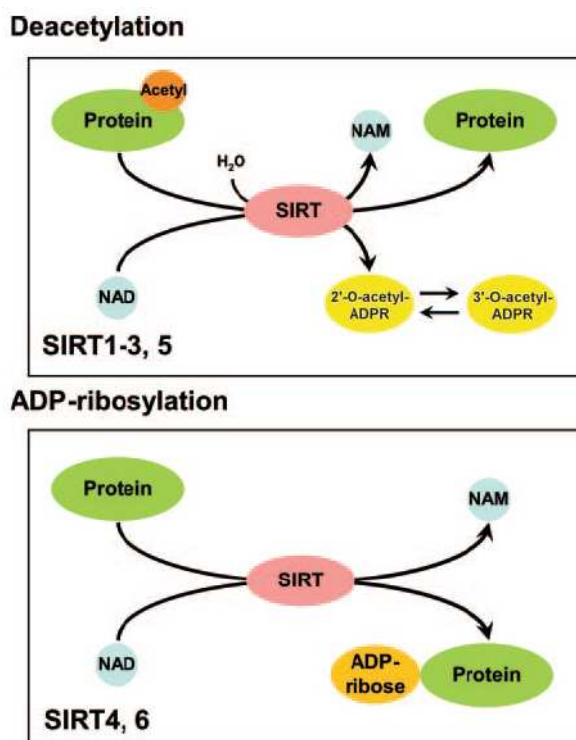


Figure 2: Deacetylation and ADP-ribosylation activity by mammalian sirtuins

Sirtuins are NAD^+ -dependent deacetylases and mono-ADP-ribosyl transferases. Sirt1-3 and Sirt5 catalyze a deacetylation reaction by transferring the acetyl lysine residues of the target protein to the ADP-ribose (ADPR) moiety of NAD^+ which generates the byproducts 2'-O- and 3'-O-acetyl-ADP-ribose (AADPR), nicotinamide (NAM) and the deacetylated protein (95-97). Sirt4 and Sirt6 possess ADP-ribosyl transferase activity (91, 92, 94). The Figure is taken from (98).

Mammalian sirtuins are found in numerous compartments within the cell (Table 1). Sirt1, Sirt6 and Sirt7 are found predominantly in the nucleus (82, 83, 99); Sirt3, Sirt4 and Sirt5 (79, 99, 100) are located in mitochondria and Sirt2 resides predominantly in the cytoplasm (79, 101). However, Sirt1 and Sirt2 were found to shuttle between the nucleus and the cytoplasm and to interact with both nuclear and cytosolic proteins (102, 103).

Sirtuin	Location	Interactions	Biology	Null phenotype
SIRT1	Nucleus	FOXO, PGC-1 α , NF- κ B, Ku70, etc.	Metabolism, stress	Developmental defects, lethal in some backgrounds
SIRT2	Cytosol	Tubulin, H4, FOXO	Cell cycle	Developmentally normal
SIRT3	Mitochondria	AceCS2, GDH complex I	Thermogenesis, ATP production	Developmentally normal
SIRT4	Mitochondria	GDH, IDE, ANT	Insulin secretion	Developmentally normal
SIRT5	Mitochondria	CPS1	Urea cycle	Developmentally normal
SIRT6	Nucleus	Histone H3, NF- κ B	Base excision repair, metabolism	Premature aging
SIRT7	Nucleolus	Pol I	rDNA transcription	Smaller size, short lifespan, heart defects

Table 1: Main characteristics of mammalian sirtuins

Abbreviations: AceCS2, acetyl-CoA-synthetase2; ANT, adenide nucleotide translocator; CPS1, carbamoyl phosphate synthetase 1; FOXO, forkhead box, subgroup O; GDH, glutamate dehydrogenase; IDE, insulin degrading enzyme; NF- κ B, nuclear factor kappa B; PGC-1 α , peroxisome proliferator-activated receptor gamma coactivator 1 alpha; Pol I, DNA polymerase I; rDNA, recombinant DNA. The table is taken from (104).

1.6 Regulatory functions of the sirtuins

1.6.1 Sirt1

The best characterized family member of the sirtuin family in terms of its endogenous function and activity is Sirt1. Sirt1 has been linked to the control of metabolic processes in adipose tissue, liver and muscle through the regulation of the nuclear receptor peroxisome-proliferator activated receptor- γ (PPAR γ) and its transcriptional co-activator PPAR γ co-activator-1 α (PGC-1 α) (105-108). A specific knockdown of Sirt1 in liver leads to decreased expression of gluconeogenic genes and glucose output (109, 110). These mice demonstrate mild hypoglycemia, increased systemic glucose as well as elevated insulin sensitivity due to the because of decreased glucose production. In pancreatic β -cells, Sirt1 is known to positively regulate glucose stimulated insulin secretion (111, 112), whereas it is able to modulate the expression (113) and secretion (114) of adiponectin, a hormone that enhances insulin sensitivity from adipocytes. Further non-histone substrates are the tumor suppressor p53, the FOXO family of forkhead box transcription factors and NF- κ B transcription factors, which are involved in the regulation of cell survival, proliferation and stress response (106, 115-117). Sirt1 has also been linked to the survival of neurons. The survival of cultured neuronal cells

can be promoted by Sirt1, probably through deacetylation-mediated downregulation of the pro-apoptotic factors p53 (115, 118) and FOXO (116, 119). Overexpression of Sirt1 and the addition of the Sirt1 agonist resveratrol reduced NF- κ B signalling in β -amyloid-induced death of microglia (120). Finally, Sirt1 null mice were shown to result in metabolically inefficient animals that failed to adapt to caloric restriction (CR) conditions, suggesting that Sirt1 is required for response to CR (121).

1.6.2 Sirt2

Compared to the Sirt1, the function of Sirt2 is less well understood. Mammalian Sirt2 resides predominantly in the cytoplasm and is involved in cytoskeleton organization by targeting the cytoskeletal protein α -tubulin (101). Sirt2 has been implicated in cell cycle regulation (102, 122-125). Its expression correlates with cell cycle progression and peaks in mitosis. Functionally, Sirt2 is considered a mitotic exit regulator. Overexpression of Sirt2 delayed mitotic exit in response of stress (123, 126, 127) whereas Sirt2 inhibition prolongs chronic mitotic arrest, preventing cell death during re-entry into the cell cycle (127). Contrastingly, under normal and non-stress inducing cell culture conditions, Sirt2 did not affect cell cycle progression (128). In addition, the Sirt2 catalytic mutant increased the number of multinucleated cells (102, 124), indicating that precise levels of Sirt2 are required for mitotic fidelity. Sirt2 has also been suggested to act as a tumor suppressor gene in human gliomas (129), since downregulation of Sirt2 gene expression or deletion of the chromosomal region harboring the Sirt2 gene is frequently observed in this type of tumor.

Sirt2 protein expression is induced by caloric restriction most predominantly in white adipose tissue and kidney. Furthermore, in 3T3-L1 murine adipocytes, Sirt2 mRNA levels were elevated by oxidative stress (130). In cultured pre-adipocytes and in adipocytes *in vivo*, Sirt2 was demonstrated to be the most abundant sirtuin (131). Moreover, overexpression of Sirt2 inhibited adipogenesis, whereas reducing Sirt2 expression had the opposite effect. This effect was attributed to Sirt2 mediated regulation of FoxO1 deacetylation (131, 132). Sirt2 can be phosphorylated by various cyclin dependent kinase complexes (124, 128) and dephosphorylated by CDC14B phosphatase (126), which might down-regulate Sirt2 function.

Amongst all sirtuins, Sirt2 expression was found strongest in the brain (128, 133). Further, Sirt2 was described as an oligodendroglial cytoplasmic protein localized in the myelin sheath, decreasing cell differentiation through α -tubulin deacetylation (133-135). It was concluded that its function might be to prevent premature differentiation or early aging of these cells. NAD⁺-mediated deacetylation activity of Sirt2 influences axonal degeneration (136) and microtubule acetylation (133), thus influencing neuronal function. In neurons, Sirt2 is rather uniformly expressed in all neurites and their growth cones (128). Whereas Sirt1 has been mainly attributed neuroprotective effect e.g. in DNA damage (137) and in model systems of Alzheimer's disease (120, 138-140), Sirt2 appears to promote neurodegeneration. For instance, Sirt2 inhibition resulted in rescue of alpha-synuclein toxicity in Parkinson's disease models (141, 142). Conversely, Sirt2 enhances axon degeneration in a mouse model of Wallerian degeneration (136).

1.6.3 Sirt3, 4 and 5

Sirt3, 4 and 5 are localized within the mitochondrial matrix (91, 100, 143-147). Sirt3 possess a mitochondrial signal peptide that is cleaved off after import into mitochondria, necessary for full enzymatic activity (100). Expression of Sirt3 is strong in brown adipose tissue and induced by cold exposure (148). It also appears to regulate mitochondrial function, as its overexpression increases respiration, while at the same time decreasing reactive oxygen species (ROS) production (148). The mitochondrial protein acetylcoenzyme A synthase 2 (AceCS2) was the first substrate identified for Sirt3 (149, 150). AceCS2 is a mitochondrial matrix enzyme that converts acetate to acetyl-CoA in the presence of ATP (151). Deacetylation of AceCS2 by SIRT3 activates its enzymatic activity (149, 150). Sirt3 also regulates ATP synthesis directly by changing the acetylation level of mitochondria electron transport Complex I (152).

Unlike Sirt3, Sirt4 lacks detectable NAD⁺-dependent deacetylase activity *in vitro*, but demonstrates ADP-ribosyl transferase activity (91, 143, 153). Sirt4 is a ubiquitously expressed gene, with highest levels in the kidney, heart, brain, liver, and pancreatic beta cells (91, 143). Furthermore, Sirt4 has been reported to down regulate glutamate dehydrogenase (GDH) by ADP ribosylation and negatively regulate both, glucose and amino acid stimulated insulin

secretion(91) whereas Sirt4 knockout mice display higher GDH activity and levels of blood insulin (91).

Recently it was demonstrated that Sirt5 regulates ammonia entry into the urea cycle (146). Sirt5 functions as a weak NAD⁺-dependent deacetylase and Sirt5 knockout mice developed normally without obvious metabolic defects (146). Sirt5 is known to interact and deacetylate carbonyl phosphate synthetase 1 (CPS1), which is the rate-limiting first step of the urea cycle. Its activity is required for clearing ammonia generated by amino acid metabolism. Mice lacking Sirt5 displayed elevated ammonia levels after a prolonged fast, suggesting that this sirtuin is necessary for dealing with byproducts of amino acid metabolism (146).

1.6.4 Sirt6 and Sirt7

Sirt6 and Sirt7 are found in the nucleus and in the nucleolus, respectively (83, 99). Beside its NAD⁺-dependent deacetylase activity and modulating telomeric chromatin (94), Sirt6 has also been shown to demonstrate a robust auto-ADP-ribosyl transferase activity, that plays a role in DNA repair and human aging (92, 154). Mice with a Sirt6 knockout displayed severe developmental defects, such as hypoglycemia, and suffered from premature aging (154). Additionally, in a recent study Sirt6 was found to regulate tumor necrosis factor (TNF) production (155).

In the nucleolus, Sirt7 associates with rDNA and interacts with RNA polymerase I (Pol I) (156). It may regulate cell growth and metabolism in response to changing metabolic conditions by driving ribosome biogenesis in dividing cells (156).

Taken together, mammalian sirtuins have diverse cellular locations, target multiple substrates including histones and non-histone substrates and affect a broad range of cellular functions. In some organisms, sirtuin have been shown to be regulated by and to mediate the effects of the dietary regimen CR. Moreover, current data indicate that these proteins are interesting therapeutic targets for metabolic and neurodegenerative diseases. Among all sirtuins, Sirt1 is the best characterized member to date, while the *in vivo* function of the other family members is incompletely understood. Moreover, *in vitro* experiments have provided results implicating Sirt2 in adipose tissue metabolism and neuronal survival, thus experiments

aiming to delineate the role of Sirt2 in energy homeostasis and neurodegenerative disease *in vivo* appear will be highly informative.

1.7 Objectives

The first part of this study aimed at the development of a system that allows temporally and spatially controlled gene silencing in mice to study directed gene function analysis in a selected tissue. To test, if this system is applicable for *in vivo* studies, the knockdown efficiency was determined, using a shRNA against the mouse endogenous target Sirt2 in mice.

The second aim was to explore the role of Sirt2 *in vivo*. To this end, transgenic mice were generated with a ubiquitous Sirt2 knockdown using an existing inducible RNAi system. These mice were physiologically characterized under conditions of a normal diet and high fat diet in terms of metabolic pathways, including adipogenesis, glucose and insulin homeostasis, embryogenesis and a model of neurodegenerative disease.

2 Material and Methods

2.1 Chemicals

Size markers for agarose gel electrophoresis (1kb Plus DNA Ladder, O`GeneRuler, ready to use) and for SDS-PAGE (peqGOLD Prestained Protein-Marker IV) were obtained from MBI Fermentas, St. Leon-Rot, Germany and from Peqlab Biotechnologie, Erlangen, Germany, accordingly. Chemicals used in this work are listed below in table 2.

Chemical	Supplier, origin
α -[³² P]-dCTP	PerkinElmer Life Science, Köln, Germany
β -mercaptoethanol	Fisher Scientific, Schwerte, Germany
10x PCR buffer	Invitrogen, Karlsruhe, Germany
20x saline-sodium citrate (SSC)	Invitrogen, Karlsruhe, Germany
4-2-hydroxyethyl-1-piperazineethanesulfonic acid (HEPES)	Sigma Aldrich, Steinheim, Germany
Agarose ultra pure	Invitrogen, Karlsruhe, Germany
Albumine from bovine serum	Sigma Aldrich, Steinheim, Germany
Ampicilin	VWR International, Langenfeld, Germany
Bromophenol blue	Merck, Darmstadt, Germany
Chloroform	Merck, Darmstadt, Germany
Complete protease inhibitor cocktail tablets	Roche Diagnostic, Mannheim, Germany
Desoxyribonukleotide triphosphate set (dNTP)	5 Prime, Hamburg, Germany
Dithiothreitol (DDT)	Sigma Aldrich, Steinheim, Germany
Doxycycline hyclate	Sigma Aldrich, Steinheim, Germany
Ethanol absolute	Merck, Darmstadt, Germany
Ethidium bromide tablets	VWR International, Langenfeld, Germany
Ethylenediaminetetraacetic (EDTA)	Sigma Aldrich, Steinheim, Germany
G153 Developer	Agfa Healthcare, Mortsels, Belgium
G354 Fix	Agfa Healthcare, Mortsels, Belgium
Geneticin (G418)	Sigma Aldrich, Steinheim, Germany

Glucose 20%	Bela-pharm, Vechta, Germany
Glycerol	Merck, Darmstadt, Germany
Guanidine hydrochloride	AppliChem, Darmstadt, Germany
Hydrochloric acid (HCl)	Sigma Aldrich, Steinheim, Germany
Insulin human	Novo Nordisk, Basvaerd, Denmark
Isopropanol	TH. Geyer & Co, Renningen, Germany
Lysogeny Broth (LB)	Sigma Aldrich, Steinheim, Germany
Magnesium chloride (MgCl)	Invitrogen, Karlsruhe, Germany
PeqGOLD TriFast	Peqlab, Erlangen, Germany
Phenol-Chloroform-Isoamyl alcohol	Applied Biosystems, Darmstadt, Germany
Phosphatase inhibitor cocktail tablets, PhosSTOP	Roche Diagnostic, Mannheim, Germany
Phosphate buffered saline (PBS) Gibco	Invitrogen, Karlsruhe, Germany
Protein A Agarose	Millipore, Eschborn, Germany
Proteinase K	5 Prime, Hamburg, Germany
QIAzol lysis reagent	Qiagen, Hilden, Germany
Reporter gene assay lysis buffer	Roche Diagnostic, Mannheim, Germany
RNAlater	Applied Biosystems, Darmstadt, Germany
Salmon sperm DNA solution ultra pure, sonificated	Fisher Scientific, Schwerte, Germany
Sodium chloride 0,9% (NaCl)	B. Braun, Melsungen, Germany
Sodium dodecyl sulfate (SDS)	Sigma Aldrich, Steinheim, Germany
Sodium hydroxide (NaOH)	VWR International, Langenfeld, Germany
Sucrose	Sigma Aldrich, Steinheim, Germany
Super Signal West Pico chemiluminescent substrate	Fisher Scientific, Schwerte, Germany
Tris acetate EDTA (TAE)	Fisher Scientific, Schwerte, Germany
Tris-glycine SDS running buffer	Invitrogen, Karlsruhe, Germany
Triton X-100	Sigma Aldrich, Steinheim, Germany
Trizma hydrochloride	Sigma Aldrich, Steinheim, Germany
Tween 20	Sigma Aldrich, Steinheim, Germany

Table 2: Chemicals

2.2 Molecular biology

Standard methods of molecular biology were performed according to Sambrook and Russell (157), if not stated otherwise.

2.2.1 Cloning of promoter fragments or genes

In general, amplified or digested DNA fragments were separated by size using agarose gel electrophoresis (1 to 3 % (w/v), (depending on fragment size); agarose; 1 x TAE; 0.5 mg/ml ethidium bromide; 1 x TAE electrophoresis buffer). To isolate DNA fragments from gel or to purify PCR amplicants the QIAquick Gel Extractions-Kit (Qiagen, Hilden, Germany) was used according to manufacturer's instructions.

The ligation of purified DNA into a vector was mediated by 12 U T4-DNA-Ligase high concentration (Invitrogen, Karlsruhe, Germany) at room temperature for 30 minutes, or alternatively at 16°C over night with an insert:vector molar ratio of 3:1 and followed by the transformation into chemically competent *Escherichia coli* (*E. coli*), growing on ampicillin containing LB agar plates. Competent *E. coli* DH5a cells were prepared according to a standard protocol (158) and used for heat shock transformation of plasmid DNA (30 min on ice; 40 sec at 42°C; 1h at 37°C in 300 µl S.O.C medium (Invitrogen, Karlsruhe, Germany).

To analyze for the presence of correct target plasmid DNA, recombinant bacterial colonies were screened with the CloneChecker System (Invitrogen, Karlsruhe, Germany) according to manufacturer's instructions. For the isolation of the plasmid DNA from transformed *E. coli* colonies a bacteria suspension of 50 ml LB-medium (Midirep-Kit) or 3 ml LB-medium (Miniprep Kit) was incubated at 37°C overnight. The preparation of plasmid DNA from transformed *E. coli* colonies was performed using PureLink HiPure Plasmid DNA Midiprep, or PureLink HiPure Plasmid Miniprep Kit (Invitrogen, Karlsruhe, Germany) according to manufacturer's instructions.

2.2.2 Cloning plasmid constructs 1, 2 and 6

Main promoter elements of plasmid constructs 1, 2 and 6 were generated by gene synthesis from Sloning Biotechnology, Puchheim, Germany. Following fragments (Table 3)

were generated by fusion PCR with primers that are listed in table 4. The fusion products, such as Fusion PCR synthetic1.1, Fusion PCR synthetic2.1 and Fusion PCR synthetic6.1 were digested each with FseI/StuI and cloned into the FseI- and StuI- sites of the final_synth1.1-vector (product from TaconicArtemis GmbH) containing an F3 site, 5' Dneo, pAhGH, zs green gene, loxP site, tet operator, shLacZ, Caggs promoter and a LacZ gene, flanked by an FRT site. The plasmids were now termed new_synth1.1, new_synth2.1 and new_synth6.1, respectively. These plasmid were transformed subsequently into the Cre expressing *E. coli* strain 294-Cre (159) for Cre mediated deletion of PIE, resulting in constructs named new_synth1.1dPIE, new_Synth2.1dPIE and new_Synth6.1dPIE, respectively.

Construct	Description	Sequence
Fusion PCR synthetic1.1	PCR1 was generated from the plasmid MRbasic with primers MR22s/oMR17as (341 bp); PCR2 was generated from final_synth1 with primers oMR21s/oMR19as (759 bp). For the fusion of PCR1 and PCR2, primers oMR22s and oMR19as (1121 bp) were used. (All PCRs were performed with High Fidelity Platinum Taq Polymerase)	GCGTTGGGTCCACTCAGTAGATGCCTGTTGAATTAAGCTTATTTA AATAGGCCGGCCAGATCTGTCGACAATTGGATCCTCACAGTAGGT GGCATCGTTCCTTTCTGACTGCCCGCCCCCGCATGCCGTCCTCCG GATATTGAGCTCCGAACCTCTCGCCCTGCCCGCCGCGGTGCTCCG TCGCCGCCGCGCCCATGGAATTCGAACGCTGACGTCATCAACC CGTCCAAGGAATCGCGGGCCAGTGTCACTAGGCGGGAACACC CAGCGCGCTGCGCCCTGGCAGGAAGATGGCTGTGAGGGACAGG GGAGTGGCGCCCTGCAATATTGCATGTCGCTATGTGTTCTGGGA AATCACCATAAACGTGAAATAACTTCGTATAATGTATGCTATAACG AAGTTATTTTTGCGTTAATTAAGTGCGATTAAGGGTGCAGCGGC CTCCGCGCCGGGTTTTGGCGCCTCCCGCGGGCGCCCCCTCTCA CGGCGAGCGCTGCCACGTCAGACGAAGGGCGCAGGAGCGTTCCT GATCCTTCCGCCCGGACGCTCAGGACAGCGGCCCGCTGCTCATAA GACTCGGCCTAGAACCCAGTATCAGCAGAAGGACATTTTAGG ACGGGACTTGGGTGACTCTAGGGCACTGGTTTTCTTTCCAGAGAG CGGAACAGGCGAGGAAAAGTAGTCCCTTCTCGGCGATTCTGCGG AGGGATCTCCGTGGGGCGGTGAACGCCGATGATTATATAAGGAC GCGCCGGGTGTGGCACAGCTAGTCCGTCGCAGCCGGGATTTGG GTCGCGGTTCTTGTGTTGTGGATCGCTGTGATCGTCACTTGGTGAGT TGCGGGCTGCTGGGCTGGCCGGGGCTTTCGTGGCCGCCGGGCCG TCGGTGGGACGGAAGCGTGTGGAGAGACCGCAAGGGCTGTAGT CTGGGTCCGCGAGCAAGGTTGCCCTGAACTGGGGGTTGGGGGGA GCGCACAAAATGGCGGCTGTCCCAGTCTTGAATGGAAGACGC TTGTAAGGCGGGCTGTGAGGTCGTTGAAACAAGGTGGGGGGCAT GGTGGGCGGCAAGAACCAAGGCTTGTAGGCCCTTCGCTAATGCG GGAAAGC

<p>Fusion PCR synthetic2.1</p>	<p>PCR1 was generated from the plasmid MRbasic with primers MR22s/oMR17as (341 bp); PCR2 was generated from final_synth2 with primers oMR21s/oMR19as (759 bp). For the fusion of PCR1 and PCR2, primers oMR22s and oMR19as (1121 bp) were used. (All PCRs were performed with High Fidelity Platinum Taq Polymerase)</p>	<p>GCGTTGGGTCCACTCAGTAGATGCCTGTTGAATTAAGCTTATTTA AATAGGCCGGCCAGATCTGTGACAATTGGATCCTCACAGTAGGT GGCATCGTTCTTTCTGACTGCCCGCCCCCGCATGCCGTCCCCG GATATTGAGCTCCGAACCTCTCGCCCTGCCGCCCGCGGTGCTCCG TCGCCCGCCGCGCCCATGGAATTCGAACGCTGACGTCATCAACC CGTCCAAGGAATCGCGGGCCAGTGTACTAGGCGGGAACACC CAGCGCGCGTGCGCCCTGGCAGGAAGATGGCTGTGAGGGACAGG GGAGTGGCGCCCTGCAATATTTGCATGTGCTATGTGTTCTGGGA AATCACCATAAACGTAAGTGTCTTATAACTTCGTATAATGTATG CTATACGAAGTTATTTTTTGGCGTTAATTAAGTGCATTAAGGGTGG CAGCGGCCTCCGCGCGGGTTTTGGCGCTCCCGCGGGCGCCCC CTCCTCACGGCGAGCGCTGCCACGTCAGACGAAGGGCGCAGGAG CGTTCCTGATCCTTCCGCCCGGACGCTCAGGACAGCGGCCCGCTG CTCATAAGACTCGGCCTTAGAACCCAGTATCAGCAGAAGGCA TTTTAGGACGGGACTTGGGTGACTCTAGGGCACTGGTTTTCTTTC CAGAGAGCGGAACAGGCGAGGAAAAGTAGTCCCTTCTCGGGCAT TCTGCGGAGGGATCTCCGTGGGGCGGTGAACGCCGATGATTATAT AAGGACGCGCCGGGTGTGGCACAGCTAGTTCGTCGACAGCGCG ATTTGGGTGCGGGTCTTGTGTTGTGGATCGCTGTGATCGTCACTTG GTGAGTTGCGGGCTGCTGGGCTGGCCGGGGCTTTCGTGCCGCCG GGCCGCTCGGTGGGACGGAAGCGTGTGGAGAGACCCCAAGGGC TGTAGTCTGGGTCCGCGAGCAAGGTTGCCCTGAACCTGAGGCTGG GGGAGCGCACAAAATGGCGGCTGTTCCCGAGTCTTGAATGGAA GACGCTTGAAGGCGGGCTGTGAGGTCGTTGAAACAAGGTGGGG GGCATGGTGGGCGCAAGAACCAAGGTCTTGAGGCCCTTCGCTA ATGCGGGAAGC</p>
<p>Fusion PCR synthetic6.1</p>	<p>PCR1 was generated from the plasmid MRbasic with primers MR22s/oMR20as (339 bp); PCR2 was generated from final_synth6 with primers oMR21s/oMR19as (759 bp). For the fusion of PCR1 and PCR2, primers oMR21s and oMR19as (1090 bp) were used. (All PCRs were performed with High Fidelity Platinum Taq Polymerase)</p>	<p>GCGTTGGGTCCACTCAGTAGATGCCTGTTGAATTAAGCTTATTTA AATAGGCCGGCCAGATCTGTGACAATTGGATCCTCACAGTAGGT GGCATCGTTCTTTCTGACTGCCCGCCCCCGCATGCCGTCCCCG GATATTGAGCTCCGAACCTCTCGCCCTGCCGCCCGCGGTGCTCCG TCGCCCGCCGCGCCCATGGAATTCGAACGCTGACGTCATCAACC CGTCCAAGGAATCGCGGGCCAGTGTACTAGGCGGGAACACC CAGCGCGCGTGCGCCCTGGCAGGAAGATGGCTGTGAGGGACAGG GGAGTGGCGCCCTGCAATATTTGCATTAGAGAATAACTTCGTATA ATGTATGCTATACGAAGTTATTTTTTGGCGTTAATTAAGTGCATTA AGGGTGCAGCGGCCTCCGCGCCGGTTTTGGCGCTCCCGCGGGC GCCCCCTCCTCACGGCGAGCGCTGCCACGTCAGACGAAGGGCG CAGGAGCGTTCCTGATCCTTCCGCCCGGACGCTCAGGACAGCGGC CCGCTGCTCATAAAGACTCGGCCTTAGAACCCAGTATCAGCAGAA GGACATTTTAGGACGGGACTTGGGTGACTCTAGGGCACTGGTTTT CTTCCAGAGAGCGGAACAGGCGAGGAAAAGTAGTCCCTTCTCG GCGATTCTGCGGAGGGATCTCCGTGGGGCGGTGAACGCCGATGA TTATATAAGGACGCGCCGGGTGTGGCACAGCTAGTTCGTCGCAG CCGGATTTGGGTGCGGGTCTTGTGTTGTGGATCGCTGTGATCGT CACTTGGTGAGTTGCGGGCTGCTGGGCTGGCCGGGGCTTTCGTGG CCGCCGGCCGCTCGGTGGGACGGAAGCGTGTGGAGAGACCGCC AAGGGCTGTAGTCTGGGTCCGCGAGCAAGGTTGCCCTGAACCTGG GGTTGGGGGAGCGCACAAAATGGCGGCTGTTCCCGAGTCTTG AATGGAAGACGCTTGAAGGCGGGCTGTGAGGTCGTTGAAACAA GGTGGGGGCGATGGTGGGCGGCAAGAACCAAGGTCTTGAGGCC TTCGCTAATGCGGGAAGC</p>

Table 3: Fusion PCR-synthetic1.1, -synthetic2.1 and –synthetic6.1

Primer	Sequence (5'-3')	T _{annealing} °C	Orientation
oMR17 as	GGTGATTTCACAGAACACATAGCG	58	antisense
oMR18 s	CGCTATGTGTTCTGGGAAATCACC	58	sense
oMR19 as	GCTTTCCCGCATTAGCGAAGG	58	antisense
oMR20 as	ATGCAAATATTGCAGGGCGCCACTCC	58	antisense
oMR21 s	CGCCCTGCAATATTTGCATTAGAGAATAA CTTCG	58	sense
oMR22 s	GCGTTGGGTCCACTCAGTAGATGC	58	sense

Table 4: Primers used for fusion PCR-synthetic1.1, -synthetic2.1 and -synthetic6.1

All primer sequences are displayed in 5'-3' order. Primer orientation is designated "sense" when coinciding with transcriptional direction. All primers were purchased from Metabion, Germany.

2.2.3 Cloning plasmid constructs 3, 4, 5 and 7

The technical challenge was to insert a loxP site at any position within the promoter sequence. Therefore, the In-Fusion™ Dry-Down PCR Cloning Kit (Clontech Laboratories, Saint-Germain-en-Laye, France) was used to amplify the required sequence by PCR reaction without the need of restriction enzymes cleavage. The amplified products contained 15 bp sequence homologies on both ends that were added through the PCR primers. Finally, the In-Fusion Enzyme promoted single-strand annealing reactions between the DNA molecules that share short sequence overlaps (or homologies) at their ends, such as the PCR amplified insert and vector backbone. A schematic overview of the In-Fusion cloning method is depicted in Figure 4.

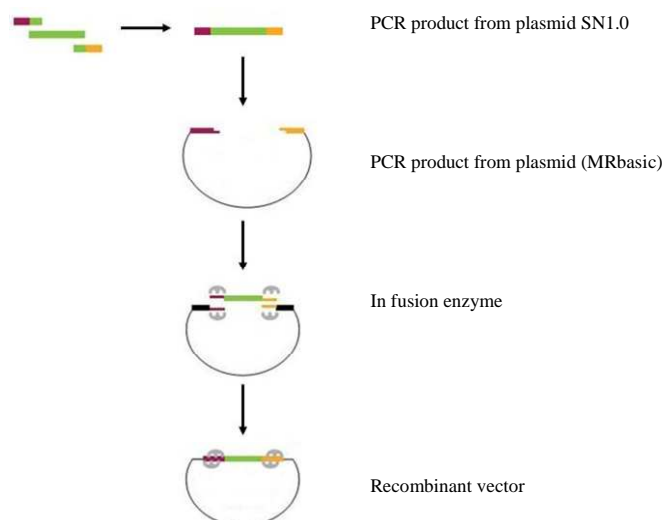


Figure 3: Overview of In-fusion cloning method

The In-fusion enzyme creates single-stranded regions at the end of the vector and PCR product, which are then fused due to the 15 bp homology. Adapted from In-Fusion Dry-Down PCR Cloning Kit User Manual (Clontech Laboratories Inc.)

PCR fragments were amplified from plasmids MRbasic and SN1.0 (both product from TaconicArtemis GmbH), respectively and fused using the In-Fusion™ Dry-Down PCR Cloning Kit (Clontech Laboratories, Saint-Germain-en-Laye, France). The primers used for amplification are listed below (Table 5). PIE was deleted by Cre-mediated recombination through transformation of the plasmids into the Cre expressing *E. coli* strain 294-Cre (159).

Construct	Primer	Sequence (5' - 3')	T _{annealing} °C	Description
3	oMR2 s	TTATAAGTCCCTATCAGTGATAGAGATT CCCAGTG	60 (4 x cycles) 65 (16 x cycles)	Used for amplification of the vector backbone consisting of following elements: F3, D-5' neo-pA, pAhGH, defined parts from 5' and 3' of H1 promoter, FRT and amp resistance gene. Template plasmid: MRbasic; Size: 5.72kb
	oMR2 as	ATTTCACGTTTATGGTGATTTCCAGAA CACATAGC		
	oMR1 s	AATCACCATAAACGTGAAATCGTATAA TGTATGCTATACGAAGTTATGCGTAATA CGACTCACTATAGGGCG	55 (4 x cycles) 65 (16 x cycles)	

	oMR1 as	TCTCTATCACTGATAGGGACTTATAAGT ATAGCATACATTATACGAAGTTATCTGT TATCCCTAGCGTAACTGGC		
4	oMR8 s	ATAAGTCCCTATCAGTGATAGAGATTCC CAGTGGATGGAGCCG	60 (4 x cycles) 65 (16 x cycles)	Used for amplification of the vector backbone consisting of following elements: F3, D-5' neo-pA, pAhGH, defined parts from 5' and 3' of H1 promoter, FRT and amp resistance gene. Template plasmid: MRbasic; Size: 5.71 kb
	oMR8 as	GGTGATTTCCAGAACACATAGCGACA TGC		
	oMR7 s	ATGTGTTCTGGGAAATCACCATAACTTC GTATAATGTATGCTATACGAAGTTATGC GTAATACGACTCACTATAGGGCG	60 (4 x cycles) 65 (16 x cycles)	Used for amplification of the H1 promoter elements implying a loxP flanked stuffer sequence called PIE (zsgreen under control of an ubiquitin promoter). Template plasmid: SN1.0; Size: 2.44 kb
	oMR7 as	CTATCACTGATAGGGACTTATAATAACT TCGTATAGCATACATTATACGAAGTTAT CTGTTATCCCTAGCGTAACTGGCGCGC		
5	oMR10 s	GCTATACGAAGTTATTGCAGTTTTAAAA TTATGTTTTAAAATGGACTATCATATGC TCACCATAAACGTGAAATGTCTTTGGAT TTGGGAATCTTATAAGTCC	60 (4 x cycles) 65 (16 x cycles)	Used for amplification of the vector backbone consisting of following elements: F3, D-5' neo-pA, pAhGH, defined parts from 5' and 3' of H1 promoter, FRT and amp resistance gene. Template plasmid: MRbasic; Size: 5.85 kb
	oMR10 as	TATTTTGTACTAATATCTTTGTGTTTACA GTCAAATTAATTCTAATTATCTCTCTAA CAGCCTTGTATCGTATATGCAAATATTG CAGGGCGCCACTCCCCTGTC		
	oMR9 s	CAAAGATATTAGTACAAAATAATAACT TCGTATAATGTATGCTATACGAAGTTAT GCGTAATACGACTCACTATAGGGCGAA TTGGAGCTCCACCGCG	60 (4 x cycles) 65 (16 x cycles)	Used for amplification of the U6 promoter DSE element including a 156 bp promoter sequence 3' from U6-DSE with the loxP flanked stuffer sequence called PIE (zsgreen under control of an ubiquitin promoter) and the PSE element from H1 promoter. Template plasmid: SN1.0; Size: 2.42 kb
	oMR9 as	CTGCAATAACTTCGTATAGCATACATTA TACGAAGTTATCTGTTATCCCTAGCGTA ACTGGCG		
	oMR14 s	TCATATGTCACCATAAACGTGAAATGTC TTTGGATTTGGG	58 (4 x cycles) 65 (16 x cycles)	Used for amplification of the vector backbone consisting of following elements: F3, D-5' neo-

	oMR14 as	TTTCCCAGAACACATAGCGACATGCAA ATATTGCAGG		
	oMR13 s	GCATGTCGCTATGTGTTCTGGGAAATAG AGAATAACTTCGTATAATGTATGCTATA CGAAGTTATGCGTAATACG	58 (4 x cycles) 65 (16 x cycles)	Used for amplification of the H1 promoter elements implying a loxP flanked stuffer sequence called PIE (zsgreen gene under control of an ubiquitin promoter). Template plasmid: SN1.0; Size: 2.45kb
	oMR13 as	CACGTTTATGGTGACATATGAATAACTT CGTATAGCATACATTATACGAAGTTATC TGTTATCCCTAGCGTAACTGGCGCG		

Table 5: Primers used for cloning of construct 3, 4, 5 and 7

All primer sequences are displayed in 5'-3' order. Primer orientation is designated "sense" when coinciding with transcriptional direction. All primers were purchased from Metabion, Germany.

2.2.4 Isolation of Genomic DNA

For genomic DNA isolation, mouse tail biopsies were incubated overnight in lysis buffer (100 mM Tris-HCl (pH 8.5), 5 mM EDTA, 0.2% (w/v) SDS, 0.2 M NaCl, 200 µg/ml proteinase K) in a thermomixer (Eppendorf, Hamburg, Germany) at 55°C and 1100 rounds per minute (rpm). Samples were centrifuged to discard debris and supernatant was transferred in a new vial. DNA-precipitation was then performed by addition of one equivalent of isopropanol. After centrifugation and a single washing step with 70% (v/v) ethanol, the DNA pellet was dried at room temperature (RT) for 15 minutes and resuspended in TE buffer (10 mM Tris-HCl (pH 7.5), 1 mM EDTA (pH 8.0)).

Mouse embryonic stem (mES) cells were incubated in lysis buffer (10 mM Tris-HCl (pH 7.5), 10 mM EDTA, and 10 mM NaCl, 5% (w/v) N-Laurylsacrosinate, 0.5 mg/ml proteinase K) at 60°C over night. DNA was precipitated with double amount of 100% ethanol, absolute, washed as described above and resuspended in double distilled water (ddH₂O).

2.2.5 Polymerase Chain Reaction (PCR)

The PCR method (160, 161) was used to genotype the mice for the presence of transgenes with customized primers listed in table 6. Reactions were performed in a

thermocycler MultiCycler PTC 225 Tetrad (Bio-Rad Laboratories, CA, USA) or in DNA engine Tetrad 2 Peltier Thermal Cycler (Bio-Rad Laboratories, München, Germany). All amplifications were performed in a total reaction volume of 50 μ l, containing a minimum of 50 ng template DNA, 5 μ M of each primer, 10 mM dNTP Mix, 50 mM MgCl₂, 10 x PCR buffer and 5 units/ μ l Taq DNA Polymerase (Invitrogen, Karlsruhe, Germany). Standard PCR programs started with 5 minutes (min) of denaturation at 95°C, followed by 35 cycles consisting of denaturation at 95°C for 30 seconds (sec), annealing at oligonucleotide-specific temperatures for 30 sec and elongation at 72°C for 1 min and a final elongation step at 72°C for 10 min.

For cloning procedures, the High Fidelity Platinum Taq Polymerase (Invitrogen, Karlsruhe, Germany) was used instead.

Primer	Sequence (5' - 3')	T _{Annealing} °C	Orientation
oRNA46	TATGGGCTATGAACTAATGACCC	60	antisense
oRNA48	CCATGGAATTCGAACGCTGACGTC	60	sense
oMRseq31as	CGGCGCGTCCTTATATAATCATCG	60	antisense
Cre1011_1	ACGACCAAGTGACAGCAATG	60	sense
Cre1011_2	CTCGACCAGTTTAGTTACCC	60	antisense
Rosawt1114_1	CTCTTCCCTCGTGATCTGCAACTCC	60	sense
Rosawt1114_2	CATGTCTTTAATCTACCTCGATGG	60	antisense
Neo1012_1	TGCTCCTGCCGAGAAAGTATCCATC ATGGC	60	sense
Neo1012_2	CGCCAAGCTCTTCAGCAATATCACG GGTAG	60	antisense
LacZ1004_3	ATCCTCTGCATGGTCAGGTC	60	sense
LacZ1004_3	CGTGGCCTGATTCATTCC	60	antisense

Table 6: Primers used for genotyping

All primer sequences are displayed in 5'-3' order. Primer orientation is designated "sense" when coinciding with transcriptional direction. All primers were purchased from Metabion, Germany.

2.2.6 Southern Blot

10 µg of genomic DNA were digested overnight at 37°C, with 40 U of HindIII or BamHI restriction enzyme (New England BioLabs GmbH, Frankfurt, Germany) and separated electrophoretically on a 0.8% (w/v) agarose gel at 90 V. The DNA was subsequently transferred to a HybondTM-XL nylon membrane (GE Healthcare, Freiburg, Germany) by an alkaline capillary transfer (162). After a washing step with 2 x SSC, DNA was crosslinked to the membrane by baking at 80°C for 1 hr. The membrane was pre-hybridized at 65°C for 1 h in hybridization solution (1 M NaCl; 50 mM Tris-HCL (pH 7.5), 10% (w/v) dextran sulfate, 0.1% (w/v) SDS; 250µg/ml sonicated salmon sperm DNA). The probes were generated by digestion of vector plasmid DNA or by PCR (Table 7, 8) and labeled with α -³²P-dCTP (PerkinElmer Life Sciences, Köln, Germany) using the Amersham Ready-To-Go DNA labeling beads (GE Healthcare, Freiburg, Germany). The radioactively labeled probe was then added to the pre-hybridization solution and hybridization was performed overnight at 65°C in a rotating cylinder. Un-specifically bound probe was removed by washing the membrane initially with 2 x SSC / 0.1 % (w/v) SDS, followed by 0.2 x SSC / 0.1% (w/v) SDS, if necessary. All washes were performed at 65°C under gentle shaking for 10-20 min. After each wash, the membrane was monitored with a scintillation detector and the washing steps were stopped when radioactivity reached 20 to 50 impulses per second (IPS). The membrane was then sealed in a plastic bag and exposed to autoradiography film (Kodak BioMax, MS; Sigma-Aldrich Chemie GmbH, Deisenhofen, Germany) at -80°C. Films were developed in an automatic developer (Agfa HealthCare GmbH, Köln, Germany).

Probe	Size (bp)	Restriction enzyme	Vector	Description
Rosa 3'	386	HindIII	JS43	external probe 3' from integration site at the <i>rosa26</i> locus
Neo	519	HindIII/ EcoRI	KD602	Internal probe
Puro	292	SpeI/XhoI	pMultilink Puro	Internal probe

Table 7: Probes for Southern Blot generated by digestion of vector DNA

The vectors are all products from TaconicArtemis GmbH.

Probe	Size (bp)	Primer (5'-3')	T _{annealing} °C	Orientation	Plasmid	Description
Rosa 5'	533	AAGGATACTGGGGCA TACG	60	sense	JS32	External probe 5' from integration site at the <i>rosa26</i> locus
		CTTCTCAGCTACCTTT ACACACC	60	antisense		

Table 8: Probes for Southern Blot generated by PCR

All primer sequences are displayed in 5'-3' order. Primer orientation is designated "sense" when coinciding with transcriptional direction. All primers were purchased from Metabion, Germany.

2.2.7 RNA Extraction and Quantitative Realtime-PCR (qPCR)

Total RNA from murine cells and tissues was extracted using the Qiagen RNeasy Plus Mini Kit (Qiagen, Hilden, Germany). 1 µg of each RNA sample was reversely transcribed using the High Capacity cDNA Reverse Transcription Kit (Applied Biosystem, Darmstadt, Germany) according to manufacturer's instructions. The analysis was performed using the ABI Prism 7900HT Fast Real-time PCR System (Applied Biosystems, Foster City, USA). The probes used during this work are listed in table 9, 10 and 11. Samples were adjusted for total RNA content to heterochromatin protein 1, binding protein 3 (Hp1bp3) and mouse glyceraldehyd-3-phosphat-dehydrogenase (GAPDH) RNA. Quantification of relative cDNA transcript amounts was calculated by comparative method ($2^{-\Delta\Delta Ct}$). Data were analyzed with the Sequence Detector System (SDS) software version 2.1 (ABI) and Ct value was automatically converted to fold change RQ value ($(RQ) = 2^{-\Delta\Delta Ct}$). The RQ values from each gene were then used to compare the gene expression across all groups.

In brief, the threshold cycle value (Ct) is the fractional PCR cycle number at which the fluorescent signal reaches the detection threshold. Therefore, the input cDNA copy number and Ct are inversely related. The higher the initial amount of the sample, the sooner the accumulated product is detected in the PCR process as a significant increase in fluorescence, and the lower is the Ct value.

Probe	Catalogue N°
Sirt2	Mm00452114_m1
Sirt1	Mm00490758_m1
PPAR γ	Mm00440940_m1
HP1bp3	Mm00802807_m1
Mouse GAPDH	Endogenous Control (VIC®/MGB Probe, Primer Limited)

Table 9: Real-Time analysis probes

Target RNA	Primer 5'	Primer 3'	Probe 5'-3'
LacZ	CTGTATGTGGTGGAT GAAGCCAATA	CGCGGATCATCGGT CAGA	ATGCCGTGGGTT TCA

Table 10: Custom Real-Time analysis probes

Target shRNA	Strand of shRNA	Sequence 5'-3' for assay design
shLacZ2	antisense	UUCAAUAUUGGCUUCAUCCAC

Table 11: Custom Real-Time analysis probes for small RNA

2.2.8 DNA sequencing

DNA-sequencing was performed using Big Dye Termination v3.1 Cycle Sequencing Kits (Applied Biosystems, Darmstadt, Germany). Therefore 1.0 μ l Ready Reaction Premix (2.5x), 3.0 μ l BigDye Sequencing Buffer (5x), 2.0 pmol/ μ l Primer and 400 ng dsDNA were adjusted to a final volume of 10 μ l and submitted to 25 cycles of the following temperature program: 30 sec at 96°C; 20 sec at 55°C; 2 min at 60°C. The fluorescently labeled DNA fragments were purified by a filtration step using Sephadex TM G-50 Medium (GE Healthcare Bio-science, Freiburg, Germany) before the sequence was automatically determined with the ABI Prism 3130xl Genetic Analyzer. The evaluation was performed with the software Sequencher 4.9 (Gene Codes Corporation, Ann Arbor, USA).

2.2.9 Quantification of DNA and RNA

Nucleic acid concentration was assessed by measuring the sample absorption at 260 nm with a NanoDrop® ND-1000 UV-Vis Spectrophotometer (Peqlab, Erlangen, Germany). The 260/280 nm absorbance ratio was used as a measure of purity for nucleic acid samples. A ratio of ~1.8 was accepted as pure DNA and a ratio of ~2.0 as pure RNA.

2.2.10 Protein extraction

Snap-frozen tissues were disrupted in organ lysis buffer (50 mM HEPES (pH7.4), 1% (v/v) Triton X-100, 50 mM sodium chloride, 10 mM EDTA, 0.1% (w/v) SDS, protease inhibitor cocktail (Roche Diagnostics, Mannheim, Germany) and phosphatase inhibitor cocktail (Roche Diagnostics, Mannheim, Germany)) at 3 ml/g tissue and homogenized by the usage of a TissueLyser II (Qiagen, Hilden, Germany) for 2 min at 30 Hz using 5 mm stainless steel beads (Qiagen, Hilden, Germany). Particulate matter was removed by centrifugation for 1 h at 4°C. The supernatant was transferred to a fresh vial. Adipose tissue was centrifuged for a second time to get rid of the fat layer. The protein concentration was determined according to manufacturer's protocol (Pierce BCA protein assay kit; Fisher Scientific, Schwerte, Germany). Protein extracts were diluted to 2.5 mg/ml with organ lysis buffer and 4 x SDS sample buffer (250 mM Tris-HCL (pH 6.8), 200 mM DTT, 8% (w/v) SDS, 40% (v/v) glycerol, and 0.04% (w/v) bromophenol blue), incubated at 95°C over 5 min and stored at -80°C

2.2.11 Western Blot

Protein lysates were thawed, centrifuged and supernatant was separated on a 4-12% Novex® Tris-Glycine polyacrylamide gel (Invitrogen, Karlsruhe, Germany) with 1 x SDS running buffer (163) and blotted onto nitrocellulose membranes (Invitrogen, Karlsruhe, Germany). Membranes were then blocked with 5% (w/v) BSA in 1x TBS, 0.1% (v/v) Tween20 or with 5% (w/v) non-fat milk in 1x TBS/0.1% (v/v) Tween, depending on the usage of the antibody, for 1h at RT. Subsequently, primary antibodies (Table 12) were diluted in freshly prepared blocking solution as described above and incubated overnight at 4°C. Nitrocellulose membranes were then washed three times for 5 min with 1 x TBS/0.01% (v/v) Tween. After 1

h incubation at RT with the respective secondary antibody, membranes were washed 3 times for 5 min with 1 x TBS/0.01% (v/v) Tween and incubated for 5 min in Pierce ECL Western Blotting Substrate (VWR international GmbH, Langenfeld, Germany), sealed in a plastic bag and exposed to chemiluminescence film (Kodak BioMax MS; Sigma-Aldrich Chemie GmbH, Deisenhofen, Germany). Films were developed in an automatic developer (Agfa HealthCare GmbH, Köln, Germany).

Antibody	Catalogue No	Distributor	Dilution
Sirt2	Sc-20966	Santa Cruz Biotechnology, Heidelberg, Germany	1:1000
Akt	9372	Cell Signaling, (NEB Biolabs, Frankfurt, Germany)	1:1000

Table 12: Antibodies used for western blot analysis

2.2.12 Enzyme-linked Immunosorbent Assay (ELISA)

Serum insulin and leptin were measured by ELISA using mouse standards according to the manufacturer's guidelines (Mouse Leptin ELISA, #90030, Crystal Chem., Downers Grove, IL, USA; Rat Insulin ELISA, #INSKR020, Crystal Chem., Downers Grove, IL, USA)

2.3 Histological analysis

White adipose tissue of high fat diet (HFD) and normal chow diet (NCD) induced control+dox and shSirt2-2+dox transgenic mice was dissected, fixed overnight in 4% (w/v) PFA (Sigma Aldrich, Seelze, Germany) and then embedded for paraffin sections. Subsequently, 7 µm thin sections were deparaffinized and stained with hematoxylin and eosin (H&E) for general histology. H&E (Sigma Aldrich, Seelze, Germany) staining was performed according to standard protocols. Quantification of adipocyte size was performed using AxioVision 4.2 (Carl Zeiss MicroImaging GmbH, Oberkochen, Germany).

2.4 Cell culture

2.4.1 Embryonic stem cell lines

The embryonic stem cell lines used in this work are listed in Table 13.

ES cell line	Strain	Origin	description
Art4.12	B6129S6F1	TaconicArtemis GmbH	Hybrid ES cell line
F1 RMCE	B6129S6F1-Gt(ROSA)26Sortm9(Flp ^e -RMCE)	TaconicArtemis GmbH	Implies an RMCE targeting system at the <i>rosa26</i> locus. Targeted ES cells include: zsgreen, PGK-Hygro, CAGGS-Flp ^e
B6/3.5	C57BL/6NTac	TaconicArtemis GmbH	Hybrid ES cell line
ArtB6 RMCE 1011	C57BL/6NTac-Gt(ROSA)26Sortm9(Flp ^e -RMCE)	TaconicArtemis GmbH	Implies an RMCE targeting system at the <i>rosa26</i> locus. Targeted ES cells include: zsgreen, PGK-Hygro, CAGGS-LacZ
Art4.12tt4RNA226 neo del	B6129S6F1	TaconicArtemis GmbH	RMCE targeting system (zsgreen, PGK-Hygro, CAGGS Flp ^e) and a dual reporter system including Firefly and Renilla luciferase transgenes (Fluc, CAGGS Rluc, FRT flanked Neomycin) at the <i>rosa26</i> locus. Subsequent deletion of the neomycin selection marker resulted by FLP as described in (164)

Table 13: Embryonic stem cell lines at TaconicArtemis GmbH

2.4.2 Embryonic stem cell culture

Culture and targeted mutagenesis of the hybrid ES cell line Art4.12 or B6 were carried out as previously described (164, 165). ES cells were cultured on a layer of mitomycinC-treated primary feeder fibroblasts. The ES cell medium for Art4.12 ES cells contains D-MEM with 15% fetal calf serum (FCS), 1x non essential amino acids (MEM), 20 mM Hepes buffer, 4 mM L-glutamine, 1 mM sodium pyruvate, 0.1 mM 2- β -mercaptoethanol and 1500 U/ml leukemia inhibitor factor (LIF) and ES cell media (20% media) for B6 ES cells contains D-MEM with 20% fetal calf serum (FCS), 1 x non essential amino acids (MEM), 2 mM L-glutamine, 1 mM sodium pyruvate, 20 mM Hepes, 0.1 mM 2- β -mercaptoethanol and 2000 U/ml LIF. ES cells were grown in culture plates (Falcon, Bedford, USA) and kept at 37°C under humid atmosphere (95%) with 7.5% CO₂.

The medium was changed every day and ES cell colony growth was stopped before they became confluent, usually every 1-3 days. Then colonies were washed once with PBS and then treated shortly with trypsin (0.25% trypsin-EDTA, Gibco, Karlsruhe, Germany) at 37°C until the cells detached from the plate. The cells were resuspended in an appropriate volume of media and splitted (usually 1:3 – 1:6) onto fresh feeder dishes.

ES cells were frozen in cryovials (Nunc, Wiesbaden, Germany) with 10% DMSO at -80°C and transferred later into liquid nitrogen for long term storage.

2.4.3 Transfection of ES cells with the exchange vector

One day before transfection, 2×10^5 ES cells were plated per well on a 6 well plate. 6 μ l Fugene6 Transfection Reagent (Roche; Catalog No. 1814443, Mannheim, Germany) was mixed with 100 μ l serum free medium (optiMEM I with Glutamax-I Invitrogen; Catalog No. 51985-035) and incubated for 5 min at room temperature. 100 μ l of the Fugene6/OptiMEM solution was added to 2 μ g circular exchange vector DNA ($c=0.5 \mu$ g/ μ l) and 2 μ g ($c=0.5 \mu$ g/ μ l) pCAGGS-flpe-ires-puro (56, 166) and incubated for 45 min at RT. This transfection complex was added drop wise to the medium and mixed by a circuiting movement. Fresh medium was added to the transfected cells at the following day. From day 2 on, the medium was changed daily, replaced by medium containing 250 μ g/ml G418 (Geneticin, Invitrogen; Catalog No 10131-019) for Art4.12 ES cells or 200 μ g/ml G418 for B6 ES cells. Seven days

after transfection, single clones were isolated by standard procedures as described (56, 167) and subsequently validated by Southern Blot analysis.

2.4.4 Doxycycline (dox) treatment of ES cells

Single ES cell clones were cultivated with ES cell medium containing 1 µg/ml doxycycline (Sigma-Aldrich, Deisenhofen, Germany) for 72 hours.

2.4.5 Analysis of doxycycline content in mouse serum

ES cells, carrying a doxycycline inducible Fluc expression cassette were cultivated in a 96 well plate. Blood serum was obtained by cardiac puncture immediately after animals have been sacrificed by CO₂ anesthesia. Cotted blood samples were centrifuged at RT for 10 min and 3000g. 10 µl of each animal serum were added to the ES cells, containing 90µl of ES cell medium per well (96 well plate) and incubated overnight 37 °C under humid atmosphere (95%) with 7.5 % CO₂. The cells were washed twice in PBS, lysed in 100 µl/well lysis reagent supplemented with protease inhibitors according to the manufacturer's protocol (β-Galactosidase Reporter Gene Assay Kit, Roche Diagnostics, Mannheim, Germany) and shaken for 20 min at RT. To determine Fluc activity, 35 µl of cell lysate was mixed with 35 µl of Steady-Glo Solution (Steady-Glo Luciferase Assay System, Promega, Mannheim, Germany) on white OptiPlate-96 plates (PerkinElmer, Rodgau, Germany) and shaken for 10 min at RT. Fluc activity was measured using a Wallac 1420 Multilabel luminescence counter (PerkinElmer LAS, Rodgau-Jügesheim, Germany). Total protein was determined according to the manufacturer's protocol (Pierce BCA protein assay kit; Fisher Scientific, Schwerte, Germany) and adjusted to Fluc activity.

2.4.6 β-Galactosidase assay

Ten days after transfection, targeted cells (Art4.12tt4RNA226 neo del) were incubated in 100 µl/well (96 well plate) lysis reagent supplemented with protease inhibitors according to the manufacturer's protocol (β-Galactosidase Reporter Gene Assay Kit, Roche Diagnostics, Mannheim, Germany) and shaken for 20 min at RT. 25 µl of cell lysate were mixed with 50 µl

of substrate reagent and 25µl of initiation solution (β-Galactosidase Reporter Gene Assay Kit, Roche Diagnostics, Mannheim, Germany). The β-galactosidase activity was determined using a Wallac 1420 Multilabel luminescence counter (PerkinElmer LAS, Rodgau-Jügesheim, Germany) and adjusted to Fluc activity. The Fluc activity measurement was performed as described in 2.4.5.

2.5 Mouse experiments

General animal handling was performed as described by Hogan and Silver (167, 168).

2.5.1 Animal care

Mice were housed in a pathogen free facility at TaconicArtemis GmbH, Köln, Germany in isolated ventilated cages (TecniplastTM; Tecniplast Deutschland GmbH, Hohenpeißenberg, Germany) that provide a HEPA (Tecniplast Deutschland GmbH, Germany) filtered supply and exhaust air (99,97 %). Mice were kept at 21°C +/- 1°C on a 12 h light / 12 h dark cycle with the light on at 6 a.m. and were fed either a normal chow diet (NCD; Table 14) or a high fat diet (HFD; Table 14). All animals had access to water *ad libitum*. Food was only withdrawn if required for an experiment. At the end of the study period, animals were sacrificed by CO₂ anesthesia or cervical dislocation. All work was performed in accordance with the “Gesetz zur Regelung der Gentechnik” (GenTGS) October 2001 (German Biologic Act) and the Tierschutzgesetz 1998 (German Animal Welfare Act). Animal procedures and euthanasia were approved by the local government authorities (Bezirksregierung Köln) and were in accordance with National Institutes of Health guidelines.

Animal food	Diet	Supplier	Nutrient information
TD.05298 Teklad Global (2018)	NCD	Harlan Laboratories GmbH, Eystrup, Germany	protein 18,2 %, carbohydrate 47,9 %, fat 5,8 %
TD.05298 Teklad Global (2018)	NCD	Harlan Laboratories GmbH, Eystrup, Germany	protein 18,2 %, carbohydrate 47,9 %, fat 5,8 %, 1 g/kg Dox
Ssniff EF R/M acc. F3282	HFD	Ssniff Spezialdiäten GmbH,	protein 20 %,

mod.		Soest, Germany	carbohydrate 35,7 %, fat 35,6 %
Ssniff EF R/M acc. F3282 mod.	HFD	Ssniff Spezialdiäten GmbH, Soest, Germany	protein 20 %, carbohydrate 35,7 %, fat 35,6 %, 1 g/kg Dox
Ssniff PS M-Z; S8289-Po12	NCD	Ssniff Spezialdiäten GmbH, Soest, Germany	protein 22,8 %, carbohydrate 32,5 %, fat 5,4 %,
Ssniff PS M-Z; S8289-Po12	NCD	Ssniff Spezialdiäten GmbH, Soest, Germany	protein 22,8 %, carbohydrate 32,5 %, fat 5,4 %, 1 g/kg Dox

Table 14: Animal food

2.5.2 Mice

C57BL/6NTac mouse strains were ordered from Taconic. Chimeric mice or fully derived ES mice were generated at TaconicArtemis GmbH by injection of trypsinized recombinant ES cell clones into diploid or tetraploid blastocysts, respectively, and implanted into the uterus of a pseudogregnant mouse. The ES mice “shLacZU6/H1tetPIE” were mated with female “Art12rosaCre” mice that were obtained from the in-house facility of TaconicArtemis GmbH. Breeding colonies were maintained by mating “Art12rosaCre-shLacZU6/H1tetPIE” (“shLacZU6/H1tet Δ PIE”) with a constitutive expressing LacZ mouse strain (TaconicArtemis GmbH) to provide a reporter target for the LacZ specific shRNA expressed from the *rosa26* locus.

Chimeric “shSirt2-2U6/H1tetPIE” mice were mated with “Art12rosaCre” mice to achieve “Art12rosaCre-shSirt2-2U6/H1tetPIE” (“shSirt2-2U6/H1tet Δ PIE”) mice expressing a Sirt2 specific shRNA from the *rosa26* locus.

All metabolic experiments were carried out with male “shSirt2-2H1tet” mice expressing a Sirt2 specific shRNA from the *rosa26* locus.

2.5.3 Body weight, blood collection and blood glucose levels

Body weight was monitored weekly for 12 weeks. Blood glucose values were determined from whole venous blood of the tail using an automatic glucose monitor (Ascensia

ELITE, Bayer Vital, Leverkusen, Germany). Collection of blood samples from living animals until a volume of 100 μ l were obtained by submandibular puncture of the *vena facialis*.

2.5.4 Glucose and insulin tolerance test

For glucose tolerance tests (GTT), mice were fasted overnight for 16 h. After determination of fasted blood glucose levels, each animal received an intraperitoneal injection of 20 % glucose solution (10 ml/kg body weight). Blood glucose was determined 15, 30, 60, and 120 min after injection. For insulin tolerance tests (ITT), each random fed animal was injected intraperitoneal with a 0.75 U/ml insulin solution (0.75 U/kg body weight) after determination of random fed blood glucose concentration. Blood glucose was determined 15, 30 and 60 min after injection.

2.5.5 Food intake and indirect calorimetry

Daily food intake was measured over a period of 7 days and calculated as the average intake of chow over the time stated. Weight of food was determined every day. Calorimetry measurements were performed in a PhenoMaster System (TSE systems, Bad Homburg, Germany), which allows measurement of metabolic performance and activity-monitoring by an infrared light-beam frame. Mice were placed at RT (22°C–24°C) in 7.1-l chambers of the PhenoMaster open circuit calorimetry. Mice were allowed to adapt to the chambers for at least 24 h. Food and water were provided *ad libitum* in the appropriate devices and measured by the build-in automated instruments. Locomotor activity and parameters of indirect calorimetry were measured for at least the following 48 h. Presented data are average values obtained in these recordings.

2.5.6 Behavioral analysis

Locomotor behavior of shSirt2-2 transgenic mice and littermate controls was determined by placing the animals in a rotarod apparatus with constant acceleration in 6 consecutive trials of 5 minutes each. The time spent in the rotating rod was recorded for each

animal and trial until mouse fell off. Animals were familiarized with the procedure under constant rod speed 1 day earlier.

2.5.7 MPTP treatment

1-methyl-4-phenyl-1,2,3,6-tetrahydropyridine hydrochloride (MPTP) was obtained from Sigma (Sigma), dissolved in 0.9% saline and injected i.p. in a volume of 1 ml/100 g body weight. Control animals received an equivalent i.p. injection of saline. The animals received up to four injections of 20 mg/kg on 1 day, at 2 h interval, for a cumulative dose of 80 mg/kg. Locomotor behavior was performed one week after treatment with MPTP or saline, respectively.

3 Results

3.1 Generation of Cre-mediated spatially and temporally regulated shRNA expression system

To derive a system for conditional activation of shRNA expression, we aimed to insert a loxP flanked stuffer sequence into the promoter such that transcription is completely abrogated whereas Cre mediated deletion of the DNA segment will restore promoter activity. The stuffer sequence, referred as promoter inhibitory element (PIE), contains the constitutive expressed reporter gene (*Zsgreen*) that is driven by an ubiquitous promoter. Since full reactivation of transcription represents a critical aspect, we first tried to define a position within the regulatory elements (Figure 4A,B) in which a single loxP site is tolerated without a significant loss of promoter activity. In a second step, inhibition of shRNA expression in the presence of PIE was tested.

3.1.1 The effect of a single loxP site on promoter activity *in vitro*

To determine if the presence of the loxP site interferes with promoter activity, various configurations have been developed and classified in three groups mimicking the promoter region after Cre-mediated recombination event (Figure 4). In group 1, a single loxP site was positioned at different positions 5' from TATA by substituting promoter sequences (Figure 4C-F). In group 2, a loxP sequence was inserted at different positions between hH1 control elements (Figure 4H-I). Finally, a hybrid configuration consisting of human H1 (hH1) and human U6 (hU6) Pol III promoter elements was generated in group 3. Since there is 156 bp stuffer sequence 3' from hU6-DSE element, promoter sequences were replaced by a single loxP site without altering the sequence and spacing of the regulatory elements (Figure 4G).

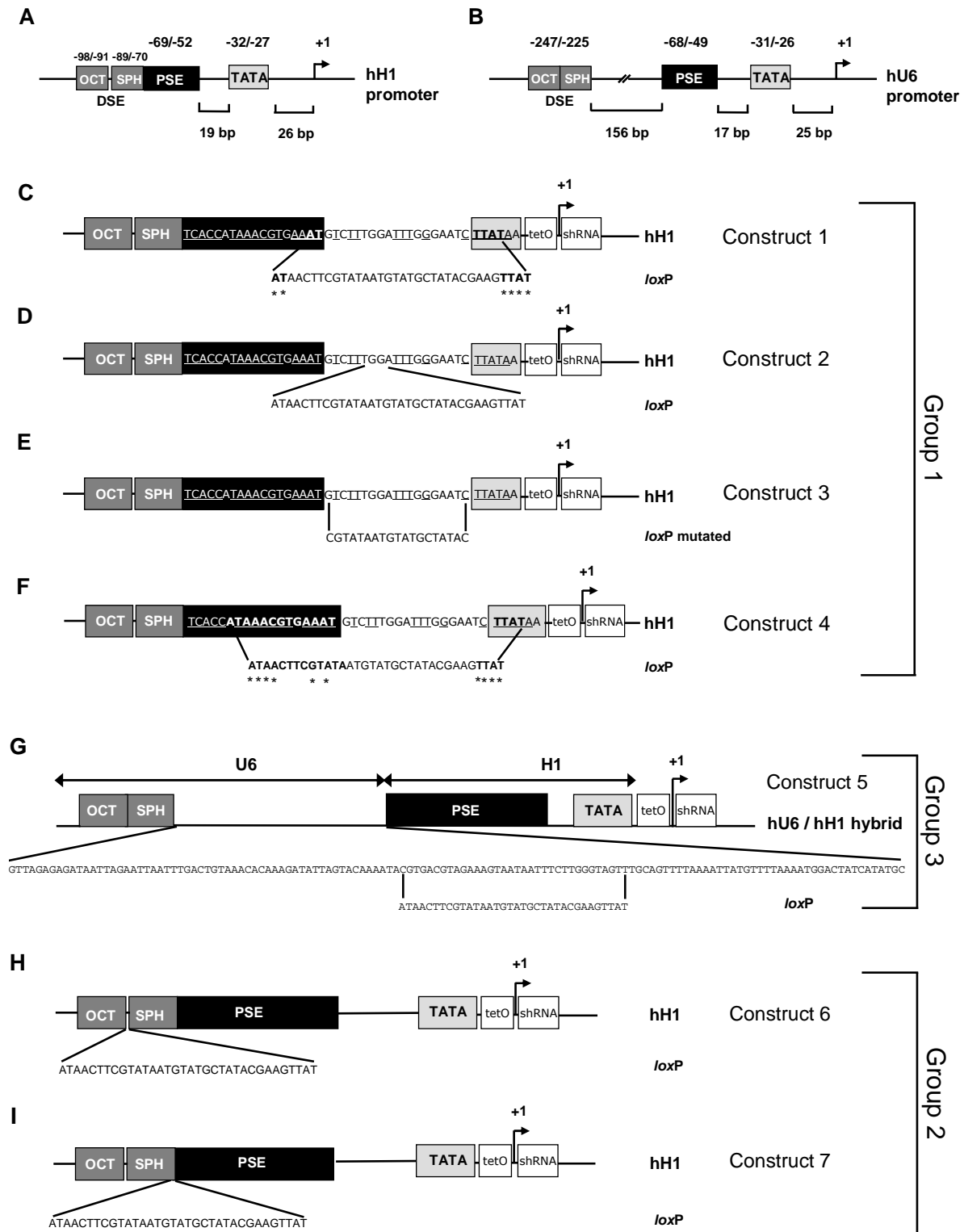
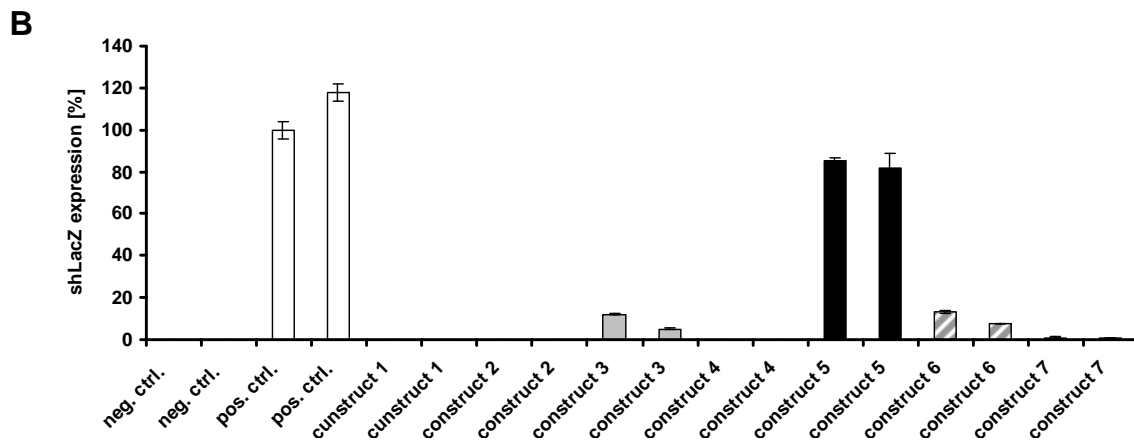
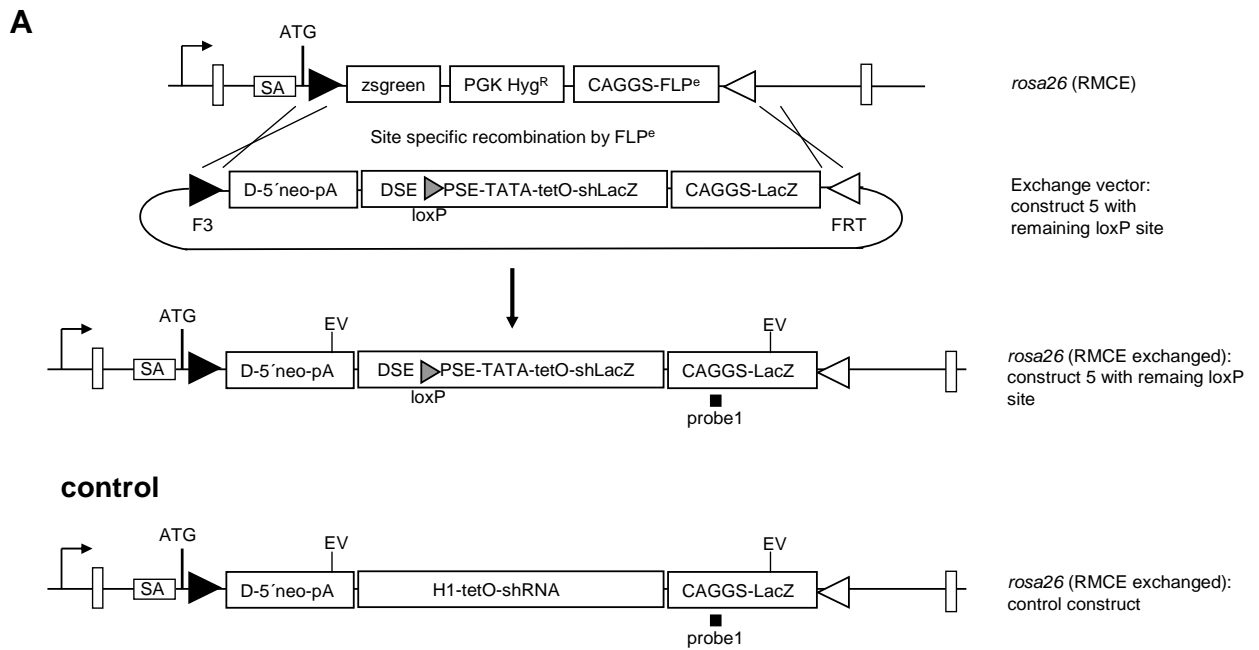


Figure 4: Schematic overview of promoter configurations after Cre-mediated recombination

A) The human H1 promoter consists of DSE (-98 to -70), PSE (-69 to -52) and a TATA box (-32 to -27). The transition from SPH/PSE is seamless and Oct/SPH is separated by one nucleotide. **B)** The human U6snRNA gene consists of a distal sequence element (DSE, -225 to -247) that enhances transcription and a core promoter composed of a proximal sequence element (PSE, -68 to -49) and a TATA box (-31 to -26). The DSE is classified in two sequence elements, SPH and OCT. The promoter elements DSE/PSE are separated by 156 bps and PSE/TATA by 17 bps, respectively. **C)** A wt-loxP was integrated between PSE/TATA (hH1), whereas exact nucleotides, indicated by an asterisk, serve for both DSE/loxP and loxP/TATA (bold letters). **D)** Three non-conserving nucleotides between PSE/TATA (hH1) were substituted by loxP. **E)** By mutating the loxP sequence, the spacing among PSE/TATA (hH1) was preserved. **F)** Nucleotides from PSE/TATA (hH1) were substituted by wt loxP site. Exact matching nucleotides are indicated by an asterisk. **G)** Hybrid H1/U6 promoter configuration including human U6 (hU6) DSE and the human H1 (hH1) PSE. Nucleotides within the 156 bp spacing region of DSE and PSE control elements were replaced by a single loxP-site. **H)** A LoxP sequence was inserted between SPH and OCT (hH1). **I)** A LoxP sequence was inserted between DSE and PSE (hH1).

However, all promoter configurations were tested by inserting a LacZ specific shRNA-sequence and a LacZ expression cassette under the control of the ubiquitous CAGGS promoter (Figure 5A). Before introduction into the *rosa26* locus by RMCE technology (56, 169) (Figure 5A), the plasmids including floxed PIE were transformed into a Cre expressing *E. coli* strain (159), removing PIE through recombination between the two loxP sites. ES cells carrying either a shRNA against LacZ or an irrelevant target (shRNA against insuline receptor), served as positive and negative controls, respectively. The shRNAs from both control constructs were driven each by a H1 promoter (Figure 5A, lower panel). Finally, the shLacZ expression levels were determined in ES cells by quantitative realtime PCR. As shown in Figure 5B, the strongest shLacZ expression amongst others could be observed for construct 5 (U6/H1tet system), demonstrating that the remaining loxP site allows activated gene silencing after Cre recombinated event.

Next, further *in vitro* analyses were performed with construct 5 in the presence and absence of PIE (Figure 5E-F). Successful integration into the *rosa26* locus using genomic DNA from transfected ES cells and an internal probe (puro) was demonstrated by Southern blot analysis (Figure 5C-D). As shown in Figure 5E, a knockdown of about 50% was noted for construct 5 after deletion of PIE compared to ~70% knockdown of the positive control consisting of a shLacZ driven by the unmodified H1 promoter. In contrast, the mRNA level of LacZ was not decreased in the presence of PIE. These results were confirmed as well on protein level using a β -Galactosidase assay. Moreover, the data were comparable to controls with a knockdown efficiency of ~90% (Figure 5F).



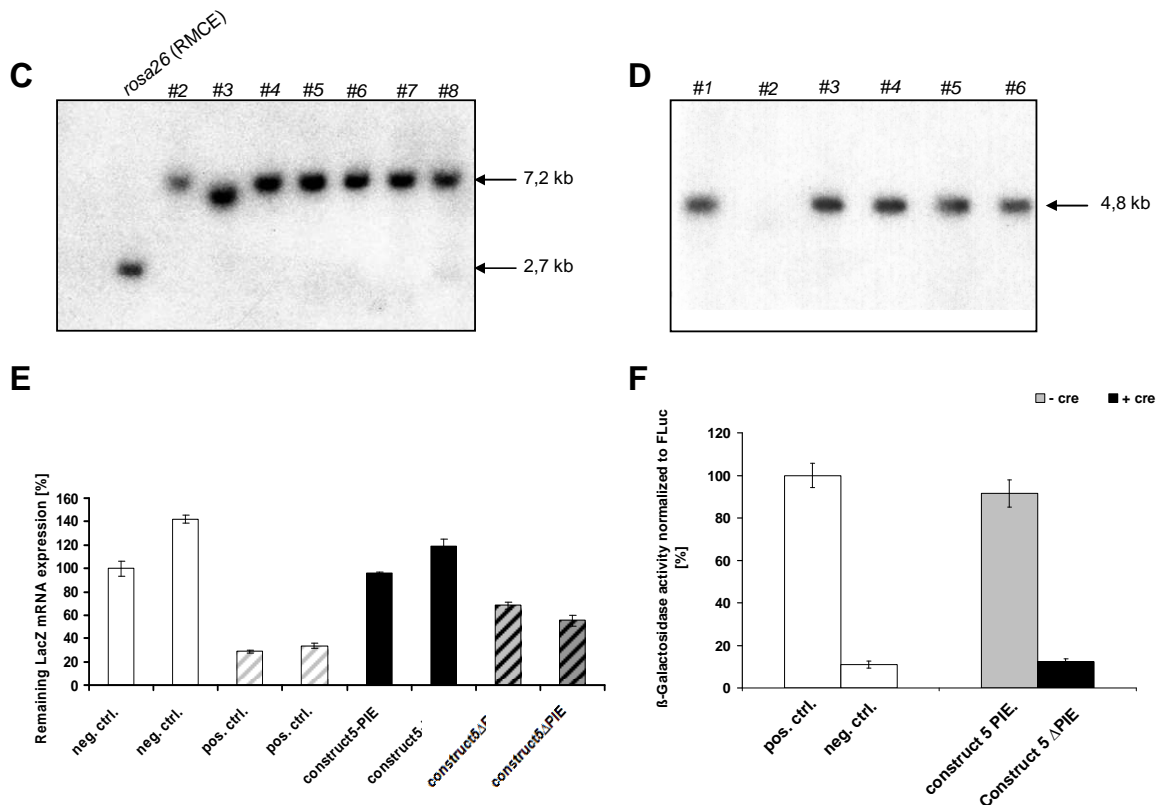


Figure 5: Analysis of seven configurations at the *rosa26* locus in mouse ES cells

A) Stable integration of a single vector cassette into the modified *rosa26* locus, called *rosa26*(RMCE), carrying the RMCE acceptor comprising ZsGreen, PGK-Hyg and CAAGS-FLP. The exchange vector carries the shRNA expression cassette under the control of the engineered promoter (here exemplified for construct5) with the single loxP site, the target gene lacZ under control of the CAGGS promoter and the F3/FRT pair. The RMCE by FLP^e-mediated recombination generates the *rosa26* (RMCE exchanged) allele. The truncated neoR gene allows for positive selection upon successful RMCE. The control constructs consist of a shRNA that is under control of the H1 promoter. (SA=splice acceptor) **B)** shLacZ expression levels were determined by quantitative realtime PCR in ES cells with a shLacZ expression control (pos.ctrl.), an irrelevant shRNA expression control (shRNA against the insulin receptor; neg.ctrl.) and ES cells carrying the promoter modification including the single loxP site after PIE deletion (construct1-7, respectively; n=2 clones per group). **C)** Southern blot analysis of genomic DNA from transfected ES cells carrying the construct5 with the promoter inhibitory element (PIE). The sizes of *rosa26* (RMCE) and *rosa26* (RMCE exchanged) are 2.7 and 7.2 kb, respectively. In clones 2, 4-8 successful RMCE had occurred. Genomic DNA was digested with EcoRV (E) and analyzed using the puro probe (probe 1). **D)** Southern blot analysis of genomic DNA from transfected ES cells carrying the construct5ΔPIE. The size of *rosa26* (RMCE exchanged) is 4.8 kb. In clones 1, 3-6 successful RMCE had occurred. Genomic DNA was digested with EcoRV (E) and analyzed using the puro probe (probe 1). **E)** Quantitative realtime PCR analysis of targeted ES cells. LacZ mRNA expression level are shown from negative control (white bars; expression of shRNA against insulin receptor), positive control (white striped bars; constitutive expressing shLacZ), shLacZ U6/H1tetPIE (construct5PIE; black bars) and of shLacZ U6/H1tetΔPIE (construct5ΔPIE). n=2. **F)** The β-Galactosidase activity of targeted ES-cells, harboring a dual reporter gene system, was measured in relative light units [RLU] from a constitutive shLacZ expression control (pos.ctrl.), a constitutive, irrelevant shRNA expression control (shRNA against the insulin receptor; neg.ctrl.) and cells carrying construct5PIE or construct5ΔPIE, respectively. Firefly Luciferase activity was used for normalization. n=4

Taken together, data from ES cells carrying construct 5 have clearly shown transcriptional inactivation in the presence of PIE. After Cre mediated deletion of PIE, promoter activity was restored resulting in shRNA expression with a knockdown efficiency of 60-90 %. Thus, next steps were performed with the modified promoter configuration of construct 5.

3.1.2 Spatially and temporally activated RNAi of LacZ in mice by the hybrid Pol

III system

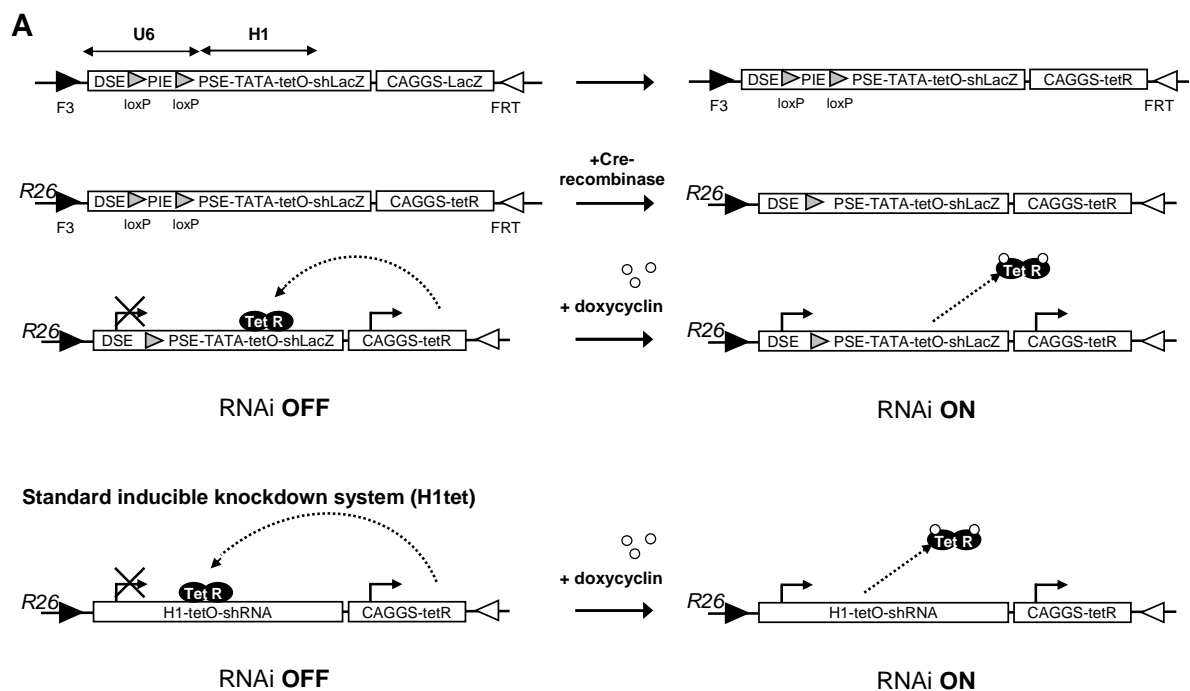
To allow for doxycycline inducible activation of shRNA expression the LacZ coding region was replaced by a transgene encoding the *E. coli* tetracycline resistance operon repressor (tetR) (56) (Figure 6A). In the absence of dox, the tet repressor (tetR) binds to operator sequence (tetO) and thereby blocks shRNA transcription. Upon administration of dox, tetR is released and shRNA mediated gene silencing proceeds (Figure 6A). After RMCE mediated insertion of the U6/H1tetPIE configuration into the *rosa26* locus, recombinant ES cells were injected into tetraploid blastocysts to achieve completely ES cell derived mice. For deletion of the loxP-flanked PIE element, shLacZ U6/H1tetPIE transgenic mice were further crossed to a Cre deleter mouse line (TaconicArtemis, unpublished), resulting in the shLacZ U6/H1tet Δ PIE allele (Figure 6A). Mice carrying the standard inducible RNAi cassette were used as positive controls (Figure 6A, lower panel). Furthermore, shRNA transgenic mice were mated with constitutively expressing LacZ mice (TaconicArtemis, unpublished), to provide a reporter target for the LacZ specific shRNA.

The knockdown level of LacZ was measured in different tissues by quantitative realtime PCR (Figure 6B). Constitutive expressing LacZ control mice (neg.ctrl.), shLacZ H1tet mice (pos.ctrl.), shLacZ U6/H1tetPIE mice and shLacZ U6/H1tet Δ PIE mice were fed either with dox food or control food for 14 days, respectively. A down regulation of LacZ mRNA was achieved with shLacZ H1tet and shLacZ U6/H1tet Δ PIE after induction with dox, but not in shLacZ U6/H1tetPIE mice, confirming that the promoter activity for shRNA expression is disrupted by PIE, even though the tetR is non-bound. No downregulation of LacZ mRNA could be observed in the un-induced state, except for brain of shLacZ H1tet and shLacZ U6/H1tet Δ PIE mice, indicating that in this tissue, the promoter may show gene silencing. The

knockdown level of shLacZ U6/H1tet Δ PIE mice was generally weaker (~ 30-40% in brain and kidney) compared to shLacZ H1tet control animals (~ 80% in EWAT, kidney, liver).

To determine a fully deletion of PIE after Cre-recombination, Zsgreen mRNA was measured by quantitative realtime PCR in shLacZ U6/H1tetPIE, wildtype and in shLacZ U6/H1tet Δ PIE mice (Figure 6C). The results show a presence of PIE in shLacZ U6/H1tetPIE mice whereas PIE is clearly disappeared in shLacZ H1/U6 Δ PIE mice after Cre-recombination, demonstrated in several tissues such as liver, brain and muscle (Figure 6C).

In conclusion, Cre-mediated recombination of the floxed PIE cassette and induction with dox results in an activation of hybrid U6/H1tet promoter in vivo. Compared to the standard inducible shLacZ H1tet system, however, the knockdown of the activated shLacZ U6/H1tet Δ PIE animals was 30-60 % weaker. Moreover, in several tissues such as EWAT and liver, no significant gene silencing was detected.



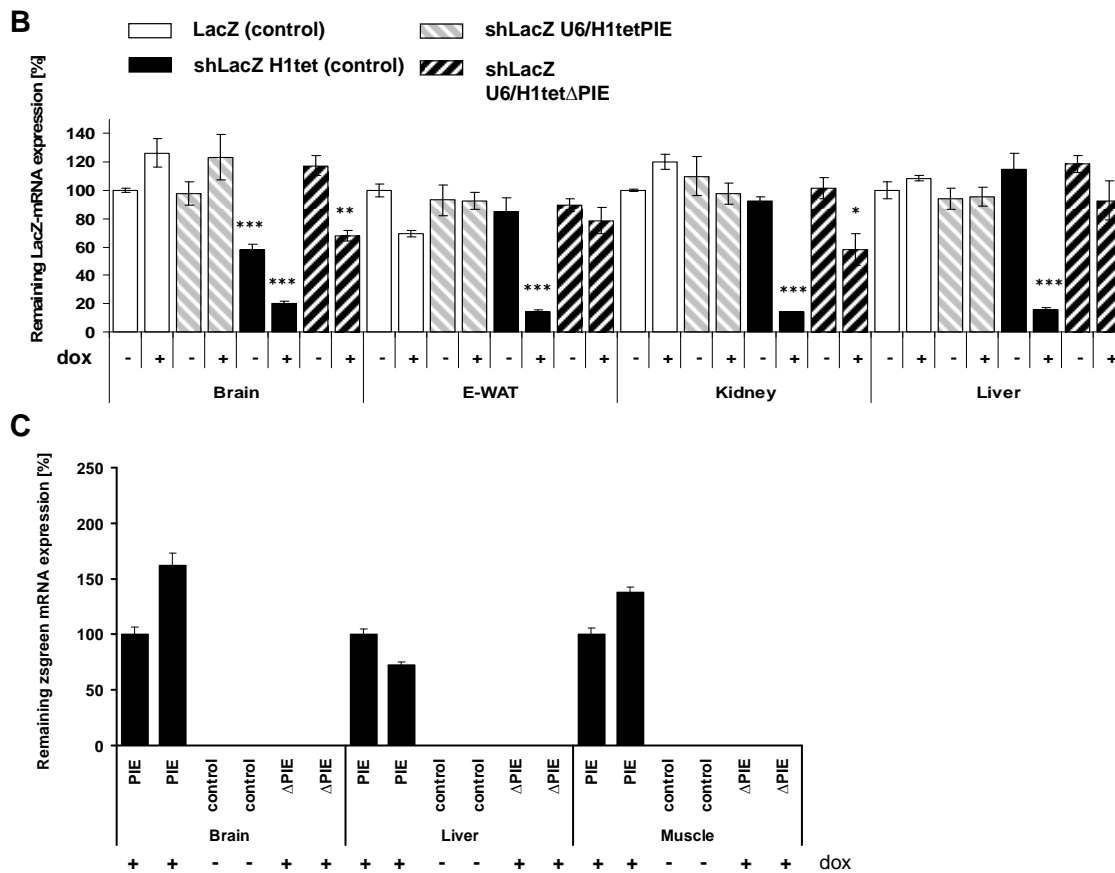


Figure 6: Schematic overview illustrating the activation of H1/U6 hybrid mediated gene silencing (A) and its analysis in vivo (B, C)

A) A single loxP site was replaced by a loxP flanked cDNA cassette named PIE (promoter inhibitory element), consisting of the reporter gene Zsgreen that is under control of a human ubiquitin promoter and placed between the elements DSE (hU6) and PSE (hH1). The LacZ coding region was changed by an *E. coli* tetracycline resistance operon repressor (tetR) (upper panel). After stable integration into the *rosa26* locus, PIE can be deleted through Cre-recombination, leaving in a single loxP site and an activation of the hybrid promoter (middle panel). Expression of shLacZ is still inhibited through binding of the tetR on tetO sequence. Only administration of dox lead to a conformational change of the tetR which then release from the tetO resulting in activated shRNA expression (lower panel). The standard inducible system was used as positive control where the shRNA (shLacZ) is driven by an inducible H1 promoter. **B)** LacZ mRNA expression levels were determined in different tissues by quantitative realtime PCR from constitutive LacZ expressing controls mice (white bars), shLacZ H1tet mice (black bars), shLacZ U6/H1tetPIE mice (grey striped bars) and shLacZ U6/H1tet Δ PIE (black striped bars) mice, respectively. 12-20 weeks old mice were fed 14 days either with control or dox-food (1g/kg dox), indicated by a minus or plus. LacZ mRNA level of non-induced control mice (black bar) was set 100%; n=3 males. **C)** Successful Cre recombination was determined by the deletion of PIE. PIE represents the reporter gene Zsgreen that is under control of an ubiquitin promoter. Zsgreen mRNA expression levels were determined in different tissues by quantitative realtime PCR from wildtype control, shLacZ U6/H1tetPIE and shLacZ U6/H1tet Δ PIE mice. 6-8 weeks old mice were induced for 10 days either with control drinking water or with drinking water supplemented with dox (2mg/ml), indicated by a minus or plus. Zsgreen mRNA expression was only measured before Cre recombination mediated event in the presence of PIE (black bars). Each bar indicates one female and on male, respectively (n=2). Hp1bp3 mRNA was used as endogenous control. (All data are presented as mean \pm SEM)

3.1.3 Spatially and temporally activated RNAi of Sirt2 in mice by the hybrid Pol

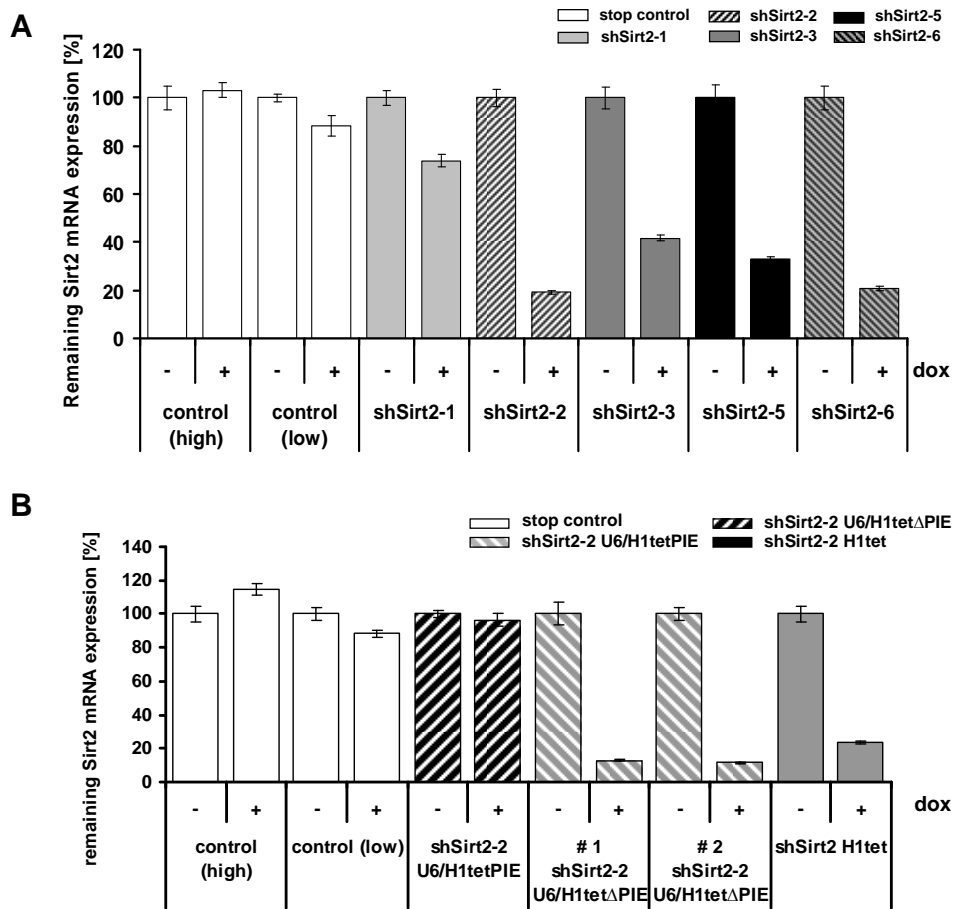
III system

To characterize the efficiency of the Pol III U6/H1tet system for silencing of an endogenous mouse target gene, Sirt2 was used for further knockdown studies. Altogether, five shRNAs were designed with an algorithm program used for the prediction of the shRNA functionality. After analyzing knockdown efficiency with the standard inducible H1-tet system in ES cells, two shRNAs (shSirt2-2 and shSirt2-6) with the highest RNAi efficiency (>80 %) were chosen for further studies (Figure 7A).

The U6/H1tet hybrid configuration containing shSirt2-2 as well as controls constructs were integrated into the *rosa26* locus of mouse ES cells by RMCE technology and validated subsequently. The knockdown of Sirt2 was investigated *in vitro* by quantitative realtime PCR (Figure 7B). Only after recombination of the floxed PIE element by Cre recombinase and in presence of dox, a knockdown of 80-90% of Sirt2 mRNA could be observed (#clone1 shSirt2-2 U6/H1tet Δ PIE; #clone2 shSirt2-2 U6/H1tet Δ PIE). Importantly, the knockdown efficiency of induced shSirt2-2 U6/H1tet Δ PIE carrying ES cells was comparable to control ES cells, harboring the standard inducible knockdown system (shSirt2-2 H1tet; grey bars). In contrast, no repression could be detected on samples with PIE configuration (black striped bars). To exclude that the confluence of the ES cells has an effect on Sirt2 mRNA expression levels, controls with a RMCE construct including a poly T stop signal instead of a shRNA (poly T control) were cultivated with high or low density, respectively (black bars) (Figure 7B).

To translate these findings into an *in vivo* setting, chimeric mice (shSirt2-2 U6/H1tetPIE) were generated and crossed with a cre-deleter line resulting in progeny carrying the activated (shSirt2-2 U6/H1tet Δ PIE) shRNA construct. In parallel, control mice were generated, harboring a tet-inducible shSirt2-2 expression cassette (shSirt2-2 H1tet). Δ PIE animals (shSirt2-2 U6/H1tet Δ PIE), shSirt2-2 H1tet and wildtype control animals (C57BL/6NTac) were induced for 17 days with dox food and tissues were prepared for quantitative realtime PCR analysis, respectively. Compared to Sirt2 expression levels in C57BL/6NTac wildtype animals, a knockdown of ~80-90% could be achieved in heart, kidney and muscle and ~60-75% in liver, EWAT and brain of dox induced shSirt2-2 U6/H1tet Δ PIE mice (grey striped bars) (Figure 7C). In the control group (shSirt2-2 H1tet; grey bars) a consistent repression of 90~95% was noted for all tissues evaluated.

Taken together, these results indicate that *in vivo* knockdown of Sirt2 caused by shSirt2-2 U6/H1tet Δ PIE is 3.6- to 5.4-fold weaker, compared to the shSirt2-2 H1tet system. Therefore, a further analysis of Cre inducible shSirt2-2 expression was not performed.



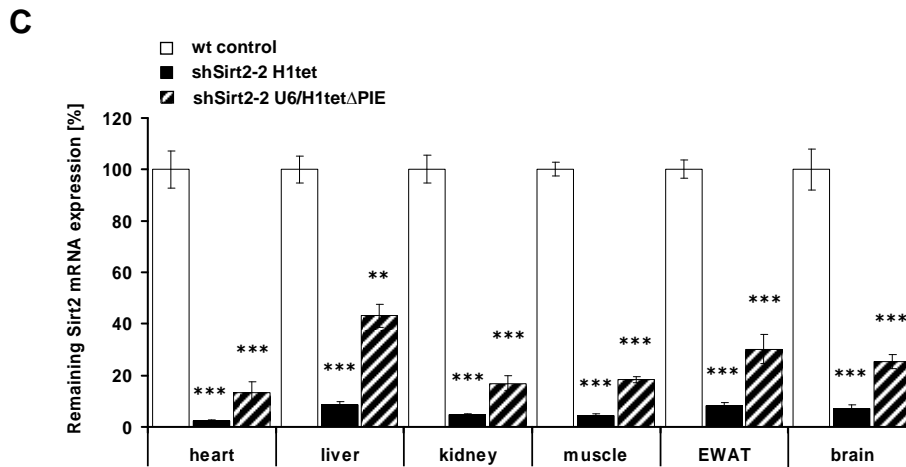


Figure 7: Knockdown level of Sirt2 *in vitro* and *in vivo* using the inducible hybrid H1/U6 system

A) Five shRNAs, shSirt2-1 (grey bars), shSirt2-2 (black striped bars), shSirt2-3 (dark grey bars), shSirt2-5 (black bars) and shSirt2-6 (grey striped bars) against Sirt2, driven by a tet-inducible H1 promoter, were analyzed in ES cells to evaluate their knockdown efficiency. The knockdown level was determined by quantitative realtime PCR analysis of targeted ES cells in presence or absence of dox (1µg/ml, 72h induction; indicated by a minus or plus). The highest Sirt2 knockdown was reached with shSirt2-2 (black striped bars) and shSirt2-6 (grey striped bars). Further experiments are performed with shSirt2-2 whereas shSirt2-6 served as a control to rule out off-target effects. Control cells (white bars) containing a poly T signal were cultivated either with high or low confluence. GAPDH mRNA was used as endogenous control. **B)** Quantitative realtime PCR analysis of targeted ES cells which were induced with or without dox (1µg/ml) for 72h, indicated with plus or minus. Sirt2 mRNA expression level are shown from shSirt2-2 H1/U6-PIE (black striped bars), two ES cell clones of shSirt2-2 H1/U6ΔPIE and shSirt2-2 H1 cells (grey bars). Control cells (white bars) containing a poly T signal were cultivated either with high or low confluence. GAPDH mRNA was used as endogenous control. **C)** Relative mRNA levels (wt control = 100%) of tissues from wt control (white bar), shSirt2-2 H1 (grey bars) and shSirt2-2 H1/U6ΔPIE (striped bars) mice analyzed by quantitative realtime PCR. 12-14 weeks old mice were fed with dox food (1g/kg) for 17days. Hp1bp3 mRNA was used as endogenous control. (All data are presented as mean ± SEM; n=3 males; wt=wildtype, C57BL/6NTac)

3.2 Phenotypical analysis of inducible Sirt2-knockdown mice

In the following experiments, the consequences of inducible Sirt2 silencing were analysed by employing the standard tet-inducible H1 system as depicted in Figure 6A (lower panel).

3.2.1 Knockdown efficiency demonstrated by two individual shRNAs against Sirt2

Inducible and ubiquitous knockdown of Sirt2 was verified on two transgenic mouse lines consisting each of an independent shRNA, shSirt2-2 or shSirt2-6, respectively. Consistently, in both mouse lines, Sirt2 mRNA was significantly reduced to 90-95% after a 14 days induction with dox (1g/kg) (Figure 8A-B). The second transgenic mouse line carrying the

shRNA2-6 has mainly been used to confirm Sirt2 knockdown, excluding off-target effects (Figure 8B).

In the absence of dox, shRNA expression is blocked by the tetR, nonetheless, a small but significant decrease of Sirt2 mRNA was found in the hypothalami of un-induced mice, indicating a low level of spontaneous shRNA expression in this tissue (Figure 8A).

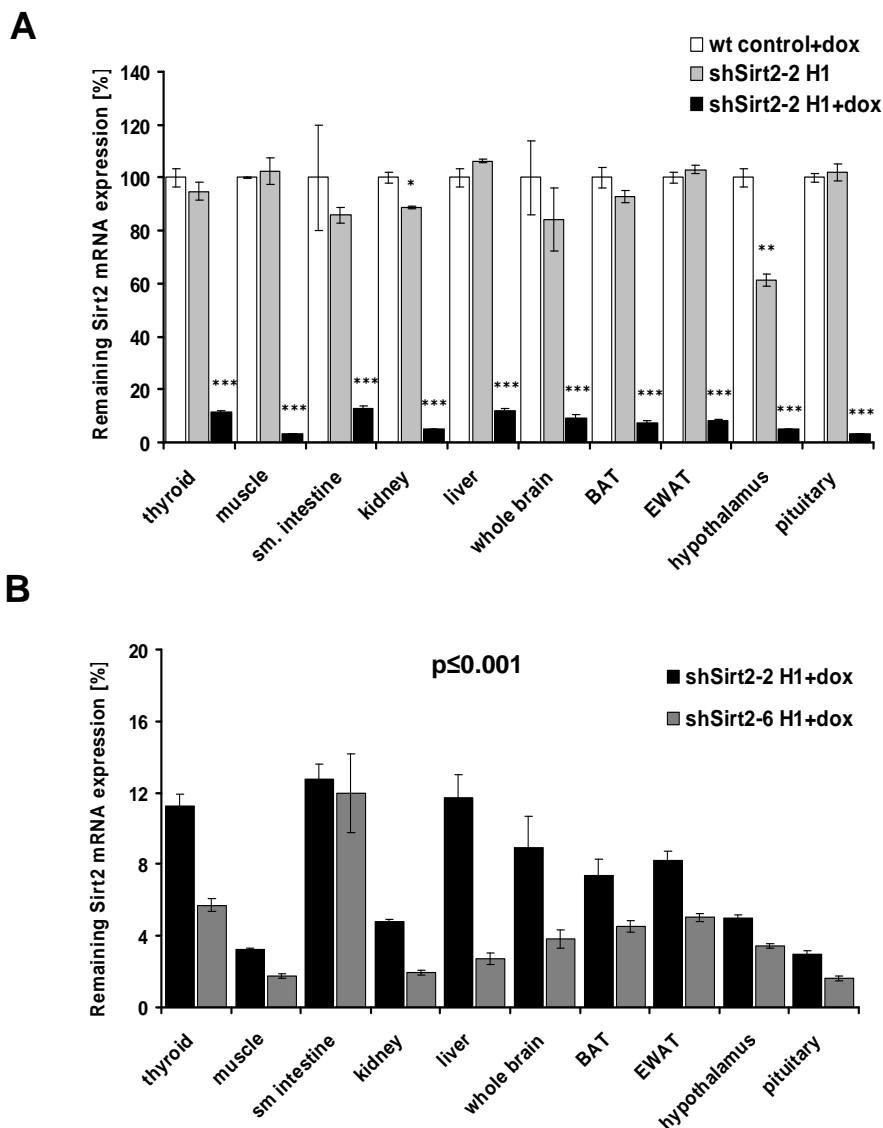


Figure 8: Two specific shRNAs against Sirt2 results each to an efficient Sirt2 knockdown *in vivo*

A) Relative mRNA levels (wt control = 100%) of tissues from wt control+dox (white bar), shSirt2-2 H1 (grey bars) and shSirt2-2 H1+dox (black bars) mice analyzed by quantitative realtime PCR. Four weeks old control and shSirt2-2 transgenic males were fed with dox food (1g/kg) for 14days. Hp1bp3 mRNA was used as endogenous control. **B)** Relative mRNA levels (wt control = 100%, not shown) of tissues from shSirt2-6 H1+dox (grey bars)

in comparison with relative mRNA levels of shSirt2-2 H1+dox animals (black bars) dedicated in A) to confirm Sirt2 knockdown. 8-14 weeks old control and shSirt2-6 transgenic females were fed with dox food (1g/kg) for 14days. Hp1bp3 mRNA was used as endogenous control. (All data are presented as mean \pm SEM; n=3; wt=wildtype, C57BL/6NTac).

To investigate the impact of ubiquitous shRNA mediated silencing of Sirt2 on diet-induced obesity, control mice and inducible Sirt2 knockdown mice were fed either a normal chow (NCD) or were exposed to a high fat diet (HFD) for 14 weeks. In addition, for induction of shRNA mediated transcription, chow diet was supplemented with 1g/kg dox and induction was started on mice at an age of 6 weeks for up to 8 weeks. Again, there was a highly and efficient decrease of 80-95% in Sirt2 mRNA expression regardless of which diet food mice were exposed to (Figure 9A-B). A weak activity of RNAi in animals fed without inductor was noticed for the brain lysate which is in accordance with similar results using tet-inducible H1 configuration (69). To exclude any dox content in the conventional NCD food, a sensitive *in vitro* assay was performed and the presence of dox in mouse-serum was analyzed. These data indicate that all mice were fed correctly with or without the inductor (Figure 9E-F). Moreover, Sirt2 knockdown could also be confirmed on protein level by an immunoblot only in mice transgenic for shSirt2-2 construct and when fed the dox-containing diet (Figure 9C-D).

In summary, regardless of which diet shSirt2-2 transgenic mice were exposed to, a significant and ubiquitous knockdown of Sirt2 has been shown on protein and on mRNA expression level. Moreover these findings could be confirmed by a second shRNA (shSirt2-6) against Sirt2 *in vivo*.

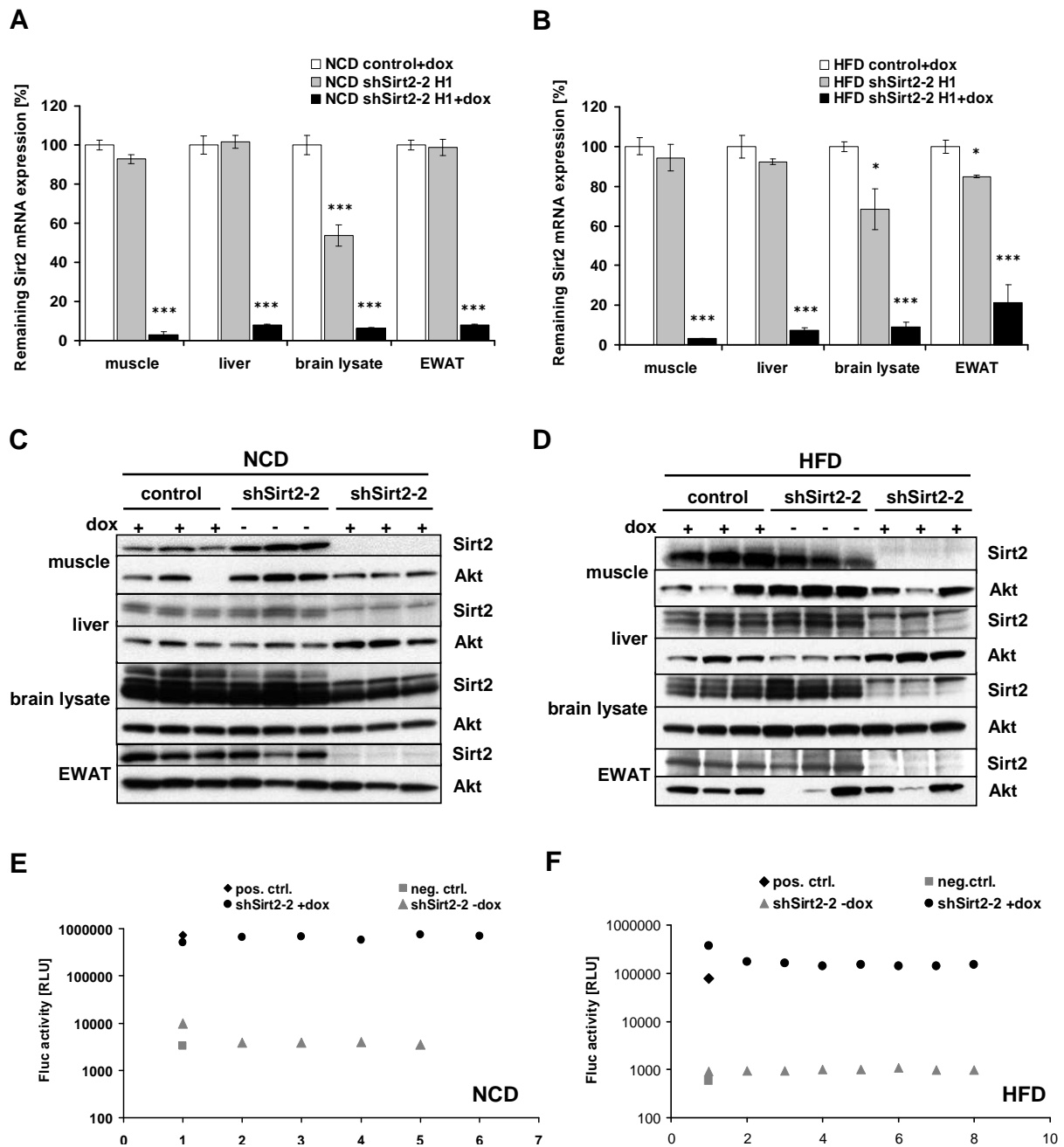


Figure 9: Sirt2 knockdown in mice exposed to a NCD or HFD

A) Expression of Sirt2 mRNA in wt control+dox (n=6; white bar), shSirt2-2 H1 (n=6; grey bars) and shSirt2-2 H1+dox (n=6; black bars) mice as measured by quantitative realtime PCR (wt control = 100%). 14 weeks old mice were fed on a NCD supplemented with dox (1g/kg) for 8 weeks. Hp1bp3 mRNA was used as endogenous control. **B**) Expression of Sirt2 mRNA in wt control+dox (n=3; white bar), shSirt2-2 H1 (n=3; grey bars) and shSirt2-2 H1+dox (n=3; black bars) mice as measured by quantitative realtime PCR (wt control = 100%). 14 weeks old mice were fed on a HFD supplemented with dox food (1g/kg) for 8 weeks. Hp1bp3 mRNA was used as endogenous control. **C, D**) Western blot analysis of Sirt2 and Protein kinase B (Akt) expression (loading control) in muscle, liver, brain lysate and epididional white adipose tissue (EWAT) of wt control and shSirt2-2 transgenic mice fed either on a NCD (n=3 per group; C) or a HFD (n=3 per group; D). **E, F**) Presence of dox in

the serum of un-induced mice transgenic for shSirt2-2 (shSirt2-2-dox) or dox induced mice transgenic for shSirt2-2 (shSirt2-2+dox) fed on NCD(E; n=6 per group) or fed on HFD (F; n=8 per group) supplemented with dox (1g/kg). As control, serum from wildtype animals which were watered with or without dox in drinking water (2mg/ml) was used. The test was performed with ES-cells harboring an inducible reporter gene expression cassette. Only in the presence of dox, high enzymatic activity of the reporter gene *Firefly Luciferase* (Fluc), which is measured in relative light units (RLU), is shown (black filled symbols). In contrast, serum from un-induced animals, have low enzymatic Fluc activity that is comparable to background activity. All data are presented as mean \pm SEM; control=C57BL/6NTac wildtype mice)

3.2.2 The effect of Sirt2 knockdown on energy homeostasis control

Under NCD all groups displayed an indistinguishable body weight growth curve (Figure 10A). Furthermore, although induction with dox was started when mice were 6 weeks, animals with a silencing in Sirt2 did not differ significantly from their respective controls illustrated in Figure 10A. In line with body weight, no differences could be observed in body fat percentage as well (Figure 10B). In the same vein, food intake analysis for one week revealed no differences in food intake of shSirt2-2+dox and control+dox mice fed NCD (Figure 10C). Calorimetric analysis revealed similar oxygen consumption between Sirt2 knockdown and control mice and also fuel preference as determined by respiratory quotient as well as activity was comparable between both groups (Figure 10D-F).

Taken together, induced Sirt2 knockdown mice show no obviously effect in the control of energy homeostasis, when fed on a normal chow diet. Thus, efficient postnatal knockdown of Sirt2 does not affect overall survival and basic metabolism.

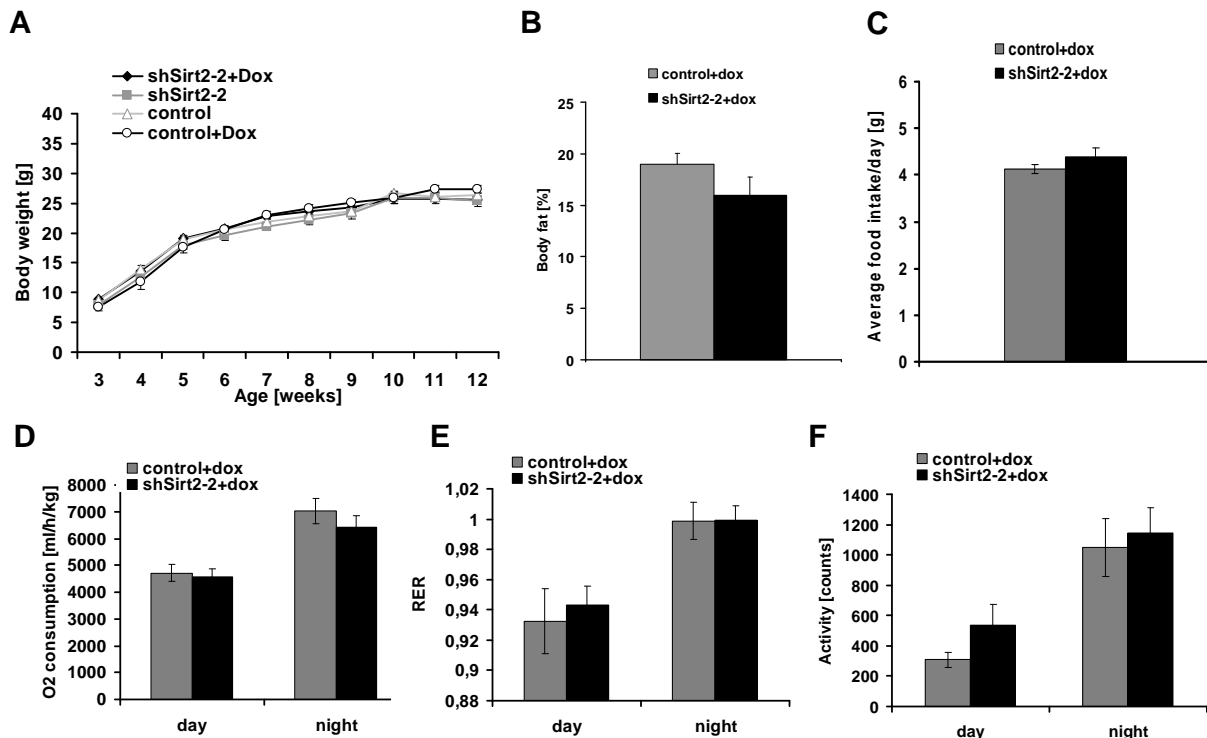


Figure 10: Knockdown of Sirt2 does not affect metabolic control on normal diet

A) Body weight curves of control (triangle, n=7), control+dox (circle, n=7), shSirt2-2 transgene (square, n=6) and shSirt2-2 transgene+dox (diamond, n=6) mice on normal diet. Animals were 6 weeks old before inducer was initiated throughout the term of the experiment. **B)** Body fat percentage of control+dox (n=6) and shSirt2-2 transgene+dox (n=6) animals of 14 weeks old mice fed for 8 weeks on normal diet, supplemented with dox. Data results from nuclear magnetic resonance (NMR) analysis. **C)** Daily food intake of 9 weeks old control+dox (n=7) and shSirt2-2 transgene+dox (n=6) animals fed for 3 weeks on normal diet, supplemented with dox. **D)** Daily and nightly oxygen consumption of 13 weeks old control+dox (n=7) and shSirt2-2 transgene+dox (n=6) animals. Oxygen consumption was calculated per kg lean mass of each individual mouse. **E, F)** Determination of respiratory quotient (RER) and activity at day and night of control+dox (n=7) and shSirt2-2 transgene+dox (n=6) animals fed for 7 weeks on normal diet, supplemented with dox. (All data are presented as mean \pm SEM)

When fed the same time with HFD, mice gained more body weight with an average maximum of approximately 31g after 11 weeks, compared to mice fed on NCD that gained about 26g. While body weight was unchanged between shSirt2-2+dox and control+dox mice, a decrease was observed surprisingly for control shSirt2-2 transgenic mice fed without an inducer (Figure 11A). Body fat content, food intake as well as calorimetric analysis were comparable between Sirt2 knockdown and control animals (Figure 11B-F).

Taken together, a knockdown of Sirt2 resulted in unchanged body weight gain, food intake and body fat composition whereas a lower activity was indicated during the night by trend when fed on a HFD.

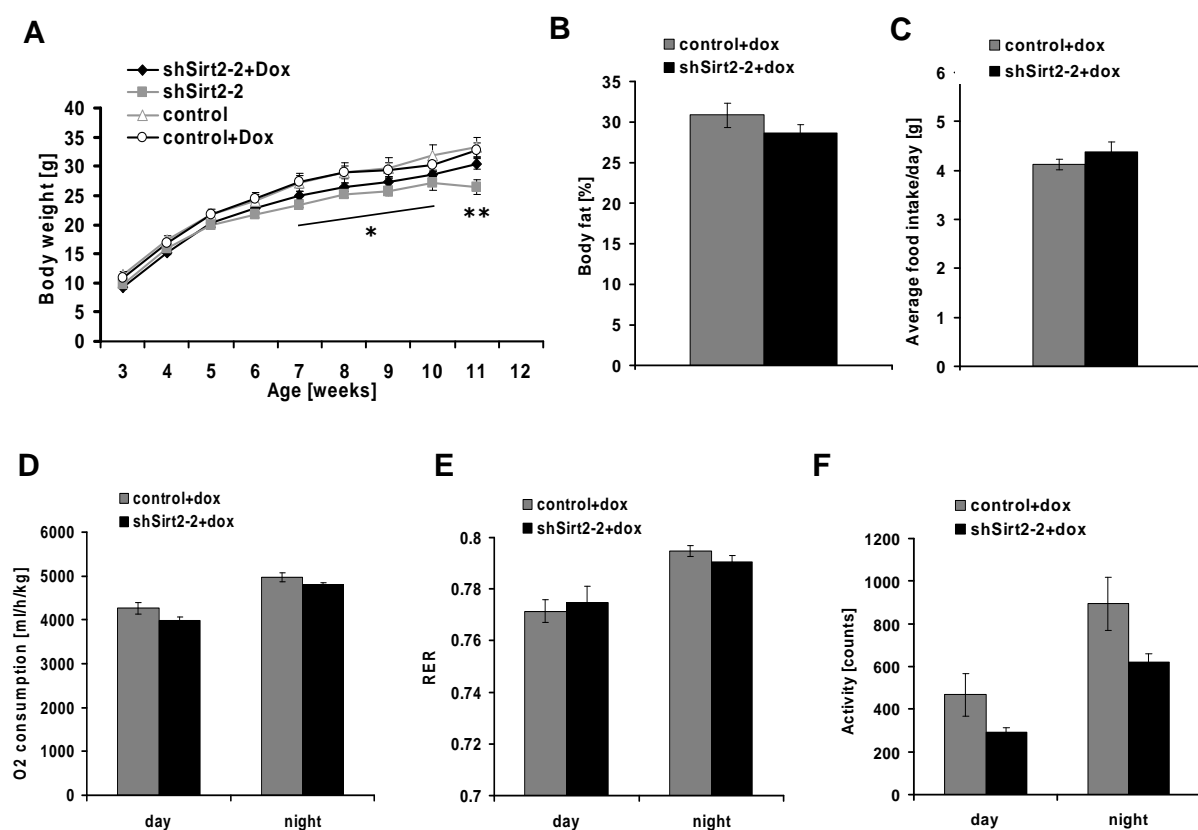


Figure 11: Knockdown of Sirt2 does not affect metabolic control on high fat diet

A) Body weight curves of control (triangle, n=7), control+dox (circle, n=7), shSirt2-2 transgene (square, n=6) and shSirt2-2 transgene+dox (diamond, n=6) mice on HFD. Animals were 6 weeks old before inductor was initiated throughout the term of the experiment. **B)** Body fat percentage of control+dox (n=6) and shSirt2-2 transgene+dox (n=6) animals of 14 weeks old mice fed for 8 weeks on normal diet, supplemented with dox. Data results from nuclear magnetic resonance (NMR) analysis. **C)** Daily food intake of 9 weeks old control+dox (n=7) and shSirt2-2 transgene+dox (n=6) animals fed for 3 weeks on normal diet, supplemented with dox. **D)** Daily and nightly oxygen consumption of 13 weeks old control+dox (n=7) and shSirt2-2 transgene+dox (n=6) animals. Oxygen consumption was calculated per kg lean mass of each individual mouse. **E, F)** Determination of respiratory quotient (RER) and activity at day and night of control+dox (n=7) and shSirt2-2 transgene+dox (n=6) animals fed for 7 weeks on normal diet, supplemented with dox. (All data are presented as mean \pm SEM; shSirt2-2 vs control *, $p \leq 0.05$; **, $p \leq 0.01$)

3.2.3 Effect of Sirt2 knockdown focused on glucose metabolism

To further elucidate whether postnatal knockdown of Sirt2 alter glucose metabolism in mice, blood glucose levels of random fed mice were analyzed. Six days after dox administration, blood glucose was comparable between all groups (Figure 12A). In addition a glucose tolerance test (GTT) was performed of 8 weeks old mice fed on NCD and 2 weeks feeding with the inductor. Mice were fasted for 16h, followed by an intraperitoneal (i.p.)

glucose injection (10 ml of 20% Glucose solution/kg body weight). Subsequently blood glucose levels were determined after 15, 30, 60 and 120 min after injection. Due to the high level of blood glucose after injection, β -cell mediated release of insulin is induced, to force glucose uptake into tissues like muscle and liver. As depicted in Figure 12B, control and Sirt2-knockdown mice obtained a similar increase in blood glucose levels after injection and both groups returned to a similar value after 120 min. Furthermore, to examine insulin sensitivity, an insulin tolerance test (ITT) was performed. Thus, blood glucose concentrations were determined 15, 30 and 60 min after an i.p. injection of insulin (0.75 U/kg BW). However, Sirt2-knockdown mice displayed no significant change in insulin sensitivity compared to their control (Figure 12C).

In summary, there are no alterations in glucose metabolism and insulin sensitivity of Sirt2 knockdown animals compared to control group when fed on NCD.

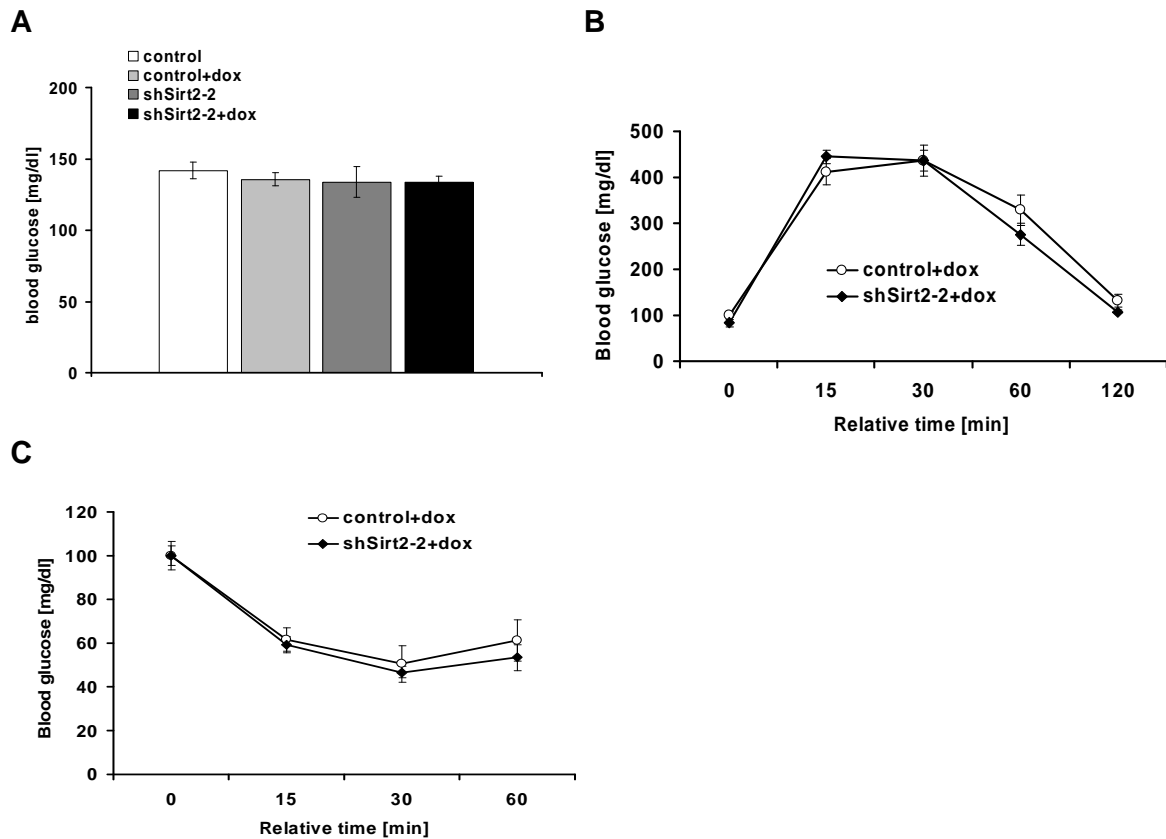


Figure 12: Unchanged glucose metabolism in Sirt2 knockdown mice on normal diet

A) Blood glucose of random fed mice was determined of control (white bar; n=7), control+dox (light grey bar; n=7), shSirt2-2 (dark grey bar; n=6) and shSirt2-2+dox (black bar; n=6) mice at the age of 6 weeks and after dox administration of 6 days on normal diet. **B)** GTT of control+dox (circle) and shSirt2-2+dox (diamond) mice on fasted state at the age of 8 weeks. **C)** ITT of control+dox (circle) and shSirt2-2+dox (diamond) mice with free access to food at the age of 9 weeks. (All data are presented as mean \pm SEM)

Mice with an induced insulin resistance due to their exposure of HFD were subjected to a GTT and ITT. Control+dox and shSirt2-2+dox mice responded similarly to exogenous glucose processing as well as to random blood glucose level (Figure 13A, C). Also during an ITT, no significant alterations were observed, compared to their control group (Figure 13B). In a further approach circulating insulin concentrations were determined from serum of fasted mice at two different time points. As shown in Figure 13D serum insulin concentrations of Sirt2 knockdown animals were comparable to controls at any time point. When measured serum leptin concentrations of fasted mice, no significant differences between both groups could be demonstrated as well (Figure 13E).

Taken together, glucose metabolism was unaffected as well as regulation of energy balance of Sirt2 knockdown mice fed on a HFD.

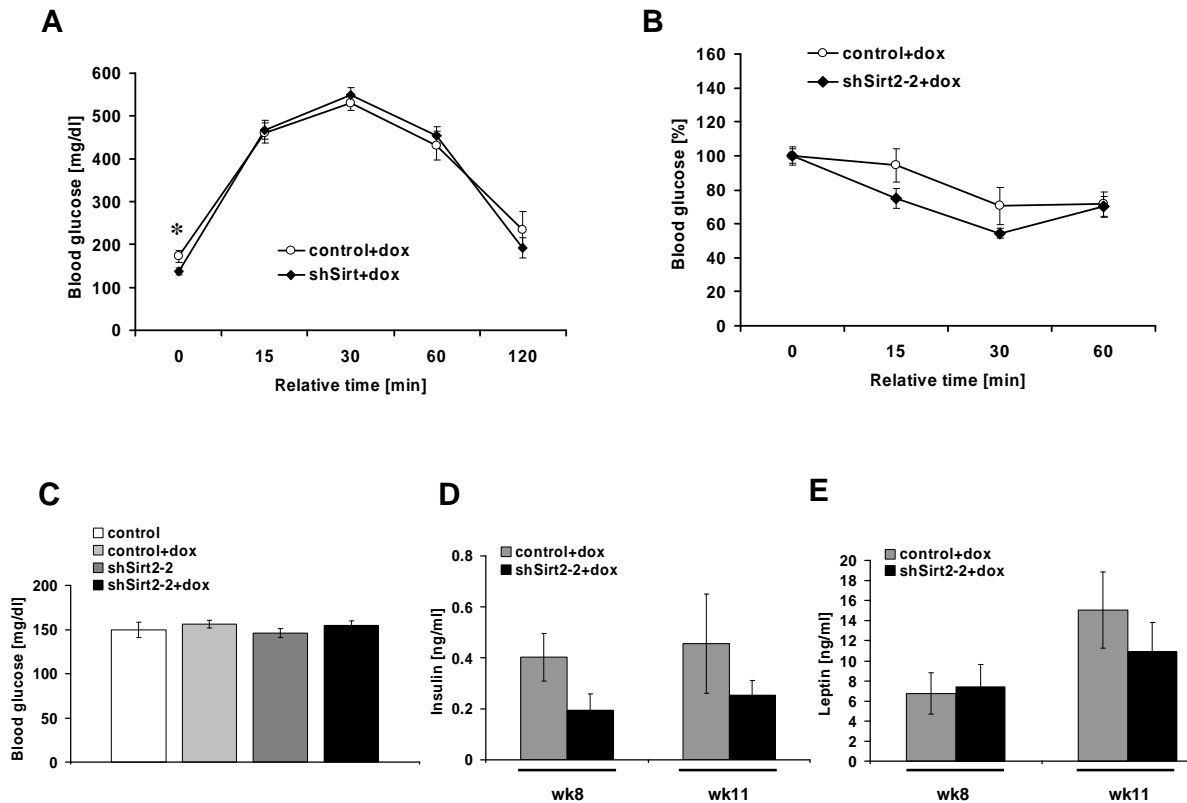


Figure 13: Unchanged glucose metabolism and energy balance in Sirt2 knockdown mice on high fat diet

A) GTT of 8 weeks old control+dox (circle) and shSirt2-2+dox (diamond) mice on fasted state. **B)** ITT of control+dox (circle) and shSirt2-2+dox (diamond) mice with free access to food at the age of 11 weeks. **C)** Blood glucose of random fed mice was determined of control (white bar; n=7), control+dox (light grey bar; n=7), shSirt2-2 (dark grey bar; n=6) and shSirt2-2+dox (black bar; n=6) mice at the age of 6 weeks and after dox administration of 6 days on high fat diet. **D)** Circulating serum insulin concentrations of fasted mice at the age of 8 and 11 weeks. **E)** Circulating leptin concentrations of fasted mice at the age of 8 and 11 weeks. (All data are presented as mean \pm SEM; shSirt2-2+dox vs control+dox *, $p \leq 0.05$)

Additionally, adipocyte size from control and Sirt2 knockdown mice was monitored on either diet. Microscopically analysis revealed no obvious alteration in morphology between both groups (Figure 14A-B). Moreover, when quantified adipocyte size, the mean cell size of mice on normal chow diet or high fat diet reached approximately 1000 μm and 2000 μm ,

respectively, with no significant changes between control mice and Sirt2 knockdown mice (Figure 14C).

In a murine adipose 3T3 cell culture system, Wang and his colleagues reported that Sirt2 knockdown cells had higher expression of markers of adipocyte differentiation, such as PPAR γ compared to controls (132). To determine these findings *in vivo*, PPAR γ mRNA was measured by quantitative realtime PCR in white adipose tissue of wt control mice, shSirt2-2 transgenic mice and shSirt2-2+dox transgenic mice (Figure 14D). The data clearly demonstrate unchanged level of PPAR γ mRNA in Sirt2 knockdown animals on either diet, compared to wt controls.

Taken together, no alteration was observed in adipocyte morphology and size of Sirt2 knockdown mice compared to control group when fed on NCD or HFD. Furthermore, a knockdown of Sirt2 did not lead to higher expressions of the key adipogenic factor PPAR γ *in vivo*.

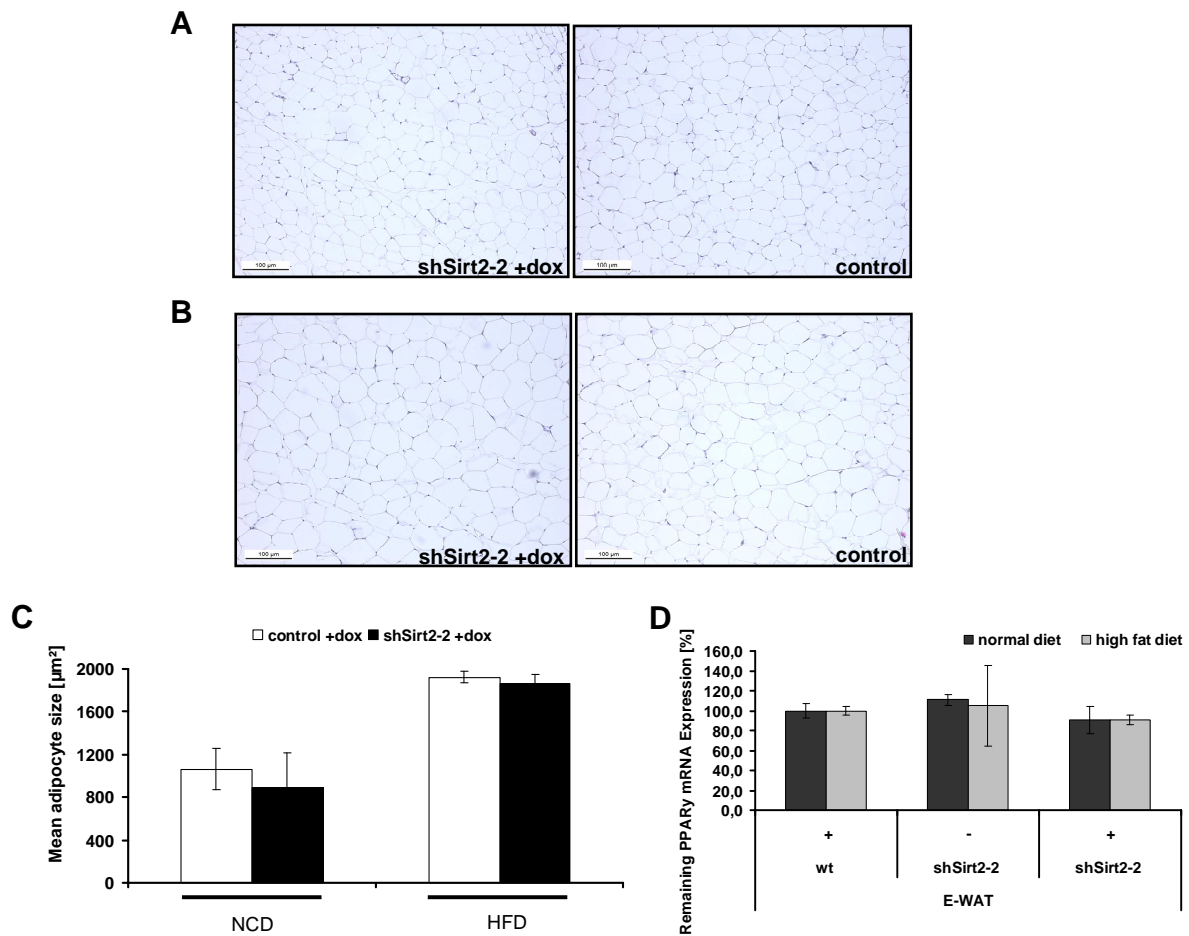


Figure 14: Effect of Sirt2 KD on adipocyte size and PPAR γ mRNA expression in EWAT

A) H&E staining of epigonadal white adipose tissue of 14 weeks old control and Sirt2 knockdown mice on NCD, supplemented with dox. Scale bar: 100 μ m. **B)** H&E staining of epigonadal white adipose tissue of 14 weeks old control and Sirt2 knockdown mice on HFD, supplemented with dox. Scale bar: 100 μ m. **C)** Quantification of mean adipocyte size in epigonadal white adipose tissue of control and Sirt2 knockdown animals on normal chow diet and high fat diet at the age of 14 weeks (n=2 per group). **D)** Expression of PPAR γ mRNA in EWAT of wt control+dox, shSirt2-2 H1 and shSirt2-2 H1+dox mice as measured by quantitative realtime PCR (wt control = 100%). 14 weeks old mice were fed on NCD or HFD. Food that is supplemented with dox (1g/kg) is indicated by a plus, whereas duration of induction was 8 weeks. Hp1bp3 mRNA was used as endogenous control.

Another objective was to check whether Sirt1 expression is changed in Sirt2 knockdown mice, since Sirt1 has been linked to metabolism in mammals. Sirt1 regulates glucose metabolism and cholesterol homeostasis by modulating PGC1 α /PPAR γ and lipid metabolism (170). In pancreatic cells, Sirt1 modulates glucose-stimulated insulin secretion in beta cell (111, 171). Moreover, in adipose tissue, Sirt1 interacts with PPAR γ and aP2 promoters, to inhibit adipogenesis (107). To investigate Sirt1 mRNA expression in mice with a Sirt2

knockdown, different tissues such as liver, muscle and EWAT were analyzed. As dedicated in Figure 15, Sirt1 mRNA expression level is unchanged in Sirt2 knockdown animals compared to wt control mice or shSirt2-2 transgenic mice that were not fed with dox containing food.

Thus, these findings suggest, that Sirt1 has no compensatory function in Sirt2 knockdown mice.

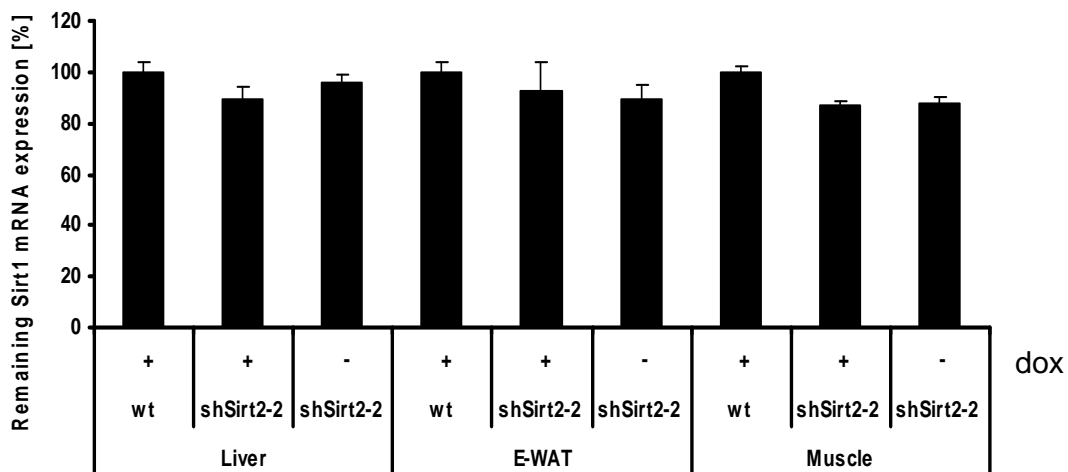


Figure 15: Sirt1 mRNA expression in Sirt2 knockdown animals fed on HFD

Expression of Sirt1 mRNA in liver, EWAT and muscle of wt control+dox, shSirt2-2 H1 and shSirt2-2 H1+dox mice as measured by quantitative realtime PCR (wt control = 100%). 14 weeks old mice were fed on HFD. Food that is supplemented with dox (1g/kg) is indicated by a plus, whereas duration of induction was 8 weeks. Hp1bp3 mRNA was used as endogenous control.

3.2.4 The effect of Sirt2 knockdown during embryogenesis

It has not yet been revealed if Sirt2 plays any essential role during development. To study any potential effect on Sirt2 knockdown during embryonic development, female wildtype controls were given dox-supplemented water for 7 days and then paired with males which were transgenic for shSirt2-2. From this time on, the breedings had access to dox in drinking water as well until one week after offspring's birth. In case of lethal embryonic effect, only wildtype littermates were expected to survive. Subsequently, one week after birth, all littermates were analyzed by PCR genotyping and hepatic Sirt2 knockdown was determined by quantitative realtime PCR. As depicted in Figure 16A, PCR revealed shSirt2-2 transgenic mice. Interestingly, the ratio of wildtype and transgenic littermate was 72% to 28%. Since 50%

wildtypes and 50% transgenic animals are to be expected, these data indicate that there might be an effect of embryonic Sirt2 knockdown on embryonic survival (Figure 16B). Nonetheless, using quantitative realtime PCR analysis, a Sirt2 knockdown of 90% on mRNA level was established for shSirt2-2 transgenic offspring compared to their wildtype littermates, indicating that in surviving transgenic animals, Sirt2 knockdown was successful (Figure 16C).

In conclusion, Sirt2 gene expression was suppressed during embryonic processes, mimicking a conventional knockout. Resulting offspring consist of viable wildtype as well transgenic mice with a rate that is shifted to wildtype littermates, indicating a possible role of Sirt2 on embryonic survival.

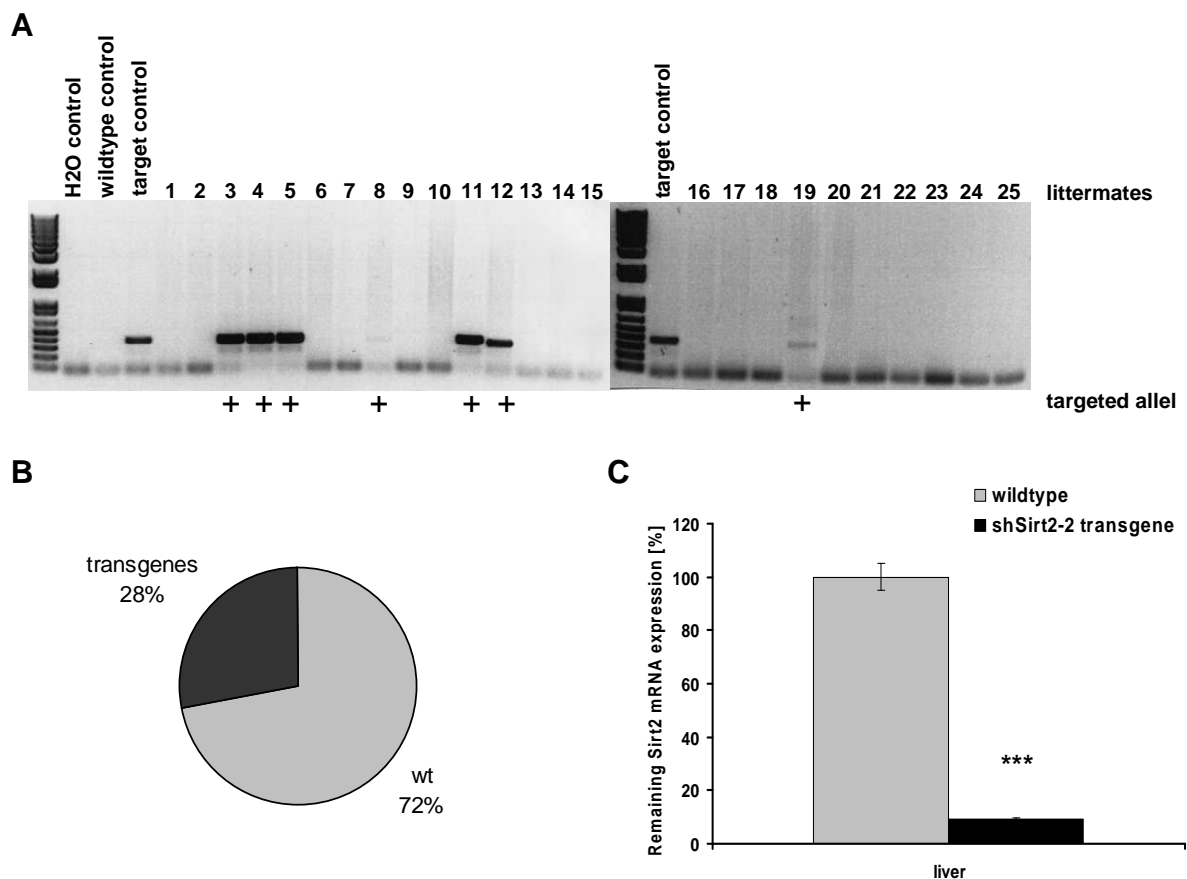


Figure 16: Possible role of Sirt2 in regulatory networks controlling embryonic processes

A) Genotyping PCR of 7 days old littermates with respective controls: H₂O control, wildtype control and a targeted control. The signal for targeted animals (No3, 4, 5, 8, 19) results in a ~365bp band indicated by a plus, whereas no signals are shown for wildtype and H₂O control. **B)** Distribution of wildtype and shSirt2-2 transgenic animals. In a total of 25 offspring, 18 mice were wildtype and 7 mice comprise the targeted allele. **C)** Quantitative

realtime PCR analysis of Sirt2mRNA from liver of 7 days old wildtype mice (grey bar; n=4) and shSirt2-2 transgenic mice (black bar; n=4). (All data are presented as mean \pm SEM; shSirt2-2+dox vs control+dox ***, $p \leq 0.001$)

3.2.5 The effect of Sirt2 knockdown in neurodegenerative disease

Parkinson Disease (PD) is characterized by the development of α -synuclein containing inclusions (termed Lewy bodies) and a loss of dopaminergic neurons in the substantia nigra (172), which is accompanied by muscle rigidity, bradykinesia, resting tremor and postural instability, eventually leading to death. Dopaminergic neurons are necessary for tasks specific to the brain regions that they innervate, including motor behavior, motivation and working memory (173) and reside mainly in the zona compacta of the substantia nigra (SNc) and ventral tegmental area (VTA) (174). A recent study demonstrated that Sirt2 inhibition by siRNAs prevented α -synuclein cytotoxicity and modified inclusion morphology in cellular models of PD. In addition, Sirt2 inhibitors were found to ameliorate dopaminergic cell death *in vitro* and in a *Drosophila* model of Parkinson's disease (141).

To study the role for SIRT2 in the control of neuronal metabolism in a mouse model of PD *in vivo*, Sirt2 transgenic and control mice were treated either with 1-methyl-4-phenyl-1,2,3,6-tetrahydropyridine (MPTP), a neurotoxin that causes permanent symptoms of Parkinson's disease by destroying dopaminergic neurons in the substantia nigra of the brain, or alternatively with saline. MPTP (20 mg/kg) was administered i.p. four times in one day at 2 hours intervals. Mice used as controls received an equivalent volume of saline (0.9%). To study motor disability, a Rotarod test was performed on control and shSirt2-2 transgenic mice one week before and one week upon treatment with MPTP or saline, respectively (Figure 17A-B). In this experiment mice are placed on an accelerating rotating rod, whereas the length of time that animals stay on the rod was monitored. The data shown in Figure 17B derived from the Rotarod performance one week after MPTP or saline treatment, while the first run on the Rotarod served for training and adaptation to the system. The control (wt) mice treated with MPTP seemed to stay shorter on the rod, indicating locomotor impairment, compared to control animals treated with saline. Data from Rotarod performances of Sirt2 knockdown mice treated with MPTP suggest a possible rescue effect for these mice since the time on the rod was similar to Sirt2 knockdown mice treated with saline. However, although not significantly, dox induced transgenic animals treated with saline seemed to stay generally shorter on the rod,

compared to wt controls treated with saline, which can likely to be misled (Figure 17B). Thus, from these results it is not yet clear, if Sirt2 knockdown mice injected with MPTP have a rescue effect, although they do not differ much from Sirt2 knockdown animals treated with saline, concerning the time on the rod. However, Rotarod performances done one week before application of MPTP or saline indicate no differences in behaviour and any impairment of Sirt2 knockdown mice at the beginning of the experiment (Figure 17A).

In addition, the knockdown of Sirt2 mRNA was measured *in vivo* by quantitative realtime PCR, from different sections of the brain tissue, such as ventral tegmental area (VTA), hypothalamus (Ht), caudate putamen (Cpu), nucleus accumbens (NaC) and frontal association cortex (Fra). A strong decrease in Sirt2 mRNA could be observed for induced mice transgenic for shSirt2-2, demonstrated for MPTP or saline treated animals (Figure 17C-D).

Taken together, with these experiments it was not possible to clarify if a Sirt2 knockdown in mouse models of PD prevents from neuronal cell death.

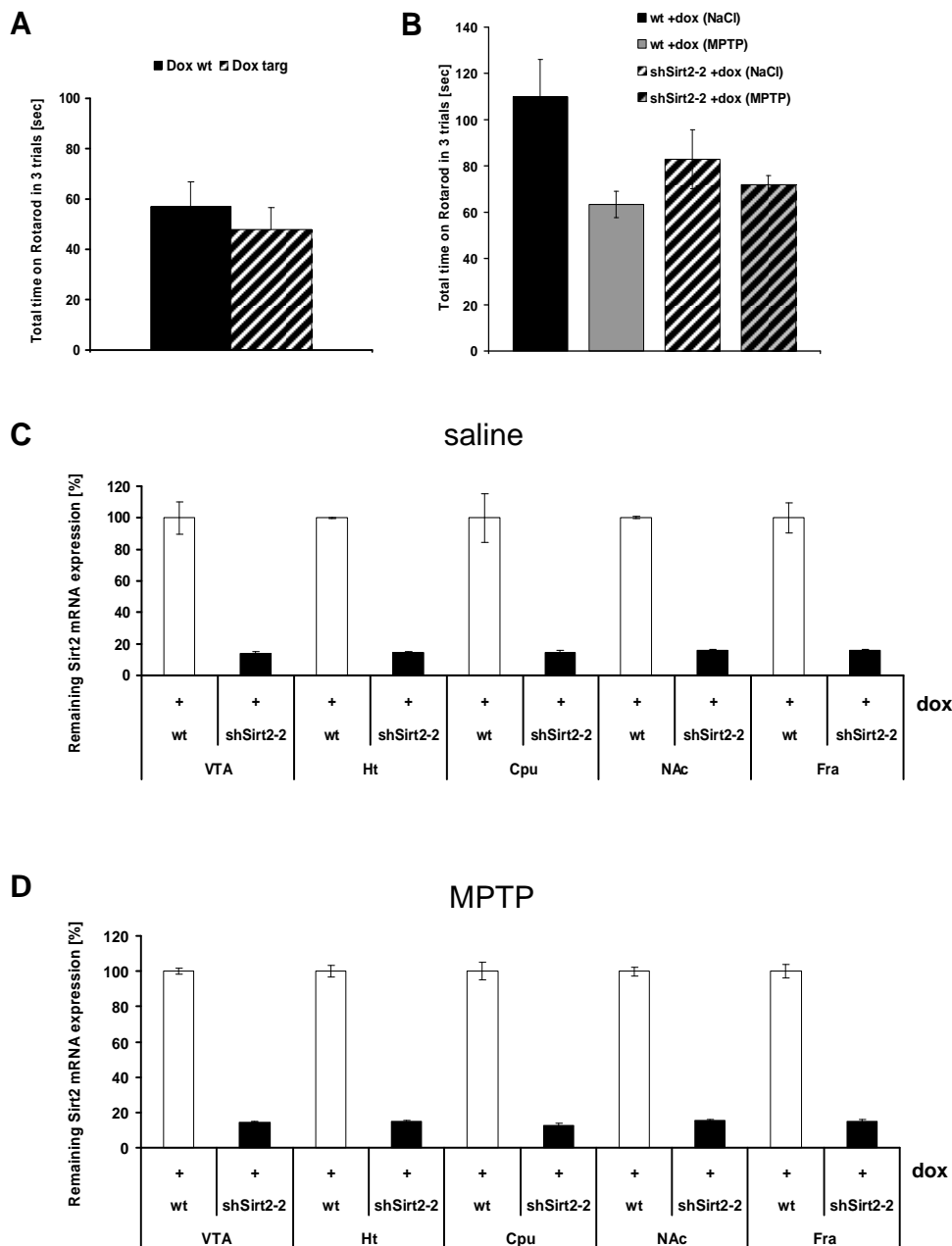


Figure 17: Rotarod analysis and knockdown efficiency of Sirt2 knockdown and wt control mice treated either with MPTP or saline

A) Rotarod analysis of Sirt2 knockdown and control mice. Total time of Sirt2 knockdown (striped bar; n=10) and control mice (black bar; n=9) staying on the rod until mice fell from the Rotarod was measured. **B)** Rotarod analysis of 22 weeks old Sirt2 knockdown and control mice one week after treatment with MPTP or saline. (wt+dox NaCl, n=5; wt+dox MPTP, n=3; shSirt2-2+dox NaCl, n=4; shSirt2-2+dox MPTP, n=3). **C, D)** Expression of Sirt2 mRNA was measured one week after treatment with saline (C) or MPTP (D) in different sections of brain tissue by quantitative realtime PCR. 22 weeks old shSirt2-2 transgenic mice and control mice were fed with NCD supplemented with dox (1g/kg) for 14 weeks (n=3 per group). VTA=ventral tegmental area; Ht=hypothalamus; CPU=caudate-putamen; NAc=nucleus accumbens; Fra=frontal association cortex

4 Discussion

During the course of this work a new system was developed to allow spatial and temporal control of gene expression by RNA interference. Therefore a dox inducible shRNA expression system was combined with a conditional Cre/loxP configuration. Analysis in mouse ES cells displayed equal levels of gene silencing compared with the standard inducible H1-tet promoter. Surprisingly, analysis of mice carrying the temporal and spatial controllable system showed a lower degree of gene silencing than mice carrying the standard inducible H1-tet promoter. Thus, this system is only suited to a limited extent for analysis of gene function *in vivo*.

4.1 Spatially and temporally controlled RNAi

Recently a H1 promoter based inducible tet-repressor system (H1-tet) has been described for ubiquitously gene silencing (69). Therefore this system was used for temporal control and combined with the Cre loxP technology to achieve spatial regulation. Various H1 promoter configurations were developed in which the promoter activity is interrupted by a loxP sites flanked stuffer sequence, called promoter inhibitory element (PIE). Recombination between the two loxP sequences through a Cre recombinase results in a deletion of PIE and a restore of the promoter activity followed by shRNA mediated gene silencing. However, the success of this approach is contingent on: i) that the promoter inhibitory element disrupts promoter action; and ii) that the presence of the remaining loxP site does not compromise promoter activity.

As the latter requirement seems to be the pivotal factor in this system, a screen was performed in mouse ES cells after the Cre recombination mediated event. Experiments revealed a deficit in promoter activity for all conformations with a modification within the H1 promoter, demonstrated by strongly reduced shRNA expression levels (Figure 5). Since the H1 promoter exhibits an extremely compact structure, this decline in promoter activity is possibly due to the residual loxP site. Myslinski and colleagues have demonstrated that sequence substitution in the region between the PSE and the TATA motif of the H1 promoter resulted in a significant reduction in RNA synthesis, both *in vitro* and *in vivo* (175). These findings are in line with our results (constructs 1, 2 and 4; Figure 4), indicating critical spacing within this

region. Although the distance between DSE and PSE was unaltered in construct 3, shRNA expression was reduced, arguing for conserved sequences between these elements. In the same line, other positions between DSE/PSE and between DSE submotifs led to an inactivation of the promoter, indicated in the results of construct 6 and 7 (Figure 5).

Altogether, each approach that included a modification of the H1 promoter resulted in promoter repression and in strongly reduced shRNA expression. Based on this data, the H1 promoter is not compatible with integration of a single loxP site.

As an alternative strategy, elements from the U6 promoter (DSE and 150bp spacing region) and the H1-tet promoter (PSE, TATA motif) were combined in which promoter sequences of the U6 spacing region were replaced by a single loxP site. Despite of the remaining loxP site, only this approach reached a shLacZ expression level comparable to the unaltered H1-tet system, as depicted in Figure 5. In contrast, shLacZ expression was not found in the presence of PIE, implementing successful interruption of the promoter activity of construct 5 (Figure 5). These findings are in line with the results of McMahon et al., who studied three regions between the PSE and DSE in the U6 promoter for optimal loxP placements by replacing promoter sequences, and no disturbance of the U6 promoter activity was found *in vitro* and *in vivo* (68). Taken together, these findings show that the U6 promoter is more compatible and suited for modifications. In combination with promoter elements of H1, a system was developed that fulfilled the criteria for promoter repression by PIE and allowed for reactivation of promoter activity after Cre mediated recombination in mouse ES cells.

To corroborate these results *in vivo*, mice were generated carrying the U6/H1-tet promoter system that is conjugated with a tet-repressor expression cassette, allowing for inducible RNAi. The U6/H1-tet configuration was explored in two mouse lines using shRNAs against the target genes LacZ or Sirt2, respectively. To study knockdown levels in all tissues after PIE deletion, these mice were further crossed with a Cre-deleter strain. Gene silencing progressed after addition of the inducer doxycycline.

Surprisingly, the knockdown level *in vivo* using the U6/H1-tet system were about 3-6 fold weaker, analyzed for both, shLacZ and shSirt2-2 carrying transgenic animals, compared to the knockdown level resulted by the commonly used inducible H1-tet promoter system. Note that the standard H1-tet promoter contains no loxP site. Incomplete recombination could result

in inefficient promoter activation followed by decreased gene silencing. The promoter inhibitory element represents the fluorescence marker gene Zsgreen that is under control of the ubiquitin promoter. To rule out incomplete recombination, mRNA levels of Zsgreen were determined of mice before and after Cre recombination. No Zsgreen mRNA was detected after Cre recombination, confirming a complete removal of PIE (Figure 6).

In conclusion, the U6/H1-tet system yields acceptable knockdown levels for Sirt2 indicating that this approach can be applied for highly efficient shRNAs. On the other hand, high and efficient gene silencing is restricted to a selection of tissues, limiting this system to use in these.

4.2. Phenotypical analysis of Sirt2 knockdown in mice

The founding member of the sirtuins, the Sir2 protein (silent information regulator 2) from the budding yeast *Saccharomyces cerevisiae*, is an NAD-dependent deacetylase that connects metabolism with longevity in yeast, worms and flies (80-82, 176). In mammals, Sir2 is represented by seven homologues, termed Sirt1 through Sirt7 (177). In addition of histones, also non-histone proteins are found to be deacetylated by sirtuins (98, 178, 179). Sirt1 is the most studied member of the sirtuin family that has been linked with metabolic control, modulating downstream biological processes by deacetylating specific transcription factors, co-repressors, and co-activators, including p53, PGC- α , NF- κ B, MyoD, PPAR γ and members of the FoxO family (105, 107, 115, 117, 180). The three sirtuins, Sirt3, Sirt4, and 5 are predominantly localized in the mitochondria (79, 99, 100). There is growing evidence linking mitochondrial sirtuins with regulating energy usage and human lifespan (148, 181), since mitochondrial dysfunction is also associated with mammalian aging and diseases, including diabetes, neurodegenerative diseases, and cancer (182). The functions of Sirt 4-7 are less known. It has been shown that Sirt6 may also be involved in aging in mice, while Sirt7 appear to regulate DNA pol I transcription (154, 156, 183).

In contrast to other sirtuins, Sirt2 protein is mainly distributed throughout the cytoplasm while only a minor fraction is located in the nucleus (102, 126, 184). Sirt2 is able to deacetylate α -tubulin that is required for normal mitotic repression (101, 124) and that controls mitotic checkpoint functions in early metaphase to prevent chromosomal instability (123, 127).

A metabolic regulation function of Sirt2 was postulated since inhibition of Sirt2 resulted in suppression of adipocyte differentiation (131, 132). A previous study reported an up-regulation of Sirt2 expression in adipose tissue by fasting (130, 132). Elevated Sirt2 expression was observed in kidney and adipose tissue when mice were dietary restricted for 18 month (130) but also by shorter-term nutrient deprivation in the form of 24 h fasting (132). Sirt2 was also described as an oligodendroglial cytoplasmic protein, localized to the outer and juxtanodal loops of the myelin sheath (134, 135). In the central nervous system the deacetylation activity of Sirt2 may appear detrimental to neuronal health. For example, SIRT2 may oppose resistance to axonal degeneration and inhibition of SIRT2 rescued α -synuclein toxicity and protected against dopaminergic cell death both *in vitro* and in a *Drosophila* model of Parkinson's disease (136, 141).

Since most functional roles for Sirt2 were studied in cellular systems, these purported roles of Sirt2 remain to be confirmed *in vivo*. In this work the effect of Sirt2 knockdown in mice was studied with the focus on glucose and energy homeostasis, developmental regulation and neurodegenerative disease.

4.2.2 The role of Sirt2 knockdown during embryogenesis

To elucidate the role of Sirt2 in regulatory networks controlling embryonic processes, Sirt2 was downregulated during gametogenesis and embryogenesis thereby mimicking a constitutive Sirt2 knockout. For this purpose a knockdown of shSirt2-2 transgenic males was initiated at mating start with wildtype females by the inducer doxycycline that was supplemented into the drinking water. A Sirt2 knockdown in early processes of embryogenesis is feasible, since it was demonstrated in rodents that dox passes the placenta of pregnant females and is also excreted into breast milk (185, 186). Data from genotyping showed that also animals carrying the shSirt2-2 allele were present among the viable offspring, but their proportion was about half what was expected. In addition, when measuring Sirt2 mRNA levels in the liver of these transgenic littermates, a strong reduction could be confirmed. However, lower levels of Sirt2 protein do not seem to induce embryonic lethality. Although offspring from most of the other sirtuin knockouts are viable, Sirt1 knockout mice experienced embryonic lethal in inbred strain backgrounds (e.g. Reference (187), or if survived in an

outbred background strain, they died in the perinatal period, exhibiting growth retardation and developmental defects in various tissues including eye, lung, pancreas, heart, and reproductive system (188, 189). In addition, Sirt6 knockout mice are born normally, but display early postnatal onset of growth retardation and failure to thrive, with a maximal lifespan of 24 days (154). In an expression profile of Sirt genes in human organs, expression levels of Sirt2 were higher in adult brain compared to fetal brain, possibly indicating a less important role in developmental processes (145). Moreover, in unpublished observations reported in Vaquero et al., Sirt2 knockout mice were described inconspicuously (125). On the other hand it was demonstrated that Sirt2 interacts with HOXA10, an evolutionarily conserved homeobox transcription factor important for cell-type determination during embryogenesis (190).

In conclusion, a Sirt2 knockdown during embryogenesis apparently has no impact in developmental processes. However, it remains to be determined whether Sirt2 knockdown animals show developmental defects in the perinatal period and if further studies confirm a proportion more shifted to wildtype littermates than transgenic animals as it was observed in this work.

4.2.2 The effect of Sirt2 knockdown on glucose and energy homeostasis

A growing interest of the sirtuin research involves the regulation of metabolism. Maintenance of energy homeostasis requires a coordinated regulation of energy intake, storage, and expenditure. Abnormal metabolic homeostasis can have severe consequences and often manifests as syndromes such as obesity and type II diabetes mellitus. Moreover, signs of metabolic imbalance, such as insulin resistance, are observed with increasing frequency during aging. The identification of central pathways that regulate metabolic homeostasis is an area of intense sirtuin research and has important implications for understanding molecular networks and for treating metabolic diseases.

In the present work, metabolic characteristics of dox induced Sirt2 knockdown mice were examined fed either a normal diet or a high fat diet and compared to their respective controls (wildtype animals fed with the inductor dox, wildtype animals and shSirt2-2 transgenic animals fed without inductor). The course of body weight gain of Sirt2 knockdown animals increased similarly to those of controls when started with dox induction. Also body fat

content of Sirt2 knockdown animals was comparable to their controls. These results were in line with data from food intake and indirect calorimetric measurements displaying no significant alteration, indicating no distinct effects in energy absorption as well as expenditure, regardless whether mice were fed on a normal or a high fat diet. Nonetheless, the knockdown of Sirt2, evaluated for various tissues was high and reached levels of about 80-90%. Western Blot analysis confirmed the strong reduction of Sirt2 protein.

Adipose tissue is a critical regulator of metabolism, being the major storage for lipids, while also regulating systemic metabolism through the release of lipids and hormones such as leptin (191, 192). Without a change in energy balance an increase in adipogenesis would result in smaller fat cells with no change in total adiposity and a reduction in adipocyte number would result in larger fat cells, but not less total adipose mass (193). In the study of Jing et al., it was demonstrated on a murine adipose 3T3 cell culture system that a knockdown of Sirt2 promotes adipogenesis, whereas overexpression leads to an opposite effect (131). Hence, white adipose tissue was investigated microscopically for changes in morphology and notably, the adipocyte size was indistinguishable between Sirt2 knockdown mice and controls, indicating that 90% knockdown of Sirt2 does not affect adipogenesis.

Another sirtuin, Sirt1, also plays a role in fat metabolism. Activation of Sirt1 in mice through fasting or resveratrol treatment, results in a reduction of white adipose tissue, a decrease in fat storage and smaller adipocytes (107, 194) whereas inhibition of Sirt1 significantly increases fat mass (195). The idea emerged that Sirt1 activity may influence the effect of Sirt2 knockdown in adipocyte differentiation.

However, Jing et al. reported elevated acetylation levels of FoxO1 in 3T3-L1 adipocytes with a Sirt2 knockdown. This effect was specifically attributed to the knockdown of Sirt2 and independent from changes in Sirt1 or FoxO1 expression. He further demonstrated in co-immunoprecipitation experiments a direct interaction of Sirt2 with FoxO1 (131), notably Sirt1 was also shown to be able to deacetylate FoxO1 (116, 180, 196). Moreover, Sirt2 expression was found to be more abundant in white adipose tissue than Sirt1, thus Sirt2 is more likely to play a major role in this regard (131). To rule out any influence of Sirt1 in adipocyte differentiation in this work, Sirt1 mRNA levels were measured in liver, white adipose tissue and muscle of Sirt2 knockdown mice. The data indicated no altered expression level of Sirt1 in Sirt2 knockdown mice compared to wildtype controls, irrespective of diet.

Increased acetylation of FoxO1 through a Sirt2 knockdown in adipocytes was associated with a decrease of FoxO1's repressive interaction with PPAR γ (131, 132). Furthermore, mRNA level of PPAR γ , a transcription factor central to adipogenic differentiation was found to be increased in Sirt2 knockdown cells (131). Nonetheless, no differential expression in PPAR γ mRNA level was observed by Sirt2 knockdown *in vivo*.

It was noted that Sirt2 knockdown has no apparent influence on the regulation of blood glucose, serum leptin and insulin concentrations.

Taken together, Sirt2 knockdown does not affect glucose or lipid metabolism *in vivo*. Effects reported in a cellular model of 3T3-L1 adipocytes with Sirt2 knockdown, could not be confirmed *in vivo* as well as regulatory modifications of Sirt2 downstream targets. Although knockdown efficiency yielded ~90%, it appears possible that the knockdown of Sirt2 was not sufficient to alter cellular function, i.e. the residual 10% of Sirt2 protein are able to adequate for its cellular functions. It appears likely that the loss of a single sirtuin might be compensated for redundant functions conferred by remaining sirtuin family members, although an increase of Sirt1 mRNA expression was not observed in this work. Furthermore, functional redundancy between sirtuins may account for the failure to confirm the physiological importance of sirtuin mediated deacetylation events. Another possibility, although less likely, is that Sirt2 was not activated under the conditions studied, suggesting a lesser role in normal physiology for Sirt2.

4.2.3 Effect of Sirt2 knockdown in a mouse model of Parkinson Disease

Parkinson's disease (PD) is one of the most common progressive neurodegenerative disorders, affecting about 2% of people over 65 years old and 4–5% of people over 85. PD is characterized by a loss of dopaminergic neurons in the substantia nigra, which is accompanied by muscle rigidity, bradykinesia, resting tremor and postural instability (106). By now, the role of sirtuins in neuroprotection is not entirely clear. Sirt2 expression was found strongest among all sirtuins in brain (128, 133). In neurons, Sirt2 is rather uniformly expressed in all neurites and their growth cones (128). Unlike SIRT2, SIRT1 is localized exclusively in neurons (93, 197-200). Moreover, Sirt2 was established as an inhibitor of oligodendroglial differentiation/aging through deacetylation of the microtubule cytoskeleton and in some instances the effect of Sirt2 appears to be detrimental to neuronal health. Pharmacological and

genetic inhibition of Sirt2 has been shown to protect against α -synuclein toxicity in cultured neurons and in *Drosophila* suggesting that Sirt2 is involved in promoting neurodegeneration (141).

In this work, the effect of Sirt2 knockdown was analyzed during a progressive loss of dopaminergic neurons, induced by the neurotoxin 1-methyl-4-phenyl-1,2,3,6-tetrahydropyridine (MPTP) that provides one of the most valuable approaches to analyze critical aspects of PD in the animal model. Dopaminergic neurons are presented within in the vertebrate central nervous system (CNS) with the largest assembly in the midbrain. There, dopamine containing neurons are separated into functionally distinct subgroups called the substantia nigra pars compacta (SNc) and the ventral tegmental area (VTA) based on their position within the midbrain (201). These dopaminergic circuits are involved in the control of voluntary movement and in emotion based behavior (173). The Rotarod is a widely used motor performance test to evaluate MPTP models (202-206). There are three MPTP protocols widely used. The acute protocol generally involves 4 injections in one day at 2 h intervals. Depending on the doses given, striatal dopamine depletion can range from 40% (14 mg/kg x 4) to approximately 90% (20 mg/kg x 4) (207). Subacute administration is a once daily injection (30 mg/kg) for five consecutive days. This regime causes apoptosis and depletes striatal dopamine by 40-50 % (207, 208). The chronic regime (25 mg/kg MPTP plus probenecid) is over 5 weeks at 3.5-day intervals and striatal dopamine levels are reduced by 90–93% within a week, and by 70–80% of the total at 3 to 24 weeks after MPTP/probenecid treatment days (209, 210).

However, in this work, using the acute protocol with four doses MPTP (20 mg/kg) in one day, a rescue effect from neuronal cell death through a knockdown of Sirt2 could not be derived from Rotarod data. Although the duration time on the rod was similar between Sirt2 knockdown mice after MPTP or saline treatment, the time on the rod differs between Sirt2 knockdown animals and wildtype control mice, handled with the placebo. Moreover, this effect was not observed on the Rotarod performance one week before injection. It is possible that the time necessary to kill dopaminergic neurons may not have been reached in acutely MPTP treated mice. This hypothesis may be unlikely given that MPTP-induced neuronal loss reaches a maximum 3 days after MPTP intoxication and is nil 7 days after intoxication (211-213). Another aspect might be compensatory mechanisms developing in the nigrostriatal pathway.

This concept can be supported by the increased ratio of dopamine metabolites to dopamine, an index of dopamine turnover seen in the striatum of acute MPTP treated mice, and the absence of motor deficit, reported by Rousselet and colleagues (214). In addition, there are other tests such as grid or pole, using skilled forepaw, or measures of sensorimotor function (forepaw placement) that are postulated to provide the most sensitive detection of dopamine loss for MPTP models, even close to the time of lesion and month later (215).

5 Summary

Within the past eight years, RNA interference (RNAi) has emerged as a powerful experimental tool for gene function analysis in mice. Reversible control of shRNA mediated RNAi has been achieved by using a tetracycline (tet)-inducible promoter. In the presence of the inducer doxycycline (dox), shRNA mediated gene silencing is initiated, whereas RNAi mechanism is blocked in the absence of dox. To achieve spatially and temporally regulated RNAi, the tet inducible system was combined with a Cre/loxP based strategy for tissue specific activation of shRNA constructs. To this end, a loxP-flanked “promoter inhibitory element” (PIE) was placed between the proximal (PSE) and distal sequence element (DSE) of a dox inducible promoter such that promoter function is completely blocked. Re-activation can be achieved through Cre mediated excision of PIE. To allow for gene silencing in a selected tissue, Cre expression can be regulated by a tissue-specific promoter. In mouse ES cells, the system mediated tight regulation of shRNA expression upon Cre mediated activation and dox administration, reaching knockdown efficiencies of >80%. Unexpectedly, the system showed a limited activity in transgenic mice when applied for conditional silencing of two different targets, LacZ and Sirt2. Sirt2 is a member of the sirtuin family which has considerably gained attention *in vitro* for its possible role in many physiological processes, including adipogenesis and neurodegenerative diseases.

To investigate the function of Sirt2 *in vivo*, the unmodified dox-responsive and tet-inducible promoter was further used for conditional RNAi in transgenic mice. Inducible shRNA expression resulted in efficient silencing of Sirt2 (>90%) in all tissues which have been analyzed. Suppression of Sirt2 during embryogenesis resulted in offspring consisting of equal ratios of wild type and transgenic pups, indicating that Sirt2 is not indispensable for development. In adult animals, glucose metabolism, insulin sensitivity and energy balance appeared to be unaffected by Sirt2 deficiency. Likewise, expression of PPAR γ , a downstream target of Sirt2, was not found to be altered upon Sirt2 inhibition. Finally, Sirt2 silencing was induced in an experimental model of Parkinson disease (PD). Data from Rotarod performances to study motor behaviour did not provide any evidence for a role of Sirt2 in PD pathogenesis as suggested by previous *in vitro* studies. Taken together, conditional Sirt2 silencing *in vivo* does not support speculation concerning a central role of Sirt2 in physiological processes, embryogenesis and in a mouse model of Parkinson disease.

6 Zusammenfassung

In den letzten acht Jahren hat sich die RNA Interferenz (RNAi) zu einer äußerst effizienten Methode entwickelt, um Funktionen von Genen in Mäusen zu untersuchen. Eine Regulierung der shRNA Transkription und des RNAi-Mechanismus wurde durch die Entwicklung von tet-induzierbaren Promotoren erreicht. In Gegenwart des Induktors Doxyzyklin (dox) findet aktiv shRNA Transkription statt, welche RNAi auslöst und zu einer Verringerung der Genexpression führt. In Abwesenheit von dox ist der RNAi-Mechanismus blockiert. Um RNAi gewebespezifisch und zeitlich regulieren zu können, wurde das tet-induzierbare System mit der Cre/loxP Technologie kombiniert. Dazu wurde ein loxP-flankiertes „Promotor inhibitorisches Element“ (PIE) zwischen das proximale (PSE) und distale (DSE) Sequenzelement des dox-induzierbaren Promotors platziert, wodurch dessen Aktivität vollständig blockiert wurde. PIE kann durch Cre-Rekombination entfernt werden, sodass die Promotorfunktion wiederhergestellt wird. Es besteht die Möglichkeit, Cre durch einen gewebespezifischen Promotor zu regulieren, womit der „Knockdown“ gezielt in einem spezifischen Gewebe stattfindet. In embryonalen Mausstammzellen konnte mit diesem System die shRNA Expression nach Aktivierung durch Cre und Induktion mit dox reguliert werden. Die Genexpression konnte dabei bis zu mehr als 80% herunterreguliert werden. In transgenen Mäusen war der „Knockdown“ von zwei verschiedenen Zielgenen, LacZ und Sirt2, unerwartet gering. Sirt2 wurde äußerst interessant, nachdem es mit grundlegenden physiologischen Prozessen wie Lipogenese und neurodegenerativen Erkrankungen *in vitro* in Verbindung gebracht wurde.

Um die Rolle von Sirt2 *in vivo* zu untersuchen, wurde das nicht-gewebespezifische und durch dox induzierbare tet-Promotor-System für induzierbare RNAi in Mäusen genutzt. Dabei führte die shRNA Transkription in allen untersuchten Geweben zu einer effizienten Herunterregulierung der Sirt2-Expression (>90%). Ein „Knockdown“ von Sirt2 während der Embryogenese hatte keine Auswirkung auf den Anteil der Wildtyp- und transgenen Nachkommen, was vermuten lässt, dass sich ein Verlust von Sirt2 während der Embryogenese nicht lethal auswirkt. In ausgewachsenen Tieren schienen Glukosemetabolismus, Insulinsensitivität und Energiebilanz nicht durch ein Sirt2 Defizit beeinflusst zu werden. Die Expression von PPAR γ , einem „Downstream“-Target von Sirt2 war ebenfalls nicht durch

einen Sirt2-„Knockdown“ verändert. Abschließend wurde die Funktion von Sirt2 in einem Parkinson-Krankheitsmodell untersucht. Ergebnisse aus Rotarod-Studien, die dazu dienen motorische Fähigkeiten zu analysieren, ließen keinen Aufschluß über eine Rolle von Sirt2 in der Krankheitsentstehung von Parkinson zu. Insgesamt unterstützt ein Sirt2-„Knockdown“ *in vivo* keine Spekulationen bezüglich einer zentralen Rolle von Sirt2 bei physiologischen Prozessen, in der Embryogenese und in einem Mausmodell der Parkinson-Krankheit.

7 References

1. Fire, A., Xu, S., Montgomery, M.K., Kostas, S.A., Driver, S.E., and Mello, C.C. 1998. Potent and specific genetic interference by double-stranded RNA in *Caenorhabditis elegans*. *Nature* 391:806-811.
2. Hutvagner, G., and Zamore, P.D. 2002. RNAi: nature abhors a double-strand. *Curr Opin Genet Dev* 12:225-232.
3. Bagasra, O., and Prilliman, K.R. 2004. RNA interference: the molecular immune system. *J Mol Histol* 35:545-553.
4. Bernstein, E., Caudy, A.A., Hammond, S.M., and Hannon, G.J. 2001. Role for a bidentate ribonuclease in the initiation step of RNA interference. *Nature* 409:363-366.
5. Elbashir, S.M., Harborth, J., Lendeckel, W., Yalcin, A., Weber, K., and Tuschl, T. 2001. Duplexes of 21-nucleotide RNAs mediate RNA interference in cultured mammalian cells. *Nature* 411:494-498.
6. Elbashir, S.M., Lendeckel, W., and Tuschl, T. 2001. RNA interference is mediated by 21- and 22-nucleotide RNAs. *Genes Dev* 15:188-200.
7. Hamilton, A., Voinnet, O., Chappell, L., and Baulcombe, D. 2002. Two classes of short interfering RNA in RNA silencing. *Embo J* 21:4671-4679.
8. Hamilton, A.J., and Baulcombe, D.C. 1999. A species of small antisense RNA in posttranscriptional gene silencing in plants. *Science* 286:950-952.
9. Rassouli, F.B., and Matin, M.M. 2009. Gene silencing in human embryonic stem cells by RNA interference. *Biochem Biophys Res Commun* 390:1106-1110.
10. Nykanen, A., Haley, B., and Zamore, P.D. 2001. ATP requirements and small interfering RNA structure in the RNA interference pathway. *Cell* 107:309-321.
11. Hannon, G.J. 2002. RNA interference. *Nature* 418:244-251.
12. McManus, M.T., and Sharp, P.A. 2002. Gene silencing in mammals by small interfering RNAs. *Nat Rev Genet* 3:737-747.
13. Collins, R.E., and Cheng, X. 2005. Structural domains in RNAi. *FEBS Lett* 579:5841-5849.
14. Khvorova, A., Reynolds, A., and Jayasena, S.D. 2003. Functional siRNAs and miRNAs exhibit strand bias. *Cell* 115:209-216.
15. Schwarz, D.S., Hutvagner, G., Du, T., Xu, Z., Aronin, N., and Zamore, P.D. 2003. Asymmetry in the assembly of the RNAi enzyme complex. *Cell* 115:199-208.
16. Reynolds, A., Leake, D., Boese, Q., Scaringe, S., Marshall, W.S., and Khvorova, A. 2004. Rational siRNA design for RNA interference. *Nat Biotechnol* 22:326-330.
17. Birmingham, A., Anderson, E.M., Reynolds, A., Ilesley-Tyree, D., Leake, D., Fedorov, Y., Baskerville, S., Maksimova, E., Robinson, K., Karpilow, J., et al. 2006. 3' UTR seed matches, but not overall identity, are associated with RNAi off-targets. *Nat Methods* 3:199-204.
18. Jackson, A.L., Bartz, S.R., Schelter, J., Kobayashi, S.V., Burchard, J., Mao, M., Li, B., Cavet, G., and Linsley, P.S. 2003. Expression profiling reveals off-target gene regulation by RNAi. *Nat Biotechnol* 21:635-637.

19. Lin, X., Ruan, X., Anderson, M.G., McDowell, J.A., Kroeger, P.E., Fesik, S.W., and Shen, Y. 2005. siRNA-mediated off-target gene silencing triggered by a 7 nt complementation. *Nucleic Acids Res* 33:4527-4535.
20. Grimm, D., Streetz, K.L., Jopling, C.L., Storm, T.A., Pandey, K., Davis, C.R., Marion, P., Salazar, F., and Kay, M.A. 2006. Fatality in mice due to oversaturation of cellular microRNA/short hairpin RNA pathways. *Nature* 441:537-541.
21. Kleinman, M.E., Yamada, K., Takeda, A., Chandrasekaran, V., Nozaki, M., Baffi, J.Z., Albuquerque, R.J., Yamasaki, S., Itaya, M., Pan, Y., et al. 2008. Sequence- and target-independent angiogenesis suppression by siRNA via TLR3. *Nature* 452:591-597.
22. Bass, B.L. 2001. RNA interference. The short answer. *Nature* 411:428-429.
23. Henschel, A., Buchholz, F., and Habermann, B. 2004. DEQOR: a web-based tool for the design and quality control of siRNAs. *Nucleic Acids Res* 32:W113-120.
24. Huesken, D., Lange, J., Mickanin, C., Weiler, J., Asselbergs, F., Warner, J., Meloon, B., Engel, S., Rosenberg, A., Cohen, D., et al. 2005. Design of a genome-wide siRNA library using an artificial neural network. *Nat Biotechnol* 23:995-1001.
25. Tilesi, F., Fradiani, P., Socci, V., Willems, D., and Ascenzioni, F. 2009. Design and validation of siRNAs and shRNAs. *Curr Opin Mol Ther* 11:156-164.
26. Omi, K., Tokunaga, K., and Hohjoh, H. 2004. Long-lasting RNAi activity in mammalian neurons. *FEBS Lett* 558:89-95.
27. Aza-Blanc, P., Cooper, C.L., Wagner, K., Batalov, S., Deveraux, Q.L., and Cooke, M.P. 2003. Identification of modulators of TRAIL-induced apoptosis via RNAi-based phenotypic screening. *Mol Cell* 12:627-637.
28. Dorsett, Y., and Tuschl, T. 2004. siRNAs: applications in functional genomics and potential as therapeutics. *Nat Rev Drug Discov* 3:318-329.
29. Berns, K., Hijmans, E.M., Mullenders, J., Brummelkamp, T.R., Velds, A., Heimerikx, M., Kerkhoven, R.M., Madiredjo, M., Nijkamp, W., Weigelt, B., et al. 2004. A large-scale RNAi screen in human cells identifies new components of the p53 pathway. *Nature* 428:431-437.
30. Brummelkamp, T.R., Nijman, S.M., Dirac, A.M., and Bernards, R. 2003. Loss of the cylindromatosis tumour suppressor inhibits apoptosis by activating NF-kappaB. *Nature* 424:797-801.
31. Zheng, L., Liu, J., Batalov, S., Zhou, D., Orth, A., Ding, S., and Schultz, P.G. 2004. An approach to genomewide screens of expressed small interfering RNAs in mammalian cells. *Proc Natl Acad Sci U S A* 101:135-140.
32. Brummelkamp, T.R., Bernards, R., and Agami, R. 2002. A system for stable expression of short interfering RNAs in mammalian cells. *Science* 296:550-553.
33. Tuschl, T. 2002. Expanding small RNA interference. *Nat Biotechnol* 20:446-448.
34. Devroe, E., and Silver, P.A. 2002. Retrovirus-delivered siRNA. *BMC Biotechnol* 2:15.
35. Hommel, J.D., Sears, R.M., Georgescu, D., Simmons, D.L., and DiLeone, R.J. 2003. Local gene knockdown in the brain using viral-mediated RNA interference. *Nat Med* 9:1539-1544.
36. Tomar, R.S., Matta, H., and Chaudhary, P.M. 2003. Use of adeno-associated viral vector for delivery of small interfering RNA. *Oncogene* 22:5712-5715.
37. Abbas-Terki, T., Blanco-Bose, W., Deglon, N., Pralong, W., and Aebischer, P. 2002. Lentiviral-mediated RNA interference. *Hum Gene Ther* 13:2197-2201.

38. Paddison, P.J., Caudy, A.A., Bernstein, E., Hannon, G.J., and Conklin, D.S. 2002. Short hairpin RNAs (shRNAs) induce sequence-specific silencing in mammalian cells. *Genes Dev* 16:948-958.
39. Yu, J.Y., DeRuiter, S.L., and Turner, D.L. 2002. RNA interference by expression of short-interfering RNAs and hairpin RNAs in mammalian cells. *Proc Natl Acad Sci U S A* 99:6047-6052.
40. Lee, S.K., and Kumar, P. 2009. Conditional RNAi: towards a silent gene therapy. *Adv Drug Deliv Rev* 61:650-664.
41. Geiduschek, E.P., and Kassavetis, G.A. 2001. The RNA polymerase III transcription apparatus. *J Mol Biol* 310:1-26.
42. Schramm, L., and Hernandez, N. 2002. Recruitment of RNA polymerase III to its target promoters. *Genes Dev* 16:2593-2620.
43. Paule, M.R., and White, R.J. 2000. Survey and summary: transcription by RNA polymerases I and III. *Nucleic Acids Res* 28:1283-1298.
44. Czauderna, F., Santel, A., Hinz, M., Fechtner, M., Durieux, B., Fisch, G., Leenders, F., Arnold, W., Giese, K., Klippel, A., et al. 2003. Inducible shRNA expression for application in a prostate cancer mouse model. *Nucleic Acids Res* 31:e127.
45. van de Wetering, M., Oving, I., Muncan, V., Pon Fong, M.T., Brantjes, H., van Leenen, D., Holstege, F.C., Brummelkamp, T.R., Agami, R., and Clevers, H. 2003. Specific inhibition of gene expression using a stably integrated, inducible small-interfering-RNA vector. *EMBO Rep* 4:609-615.
46. Wiznerowicz, M., and Trono, D. 2003. Conditional suppression of cellular genes: lentivirus vector-mediated drug-inducible RNA interference. *J Virol* 77:8957-8961.
47. Sandy, P., Ventura, A., and Jacks, T. 2005. Mammalian RNAi: a practical guide. *Biotechniques* 39:215-224.
48. Lewis, D.L., Hagstrom, J.E., Loomis, A.G., Wolff, J.A., and Herweijer, H. 2002. Efficient delivery of siRNA for inhibition of gene expression in postnatal mice. *Nat Genet* 32:107-108.
49. McCaffrey, A.P., Meuse, L., Pham, T.T., Conklin, D.S., Hannon, G.J., and Kay, M.A. 2002. RNA interference in adult mice. *Nature* 418:38-39.
50. Dann, C.T., Alvarado, A.L., Hammer, R.E., and Garbers, D.L. 2006. Heritable and stable gene knockdown in rats. *Proc Natl Acad Sci U S A* 103:11246-11251.
51. Hasuwa, H., Kaseda, K., Einarsdottir, T., and Okabe, M. 2002. Small interfering RNA and gene silencing in transgenic mice and rats. *FEBS Lett* 532:227-230.
52. Kunath, T., Gish, G., Lickert, H., Jones, N., Pawson, T., and Rossant, J. 2003. Transgenic RNA interference in ES cell-derived embryos recapitulates a genetic null phenotype. *Nat Biotechnol* 21:559-561.
53. Peng, S., York, J.P., and Zhang, P. 2006. A transgenic approach for RNA interference-based genetic screening in mice. *Proc Natl Acad Sci U S A* 103:2252-2256.
54. Rubinson, D.A., Dillon, C.P., Kwiatkowski, A.V., Sievers, C., Yang, L., Kopinja, J., Rooney, D.L., Zhang, M., Ibragimov, M.M., McManus, M.T., et al. 2003. A lentivirus-based system to functionally silence genes in primary mammalian cells, stem cells and transgenic mice by RNA interference. *Nat Genet* 33:401-406.
55. Tiscornia, G., Singer, O., Ikawa, M., and Verma, I.M. 2003. A general method for gene knockdown in mice by using lentiviral vectors expressing small interfering RNA. *Proc Natl Acad Sci U S A* 100:1844-1848.

56. Seibler, J., Kuter-Luks, B., Kern, H., Streu, S., Plum, L., Mauer, J., Kuhn, R., Bruning, J.C., and Schwenk, F. 2005. Single copy shRNA configuration for ubiquitous gene knockdown in mice. *Nucleic Acids Res* 33:e67.
57. Hoess, R.H., Ziese, M., and Sternberg, N. 1982. P1 site-specific recombination: nucleotide sequence of the recombining sites. *Proc Natl Acad Sci U S A* 79:3398-3402.
58. Chang, H.S., Lin, C.H., Chen, Y.C., and Yu, W.C. 2004. Using siRNA technique to generate transgenic animals with spatiotemporal and conditional gene knockdown. *Am J Pathol* 165:1535-1541.
59. Coumoul, X., Shukla, V., Li, C., Wang, R.H., and Deng, C.X. 2005. Conditional knockdown of Fgfr2 in mice using Cre-LoxP induced RNA interference. *Nucleic Acids Res* 33:e102.
60. Fritsch, L., Martinez, L.A., Sekhri, R., Naguibneva, I., Gerard, M., Vandromme, M., Schaeffer, L., and Harel-Bellan, A. 2004. Conditional gene knock-down by CRE-dependent short interfering RNAs. *EMBO Rep* 5:178-182.
61. Hitz, C., Wurst, W., and Kuhn, R. 2007. Conditional brain-specific knockdown of MAPK using Cre/loxP regulated RNA interference. *Nucleic Acids Res* 35:e90.
62. Kasim, V., Miyagishi, M., and Taira, K. 2004. Control of siRNA expression using the Cre-loxP recombination system. *Nucleic Acids Res* 32:e66.
63. Oberdoerffer, P., Kanellopoulou, C., Heissmeyer, V., Paeper, C., Borowski, C., Aifantis, I., Rao, A., and Rajewsky, K. 2005. Efficiency of RNA interference in the mouse hematopoietic system varies between cell types and developmental stages. *Mol Cell Biol* 25:3896-3905.
64. Tiscornia, G., Tergaonkar, V., Galimi, F., and Verma, I.M. 2004. CRE recombinase-inducible RNA interference mediated by lentiviral vectors. *Proc Natl Acad Sci U S A* 101:7347-7351.
65. Ventura, A., Meissner, A., Dillon, C.P., McManus, M., Sharp, P.A., Van Parijs, L., Jaenisch, R., and Jacks, T. 2004. Cre-lox-regulated conditional RNA interference from transgenes. *Proc Natl Acad Sci U S A* 101:10380-10385.
66. Ryding, A.D., Sharp, M.G., and Mullins, J.J. 2001. Conditional transgenic technologies. *J Endocrinol* 171:1-14.
67. Yamamoto, A., Hen, R., and Dauer, W.T. 2001. The ons and offs of inducible transgenic technology: a review. *Neurobiol Dis* 8:923-932.
68. Yu, J., and McMahon, A.P. 2006. Reproducible and inducible knockdown of gene expression in mice. *Genesis* 44:252-261.
69. Seibler, J., Kleinriders, A., Kuter-Luks, B., Niehaves, S., Bruning, J.C., and Schwenk, F. 2007. Reversible gene knockdown in mice using a tight, inducible shRNA expression system. *Nucleic Acids Res* 35:e54.
70. Gossen, M., and Bujard, H. 1992. Tight control of gene expression in mammalian cells by tetracycline-responsive promoters. *Proc Natl Acad Sci U S A* 89:5547-5551.
71. Ohkawa, J., and Taira, K. 2000. Control of the functional activity of an antisense RNA by a tetracycline-responsive derivative of the human U6 snRNA promoter. *Hum Gene Ther* 11:577-585.
72. Yao, F., Svensjo, T., Winkler, T., Lu, M., Eriksson, C., and Eriksson, E. 1998. Tetracycline repressor, tetR, rather than the tetR-mammalian cell transcription factor fusion derivatives, regulates inducible gene expression in mammalian cells. *Hum Gene Ther* 9:1939-1950.

73. Matsukura, S., Jones, P.A., and Takai, D. 2003. Establishment of conditional vectors for hairpin siRNA knockdowns. *Nucleic Acids Res* 31:e77.
74. Herold, M.J., van den Brandt, J., Seibler, J., and Reichardt, H.M. 2008. Inducible and reversible gene silencing by stable integration of an shRNA-encoding lentivirus in transgenic rats. *Proc Natl Acad Sci U S A* 105:18507-18512.
75. Kotnik, K., Popova, E., Todiras, M., Mori, M.A., Alenina, N., Seibler, J., and Bader, M. 2009. Inducible transgenic rat model for diabetes mellitus based on shRNA-mediated gene knockdown. *PLoS One* 4:e5124.
76. Anastassiadis, K., Kim, J., Daigle, N., Sprengel, R., Scholer, H.R., and Stewart, A.F. 2002. A predictable ligand regulated expression strategy for stably integrated transgenes in mammalian cells in culture. *Gene* 298:159-172.
77. Ngo, V.N., Davis, R.E., Lamy, L., Yu, X., Zhao, H., Lenz, G., Lam, L.T., Dave, S., Yang, L., Powell, J., et al. 2006. A loss-of-function RNA interference screen for molecular targets in cancer. *Nature* 441:106-110.
78. Dickins, R.A., McJunkin, K., Hernando, E., Premssirut, P.K., Krizhanovsky, V., Burgess, D.J., Kim, S.Y., Cordon-Cardo, C., Zender, L., Hannon, G.J., et al. 2007. Tissue-specific and reversible RNA interference in transgenic mice. *Nat Genet* 39:914-921.
79. Frye, R.A. 1999. Characterization of five human cDNAs with homology to the yeast SIR2 gene: Sir2-like proteins (sirtuins) metabolize NAD and may have protein ADP-ribosyltransferase activity. *Biochem Biophys Res Commun* 260:273-279.
80. Kaeberlein, M., McVey, M., and Guarente, L. 1999. The SIR2/3/4 complex and SIR2 alone promote longevity in *Saccharomyces cerevisiae* by two different mechanisms. *Genes Dev* 13:2570-2580.
81. Sinclair, D.A., and Guarente, L. 1997. Extrachromosomal rDNA circles--a cause of aging in yeast. *Cell* 91:1033-1042.
82. Imai, S., Armstrong, C.M., Kaeberlein, M., and Guarente, L. 2000. Transcriptional silencing and longevity protein Sir2 is an NAD-dependent histone deacetylase. *Nature* 403:795-800.
83. Haigis, M.C., and Guarente, L.P. 2006. Mammalian sirtuins--emerging roles in physiology, aging, and calorie restriction. *Genes Dev* 20:2913-2921.
84. Sauve, A.A., Wolberger, C., Schramm, V.L., and Boeke, J.D. 2006. The biochemistry of sirtuins. *Annu Rev Biochem* 75:435-465.
85. Anderson, R.M., Bitterman, K.J., Wood, J.G., Medvedik, O., and Sinclair, D.A. 2003. Nicotinamide and PNC1 govern lifespan extension by calorie restriction in *Saccharomyces cerevisiae*. *Nature* 423:181-185.
86. Lin, S.J., Defossez, P.A., and Guarente, L. 2000. Requirement of NAD and SIR2 for life-span extension by calorie restriction in *Saccharomyces cerevisiae*. *Science* 289:2126-2128.
87. Lin, S.J., Ford, E., Haigis, M., Liszt, G., and Guarente, L. 2004. Calorie restriction extends yeast life span by lowering the level of NADH. *Genes Dev* 18:12-16.
88. Lin, S.J., Kaeberlein, M., Andalis, A.A., Sturtz, L.A., Defossez, P.A., Culotta, V.C., Fink, G.R., and Guarente, L. 2002. Calorie restriction extends *Saccharomyces cerevisiae* lifespan by increasing respiration. *Nature* 418:344-348.

89. Revollo, J.R., Grimm, A.A., and Imai, S. 2004. The NAD biosynthesis pathway mediated by nicotinamide phosphoribosyltransferase regulates Sir2 activity in mammalian cells. *J Biol Chem* 279:50754-50763.
90. Yu, J., and Auwerx, J. 2009. The role of sirtuins in the control of metabolic homeostasis. *Ann N Y Acad Sci* 1173 Suppl 1:E10-19.
91. Haigis, M.C., Mostoslavsky, R., Haigis, K.M., Fahie, K., Christodoulou, D.C., Murphy, A.J., Valenzuela, D.M., Yancopoulos, G.D., Karow, M., Blander, G., et al. 2006. SIRT4 inhibits glutamate dehydrogenase and opposes the effects of calorie restriction in pancreatic beta cells. *Cell* 126:941-954.
92. Liszt, G., Ford, E., Kurtev, M., and Guarente, L. 2005. Mouse Sir2 homolog SIRT6 is a nuclear ADP-ribosyltransferase. *J Biol Chem* 280:21313-21320.
93. Michan, S., and Sinclair, D. 2007. Sirtuins in mammals: insights into their biological function. *Biochem J* 404:1-13.
94. Michishita, E., McCord, R.A., Berber, E., Kioi, M., Padilla-Nash, H., Damian, M., Cheung, P., Kusumoto, R., Kawahara, T.L., Barrett, J.C., et al. 2008. SIRT6 is a histone H3 lysine 9 deacetylase that modulates telomeric chromatin. *Nature* 452:492-496.
95. Borra, M.T., Langer, M.R., Slama, J.T., and Denu, J.M. 2004. Substrate specificity and kinetic mechanism of the Sir2 family of NAD⁺-dependent histone/protein deacetylases. *Biochemistry* 43:9877-9887.
96. Sauve, A.A., Celic, I., Avalos, J., Deng, H., Boeke, J.D., and Schramm, V.L. 2001. Chemistry of gene silencing: the mechanism of NAD⁺-dependent deacetylation reactions. *Biochemistry* 40:15456-15463.
97. Schmidt, M.T., Smith, B.C., Jackson, M.D., and Denu, J.M. 2004. Coenzyme specificity of Sir2 protein deacetylases: implications for physiological regulation. *J Biol Chem* 279:40122-40129.
98. Yamamoto, H., Schoonjans, K., and Auwerx, J. 2007. Sirtuin functions in health and disease. *Mol Endocrinol* 21:1745-1755.
99. Blander, G., and Guarente, L. 2004. The Sir2 family of protein deacetylases. *Annu Rev Biochem* 73:417-435.
100. Schwer, B., North, B.J., Frye, R.A., Ott, M., and Verdin, E. 2002. The human silent information regulator (Sir)2 homologue hSIRT3 is a mitochondrial nicotinamide adenine dinucleotide-dependent deacetylase. *J Cell Biol* 158:647-657.
101. North, B.J., Marshall, B.L., Borra, M.T., Denu, J.M., and Verdin, E. 2003. The human Sir2 ortholog, SIRT2, is an NAD⁺-dependent tubulin deacetylase. *Mol Cell* 11:437-444.
102. North, B.J., and Verdin, E. 2007. Interphase nucleo-cytoplasmic shuttling and localization of SIRT2 during mitosis. *PLoS One* 2:e784.
103. Tanno, M., Sakamoto, J., Miura, T., Shimamoto, K., and Horio, Y. 2007. Nucleocytoplasmic shuttling of the NAD⁺-dependent histone deacetylase SIRT1. *J Biol Chem* 282:6823-6832.
104. Haigis, M.C., and Sinclair, D.A. 2010. Mammalian sirtuins: biological insights and disease relevance. *Annu Rev Pathol* 5:253-295.
105. Nemoto, S., Fergusson, M.M., and Finkel, T. 2005. SIRT1 functionally interacts with the metabolic regulator and transcriptional coactivator PGC-1{alpha}. *J Biol Chem* 280:16456-16460.

106. Outeiro, T.F., Marques, O., and Kazantsev, A. 2008. Therapeutic role of sirtuins in neurodegenerative disease. *Biochim Biophys Acta* 1782:363-369.
107. Picard, F., Kurtev, M., Chung, N., Topark-Ngarm, A., Senawong, T., Machado De Oliveira, R., Leid, M., McBurney, M.W., and Guarente, L. 2004. Sirt1 promotes fat mobilization in white adipocytes by repressing PPAR-gamma. *Nature* 429:771-776.
108. Fulco, M., Schiltz, R.L., Iezzi, S., King, M.T., Zhao, P., Kashiwaya, Y., Hoffman, E., Veech, R.L., and Sartorelli, V. 2003. Sir2 regulates skeletal muscle differentiation as a potential sensor of the redox state. *Mol Cell* 12:51-62.
109. Rodgers, J.T., Lerin, C., Haas, W., Gygi, S.P., Spiegelman, B.M., and Puigserver, P. 2005. Nutrient control of glucose homeostasis through a complex of PGC-1alpha and SIRT1. *Nature* 434:113-118.
110. Rodgers, J.T., and Puigserver, P. 2007. Fasting-dependent glucose and lipid metabolic response through hepatic sirtuin 1. *Proc Natl Acad Sci U S A* 104:12861-12866.
111. Moynihan, K.A., Grimm, A.A., Plueger, M.M., Bernal-Mizrachi, E., Ford, E., Cras-Meneur, C., Permutt, M.A., and Imai, S. 2005. Increased dosage of mammalian Sir2 in pancreatic beta cells enhances glucose-stimulated insulin secretion in mice. *Cell Metab* 2:105-117.
112. Bordone, L., Motta, M.C., Picard, F., Robinson, A., Jhala, U.S., Apfeld, J., McDonagh, T., Lemieux, M., McBurney, M., Szilvasi, A., et al. 2006. Sirt1 regulates insulin secretion by repressing UCP2 in pancreatic beta cells. *PLoS Biol* 4:e31.
113. Qiao, L., and Shao, J. 2006. SIRT1 regulates adiponectin gene expression through Foxo1-C/enhancer-binding protein alpha transcriptional complex. *J Biol Chem* 281:39915-39924.
114. Qiang, L., Wang, H., and Farmer, S.R. 2007. Adiponectin secretion is regulated by SIRT1 and the endoplasmic reticulum oxidoreductase Ero1-L alpha. *Mol Cell Biol* 27:4698-4707.
115. Luo, J., Nikolaev, A.Y., Imai, S., Chen, D., Su, F., Shiloh, A., Guarente, L., and Gu, W. 2001. Negative control of p53 by Sir2alpha promotes cell survival under stress. *Cell* 107:137-148.
116. Motta, M.C., Divecha, N., Lemieux, M., Kamel, C., Chen, D., Gu, W., Bultsma, Y., McBurney, M., and Guarente, L. 2004. Mammalian SIRT1 represses forkhead transcription factors. *Cell* 116:551-563.
117. Yeung, F., Hoberg, J.E., Ramsey, C.S., Keller, M.D., Jones, D.R., Frye, R.A., and Mayo, M.W. 2004. Modulation of NF-kappaB-dependent transcription and cell survival by the SIRT1 deacetylase. *Embo J* 23:2369-2380.
118. Vaziri, H., Dessain, S.K., Ng Eaton, E., Imai, S.I., Frye, R.A., Pandita, T.K., Guarente, L., and Weinberg, R.A. 2001. hSIR2(SIRT1) functions as an NAD-dependent p53 deacetylase. *Cell* 107:149-159.
119. Brunet, A., Sweeney, L.B., Sturgill, J.F., Chua, K.F., Greer, P.L., Lin, Y., Tran, H., Ross, S.E., Mostoslavsky, R., Cohen, H.Y., et al. 2004. Stress-dependent regulation of FOXO transcription factors by the SIRT1 deacetylase. *Science* 303:2011-2015.
120. Chen, J., Zhou, Y., Mueller-Steiner, S., Chen, L.F., Kwon, H., Yi, S., Mucke, L., and Gan, L. 2005. SIRT1 protects against microglia-dependent amyloid-beta toxicity through inhibiting NF-kappaB signaling. *J Biol Chem* 280:40364-40374.

121. Boily, G., Seifert, E.L., Bevilacqua, L., He, X.H., Sabourin, G., Estey, C., Moffat, C., Crawford, S., Saliba, S., Jardine, K., et al. 2008. SirT1 regulates energy metabolism and response to caloric restriction in mice. *PLoS One* 3:e1759.
122. Inoue, T., Hiratsuka, M., Osaki, M., and Oshimura, M. 2007. The molecular biology of mammalian SIRT proteins: SIRT2 in cell cycle regulation. *Cell Cycle* 6:1011-1018.
123. Inoue, T., Hiratsuka, M., Osaki, M., Yamada, H., Kishimoto, I., Yamaguchi, S., Nakano, S., Katoh, M., Ito, H., and Oshimura, M. 2007. SIRT2, a tubulin deacetylase, acts to block the entry to chromosome condensation in response to mitotic stress. *Oncogene* 26:945-957.
124. North, B.J., and Verdin, E. 2007. Mitotic regulation of SIRT2 by cyclin-dependent kinase 1-dependent phosphorylation. *J Biol Chem* 282:19546-19555.
125. Vaquero, A., Scher, M.B., Lee, D.H., Sutton, A., Cheng, H.L., Alt, F.W., Serrano, L., Sternglanz, R., and Reinberg, D. 2006. SirT2 is a histone deacetylase with preference for histone H4 Lys 16 during mitosis. *Genes Dev* 20:1256-1261.
126. Dryden, S.C., Nahhas, F.A., Nowak, J.E., Goustin, A.S., and Tainsky, M.A. 2003. Role for human SIRT2 NAD-dependent deacetylase activity in control of mitotic exit in the cell cycle. *Mol Cell Biol* 23:3173-3185.
127. Inoue, T., Nakayama, Y., Yamada, H., Li, Y.C., Yamaguchi, S., Osaki, M., Kurimasa, A., Hiratsuka, M., Katoh, M., and Oshimura, M. 2009. SIRT2 downregulation confers resistance to microtubule inhibitors by prolonging chronic mitotic arrest. *Cell Cycle* 8:1279-1291.
128. Pandithage, R., Lilischkis, R., Harting, K., Wolf, A., Jedamzik, B., Luscher-Firzlauff, J., Vervoorts, J., Lasonder, E., Kremmer, E., Knoll, B., et al. 2008. The regulation of SIRT2 function by cyclin-dependent kinases affects cell motility. *J Cell Biol* 180:915-929.
129. Hiratsuka, M., Inoue, T., Toda, T., Kimura, N., Shirayoshi, Y., Kamitani, H., Watanabe, T., Ohama, E., Tahimic, C.G., Kurimasa, A., et al. 2003. Proteomics-based identification of differentially expressed genes in human gliomas: down-regulation of SIRT2 gene. *Biochem Biophys Res Commun* 309:558-566.
130. Wang, F., Nguyen, M., Qin, F.X., and Tong, Q. 2007. SIRT2 deacetylates FOXO3a in response to oxidative stress and caloric restriction. *Aging Cell* 6:505-514.
131. Jing, E., Gesta, S., and Kahn, C.R. 2007. SIRT2 regulates adipocyte differentiation through FoxO1 acetylation/deacetylation. *Cell Metab* 6:105-114.
132. Wang, F., and Tong, Q. 2009. SIRT2 suppresses adipocyte differentiation by deacetylating FOXO1 and enhancing FOXO1's repressive interaction with PPARgamma. *Mol Biol Cell* 20:801-808.
133. Southwood, C.M., Peppi, M., Dryden, S., Tainsky, M.A., and Gow, A. 2007. Microtubule deacetylases, SirT2 and HDAC6, in the nervous system. *Neurochem Res* 32:187-195.
134. Li, W., Zhang, B., Tang, J., Cao, Q., Wu, Y., Wu, C., Guo, J., Ling, E.A., and Liang, F. 2007. Sirtuin 2, a mammalian homolog of yeast silent information regulator-2 longevity regulator, is an oligodendroglial protein that decelerates cell differentiation through deacetylating alpha-tubulin. *J Neurosci* 27:2606-2616.
135. Werner, H.B., Kuhlmann, K., Shen, S., Uecker, M., Schardt, A., Dimova, K., Orfaniotou, F., Dhaunchak, A., Brinkmann, B.G., Mobius, W., et al. 2007. Proteolipid protein is required for transport of sirtuin 2 into CNS myelin. *J Neurosci* 27:7717-7730.

136. Suzuki, K., and Koike, T. 2007. Mammalian Sir2-related protein (SIRT) 2-mediated modulation of resistance to axonal degeneration in slow Wallerian degeneration mice: a crucial role of tubulin deacetylation. *Neuroscience* 147:599-612.
137. Hasegawa, K., and Yoshikawa, K. 2008. Necdin regulates p53 acetylation via Sirtuin1 to modulate DNA damage response in cortical neurons. *J Neurosci* 28:8772-8784.
138. Anekonda, T.S. 2006. Resveratrol--a boon for treating Alzheimer's disease? *Brain Res Rev* 52:316-326.
139. Kim, D., Nguyen, M.D., Dobbin, M.M., Fischer, A., Sananbenesi, F., Rodgers, J.T., Delalle, I., Baur, J.A., Sui, G., Armour, S.M., et al. 2007. SIRT1 deacetylase protects against neurodegeneration in models for Alzheimer's disease and amyotrophic lateral sclerosis. *Embo J* 26:3169-3179.
140. Qin, W., Chachich, M., Lane, M., Roth, G., Bryant, M., de Cabo, R., Ottinger, M.A., Mattison, J., Ingram, D., Gandy, S., et al. 2006. Calorie restriction attenuates Alzheimer's disease type brain amyloidosis in Squirrel monkeys (*Saimiri sciureus*). *J Alzheimers Dis* 10:417-422.
141. Outeiro, T.F., Kontopoulos, E., Altmann, S.M., Kufareva, I., Strathearn, K.E., Amore, A.M., Volk, C.B., Maxwell, M.M., Rochet, J.C., McLean, P.J., et al. 2007. Sirtuin 2 inhibitors rescue alpha-synuclein-mediated toxicity in models of Parkinson's disease. *Science* 317:516-519.
142. Garske, A.L., Smith, B.C., and Denu, J.M. 2007. Linking SIRT2 to Parkinson's disease. *ACS Chem Biol* 2:529-532.
143. Ahuja, N., Schwer, B., Carobbio, S., Waltregny, D., North, B.J., Castronovo, V., Maechler, P., and Verdin, E. 2007. Regulation of insulin secretion by SIRT4, a mitochondrial ADP-ribosyltransferase. *J Biol Chem* 282:33583-33592.
144. Lombard, D.B., Alt, F.W., Cheng, H.L., Bunkenborg, J., Streeper, R.S., Mostoslavsky, R., Kim, J., Yancopoulos, G., Valenzuela, D., Murphy, A., et al. 2007. Mammalian Sir2 homolog SIRT3 regulates global mitochondrial lysine acetylation. *Mol Cell Biol* 27:8807-8814.
145. Michishita, E., Park, J.Y., Burneskis, J.M., Barrett, J.C., and Horikawa, I. 2005. Evolutionarily conserved and nonconserved cellular localizations and functions of human SIRT proteins. *Mol Biol Cell* 16:4623-4635.
146. Nakagawa, T., Lomb, D.J., Haigis, M.C., and Guarente, L. 2009. SIRT5 Deacetylates carbamoyl phosphate synthetase 1 and regulates the urea cycle. *Cell* 137:560-570.
147. Onyango, P., Celic, I., McCaffery, J.M., Boeke, J.D., and Feinberg, A.P. 2002. SIRT3, a human SIR2 homologue, is an NAD-dependent deacetylase localized to mitochondria. *Proc Natl Acad Sci U S A* 99:13653-13658.
148. Shi, T., Wang, F., Stieren, E., and Tong, Q. 2005. SIRT3, a mitochondrial sirtuin deacetylase, regulates mitochondrial function and thermogenesis in brown adipocytes. *J Biol Chem* 280:13560-13567.
149. Hallows, W.C., Lee, S., and Denu, J.M. 2006. Sirtuins deacetylate and activate mammalian acetyl-CoA synthetases. *Proc Natl Acad Sci U S A* 103:10230-10235.
150. Schwer, B., Bunkenborg, J., Verdin, R.O., Andersen, J.S., and Verdin, E. 2006. Reversible lysine acetylation controls the activity of the mitochondrial enzyme acetyl-CoA synthetase 2. *Proc Natl Acad Sci U S A* 103:10224-10229.

151. Fujino, T., Kondo, J., Ishikawa, M., Morikawa, K., and Yamamoto, T.T. 2001. Acetyl-CoA synthetase 2, a mitochondrial matrix enzyme involved in the oxidation of acetate. *J Biol Chem* 276:11420-11426.
152. Ahn, B.H., Kim, H.S., Song, S., Lee, I.H., Liu, J., Vassilopoulos, A., Deng, C.X., and Finkel, T. 2008. A role for the mitochondrial deacetylase Sirt3 in regulating energy homeostasis. *Proc Natl Acad Sci U S A* 105:14447-14452.
153. Verdin, E., Dequiedt, F., Fischle, W., Frye, R., Marshall, B., and North, B. 2004. Measurement of mammalian histone deacetylase activity. *Methods Enzymol* 377:180-196.
154. Mostoslavsky, R., Chua, K.F., Lombard, D.B., Pang, W.W., Fischer, M.R., Gellon, L., Liu, P., Mostoslavsky, G., Franco, S., Murphy, M.M., et al. 2006. Genomic instability and aging-like phenotype in the absence of mammalian SIRT6. *Cell* 124:315-329.
155. Van Gool, F., Galli, M., Gueydan, C., Kruys, V., Prevot, P.P., Bedalov, A., Mostoslavsky, R., Alt, F.W., De Smedt, T., and Leo, O. 2009. Intracellular NAD levels regulate tumor necrosis factor protein synthesis in a sirtuin-dependent manner. *Nat Med* 15:206-210.
156. Ford, E., Voit, R., Liszt, G., Magin, C., Grummt, I., and Guarente, L. 2006. Mammalian Sir2 homolog SIRT7 is an activator of RNA polymerase I transcription. *Genes Dev* 20:1075-1080.
157. Sambrook, J., Fritschy, E.F., and Maniatis, T. 2001. Molecular cloning: a laboratory manual. (CSHL Press).
158. Inoue, H., Nojima, H., and Okayama, H. 1990. High efficiency transformation of *Escherichia coli* with plasmids. *Gene* 96:23-28.
159. Buchholz, F., Angrand, P.O., and Stewart, A.F. 1996. A simple assay to determine the functionality of Cre or FLP recombination targets in genomic manipulation constructs. *Nucleic Acids Res* 24:3118-3119.
160. Mullis, K.B., and Faloona, F.A. 1987. Specific synthesis of DNA in vitro via a polymerase-catalyzed chain reaction. *Methods Enzymol* 155:335-350.
161. Saiki, R.K., Gelfand, D.H., Stoffel, S., Scharf, S.J., Higuchi, R., Horn, G.T., Mullis, K.B., and Erlich, H.A. 1988. Primer-directed enzymatic amplification of DNA with a thermostable DNA polymerase. *Science* 239:487-491.
162. Chomczynski, P., and Qasba, P.K. 1984. Alkaline transfer of DNA to plastic membrane. *Biochem Biophys Res Commun* 122:340-344.
163. Laemmli, U.K. 1970. Cleavage of structural proteins during the assembly of the head of bacteriophage T4. *Nature* 227:680-685.
164. Seibler, J., Zevnik, B., Kuter-Luks, B., Andreas, S., Kern, H., Hennek, T., Rode, A., Heimann, C., Faust, N., Kauselmann, G., et al. 2003. Rapid generation of inducible mouse mutants. *Nucleic Acids Res* 31:e12.
165. Eggan, K., Rode, A., Jentsch, I., Samuel, C., Hennek, T., Tintrup, H., Zevnik, B., Erwin, J., Loring, J., Jackson-Grusby, L., et al. 2002. Male and female mice derived from the same embryonic stem cell clone by tetraploid embryo complementation. *Nat Biotechnol* 20:455-459.
166. Schaft, J., Ashery-Padan, R., van der Hoeven, F., Gruss, P., and Stewart, A.F. 2001. Efficient FLP recombination in mouse ES cells and oocytes. *Genesis* 31:6-10.
167. Hogan, B., Beddington, R., Costantini, F. and Lacey, E. 1994. Manipulating the Mouse Embryo: A Laboratory Manual. CSHL Press.

168. Silver, L.M. 1995. Mouse Genetics: Concepts and Applications. *Oxford University Press*.
169. Soriano, P. 1999. Generalized lacZ expression with the ROSA26 Cre reporter strain. *Nat Genet* 21:70-71.
170. Shoba, B., Lwin, Z.M., Ling, L.S., Bay, B.H., Yip, G.W., and Kumar, S.D. 2009. Function of sirtuins in biological tissues. *Anat Rec (Hoboken)* 292:536-543.
171. Leibiger, I.B., and Berggren, P.O. 2005. A SIRTain role in pancreatic beta cell function. *Cell Metab* 2:80-82.
172. Spillantini, M.G., Schmidt, M.L., Lee, V.M., Trojanowski, J.Q., Jakes, R., and Goedert, M. 1997. Alpha-synuclein in Lewy bodies. *Nature* 388:839-840.
173. Chinta, S.J., and Andersen, J.K. 2005. Dopaminergic neurons. *Int J Biochem Cell Biol* 37:942-946.
174. Bjorklund, A., Lindvall, O. 1984. Dopamine-containing systems in the CNS. *Handbook of Chemical Neuroanatomy (Classical Transmitters in the CNS, Part I)* 2:55-113.
175. Myslinski, E., Ame, J.C., Krol, A., and Carbon, P. 2001. An unusually compact external promoter for RNA polymerase III transcription of the human H1RNA gene. *Nucleic Acids Res* 29:2502-2509.
176. Tissenbaum, H.A., and Guarente, L. 2001. Increased dosage of a sir-2 gene extends lifespan in *Caenorhabditis elegans*. *Nature* 410:227-230.
177. Frye, R.A. 2000. Phylogenetic classification of prokaryotic and eukaryotic Sir2-like proteins. *Biochem Biophys Res Commun* 273:793-798.
178. Liou, G.G., Tanny, J.C., Kruger, R.G., Walz, T., and Moazed, D. 2005. Assembly of the SIR complex and its regulation by O-acetyl-ADP-ribose, a product of NAD-dependent histone deacetylation. *Cell* 121:515-527.
179. Vaquero, A., Scher, M., Lee, D., Erdjument-Bromage, H., Tempst, P., and Reinberg, D. 2004. Human SirT1 interacts with histone H1 and promotes formation of facultative heterochromatin. *Mol Cell* 16:93-105.
180. Daitoku, H., Hatta, M., Matsuzaki, H., Aratani, S., Ohshima, T., Miyagishi, M., Nakajima, T., and Fukamizu, A. 2004. Silent information regulator 2 potentiates Foxo1-mediated transcription through its deacetylase activity. *Proc Natl Acad Sci U S A* 101:10042-10047.
181. Rose, G., Dato, S., Altomare, K., Bellizzi, D., Garasto, S., Greco, V., Passarino, G., Feraco, E., Mari, V., Barbi, C., et al. 2003. Variability of the SIRT3 gene, human silent information regulator Sir2 homologue, and survivorship in the elderly. *Exp Gerontol* 38:1065-1070.
182. Wallace, D.C. 2005. A mitochondrial paradigm of metabolic and degenerative diseases, aging, and cancer: a dawn for evolutionary medicine. *Annu Rev Genet* 39:359-407.
183. Lombard, D.B., Schwer, B., Alt, F.W., and Mostoslavsky, R. 2008. SIRT6 in DNA repair, metabolism and ageing. *J Intern Med* 263:128-141.
184. Yang, Y.H., Chen, Y.H., Zhang, C.Y., Nimmakayalu, M.A., Ward, D.C., and Weissman, S. 2000. Cloning and characterization of two mouse genes with homology to the yeast Sir2 gene. *Genomics* 69:355-369.
185. Shin, M.K., Levorse, J.M., Ingram, R.S., and Tilghman, S.M. 1999. The temporal requirement for endothelin receptor-B signalling during neural crest development. *Nature* 402:496-501.

-
186. Zhou, H., Huang, C., Yang, M., Landel, C.P., Xia, P.Y., Liu, Y.J., and Xia, X.G. 2009. Developing tTA transgenic rats for inducible and reversible gene expression. *Int J Biol Sci* 5:171-181.
 187. Kim, J.E., Chen, J., and Lou, Z. 2008. DBC1 is a negative regulator of SIRT1. *Nature* 451:583-586.
 188. McBurney, M.W., Yang, X., Jardine, K., Hixon, M., Boekelheide, K., Webb, J.R., Lansdorp, P.M., and Lemieux, M. 2003. The mammalian SIR2alpha protein has a role in embryogenesis and gametogenesis. *Mol Cell Biol* 23:38-54.
 189. Cheng, H.L., Mostoslavsky, R., Saito, S., Manis, J.P., Gu, Y., Patel, P., Bronson, R., Appella, E., Alt, F.W., and Chua, K.F. 2003. Developmental defects and p53 hyperacetylation in Sir2 homolog (SIRT1)-deficient mice. *Proc Natl Acad Sci U S A* 100:10794-10799.
 190. Bae, N.S., Swanson, M.J., Vassilev, A., and Howard, B.H. 2004. Human histone deacetylase SIRT2 interacts with the homeobox transcription factor HOXA10. *J Biochem* 135:695-700.
 191. Ahima, R.S. 2006. Adipose tissue as an endocrine organ. *Obesity (Silver Spring)* 14 Suppl 5:242S-249S.
 192. Scherer, P.E. 2006. Adipose tissue: from lipid storage compartment to endocrine organ. *Diabetes* 55:1537-1545.
 193. Rosen, E.D., and Spiegelman, B.M. 2006. Adipocytes as regulators of energy balance and glucose homeostasis. *Nature* 444:847-853.
 194. Lagouge, M., Argmann, C., Gerhart-Hines, Z., Meziane, H., Lerin, C., Daussin, F., Messadeq, N., Milne, J., Lambert, P., Elliott, P., et al. 2006. Resveratrol improves mitochondrial function and protects against metabolic disease by activating SIRT1 and PGC-1alpha. *Cell* 127:1109-1122.
 195. Sun, C., Zhang, F., Ge, X., Yan, T., Chen, X., Shi, X., and Zhai, Q. 2007. SIRT1 improves insulin sensitivity under insulin-resistant conditions by repressing PTP1B. *Cell Metab* 6:307-319.
 196. Yang, Y., Hou, H., Haller, E.M., Nicosia, S.V., and Bai, W. 2005. Suppression of FOXO1 activity by FHL2 through SIRT1-mediated deacetylation. *Embo J* 24:1021-1032.
 197. Hisahara, S., Chiba, S., Matsumoto, H., Tanno, M., Yagi, H., Shimohama, S., Sato, M., and Horio, Y. 2008. Histone deacetylase SIRT1 modulates neuronal differentiation by its nuclear translocation. *Proc Natl Acad Sci U S A* 105:15599-15604.
 198. Prozorovski, T., Schulze-Topphoff, U., Glumm, R., Baumgart, J., Schroter, F., Ninnemann, O., Siegert, E., Bendix, I., Brustle, O., Nitsch, R., et al. 2008. Sirt1 contributes critically to the redox-dependent fate of neural progenitors. *Nat Cell Biol* 10:385-394.
 199. Ramadori, G., Lee, C.E., Bookout, A.L., Lee, S., Williams, K.W., Anderson, J., Elmquist, J.K., and Coppari, R. 2008. Brain SIRT1: anatomical distribution and regulation by energy availability. *J Neurosci* 28:9989-9996.
 200. Sakamoto, J., Miura, T., Shimamoto, K., and Horio, Y. 2004. Predominant expression of Sir2alpha, an NAD-dependent histone deacetylase, in the embryonic mouse heart and brain. *FEBS Lett* 556:281-286.
 201. Gale, E., and Li, M. 2008. Midbrain dopaminergic neuron fate specification: Of mice and embryonic stem cells. *Mol Brain* 1:8.

-
202. Colotla, V.A., Flores, E., Oscos, A., Meneses, A., and Tapia, R. 1990. Effects of MPTP on locomotor activity in mice. *Neurotoxicol Teratol* 12:405-407.
 203. Petroske, E., Meredith, G.E., Callen, S., Totterdell, S., and Lau, Y.S. 2001. Mouse model of Parkinsonism: a comparison between subacute MPTP and chronic MPTP/probenecid treatment. *Neuroscience* 106:589-601.
 204. Rozas, G., Lopez-Martin, E., Guerra, M.J., and Labandeira-Garcia, J.L. 1998. The overall rod performance test in the MPTP-treated-mouse model of Parkinsonism. *J Neurosci Methods* 83:165-175.
 205. Sedelis, M., Hofele, K., Auburger, G.W., Morgan, S., Huston, J.P., and Schwarting, R.K. 2000. MPTP susceptibility in the mouse: behavioral, neurochemical, and histological analysis of gender and strain differences. *Behav Genet* 30:171-182.
 206. Tillerson, J.L., Caudle, W.M., Reveron, M.E., and Miller, G.W. 2002. Detection of behavioral impairments correlated to neurochemical deficits in mice treated with moderate doses of 1-methyl-4-phenyl-1,2,3,6-tetrahydropyridine. *Exp Neurol* 178:80-90.
 207. Jackson-Lewis, V., and Przedborski, S. 2007. Protocol for the MPTP mouse model of Parkinson's disease. *Nat Protoc* 2:141-151.
 208. Tatton, N.A., and Kish, S.J. 1997. In situ detection of apoptotic nuclei in the substantia nigra compacta of 1-methyl-4-phenyl-1,2,3,6-tetrahydropyridine-treated mice using terminal deoxynucleotidyl transferase labelling and acridine orange staining. *Neuroscience* 77:1037-1048.
 209. Meredith, G.E., Totterdell, S., Potashkin, J.A., and Surmeier, D.J. 2008. Modeling PD pathogenesis in mice: advantages of a chronic MPTP protocol. *Parkinsonism Relat Disord* 14 Suppl 2:S112-115.
 210. Potashkin, J.A., Kang, U.J., Loomis, P.A., Jodelka, F.M., Ding, Y., and Meredith, G.E. 2007. MPTP administration in mice changes the ratio of splice isoforms of fosB and rgs9. *Brain Res* 1182:1-10.
 211. Bezard, E., Jaber, M., Gonon, F., Boireau, A., Bloch, B., and Gross, C.E. 2000. Adaptive changes in the nigrostriatal pathway in response to increased 1-methyl-4-phenyl-1,2,3,6-tetrahydropyridine-induced neurodegeneration in the mouse. *Eur J Neurosci* 12:2892-2900.
 212. Jackson-Lewis, V., Jakowec, M., Burke, R.E., and Przedborski, S. 1995. Time course and morphology of dopaminergic neuronal death caused by the neurotoxin 1-methyl-4-phenyl-1,2,3,6-tetrahydropyridine. *Neurodegeneration* 4:257-269.
 213. Turmel, H., Hartmann, A., Parain, K., Douhou, A., Srinivasan, A., Agid, Y., and Hirsch, E.C. 2001. Caspase-3 activation in 1-methyl-4-phenyl-1,2,3,6-tetrahydropyridine (MPTP)-treated mice. *Mov Disord* 16:185-189.
 214. Rousselet, E., Joubert, C., Callebert, J., Parain, K., Tremblay, L., Orioux, G., Launay, J.M., Cohen-Salmon, C., and Hirsch, E.C. 2003. Behavioral changes are not directly related to striatal monoamine levels, number of nigral neurons, or dose of parkinsonian toxin MPTP in mice. *Neurobiol Dis* 14:218-228.
 215. Meredith, G.E., and Kang, U.J. 2006. Behavioral models of Parkinson's disease in rodents: a new look at an old problem. *Mov Disord* 21:1595-1606.

8 Acknowledgements

Diese Arbeit wurde durch das Bundesministerium für Bildung und Forschung (BMBF) im Rahmen des FH3 Programms (FKZ: 1726X06) der Fachhochschule Gelsenkirchen gefördert. Die Arbeit erfolgte in einer Forschungs Kooperation zwischen der Fachhochschule Gelsenkirchen (AG Prof. Dr. Frieder Schwenk), der Universität zu Köln (AG Prof. Dr. Jens Brüning) und der TaconicArtemis GmbH in Köln.

Mein Dank geht an Prof. Dr. Jens Brüning für seine Unterstützung und Diskussionsbereitschaft bei dieser Arbeit. Prof. Dr. Frieder Schwenk und Dr. Jost Seibler danke ich für die Möglichkeit an diesem interessanten Thema zu arbeiten und ihrer ständigen Diskussionsbereitschaft.

Ich möchte Prof. Peter Kloppenburg, Prof. Matthias Hammerschmidt und Dr. Ursula Lichtenberg dafür danken, dass sie sich dazu bereit erklärt haben, mein Prüfungskomitee zu bilden.

Mein besonderer Dank gilt meinen Kollegen Sonja Ortmann, Simone Janzen und Fabian Schütte. Danke für die einmalige und unterhaltsame Laborzeit, Diskussionen und Freundschaft. Allen weiteren Mitarbeitern danke ich, die zum Gelingen dieser Arbeit beigetragen haben und für die vielen schönen Momente und dem äußerst angenehmen Arbeitsklima. Außerdem danke ich Friedemann Pohlig, der mir mit sehr viel Geduld und Ruhe das „Tierhandling“ beigebracht hat. Danke an Jost Seibler, Frieder Schwenk, Bengt Belgardt und Sonja Ortmann, Simone Janzen und Fabian Schütte für die exzellente Korrekturarbeit.

Bei der AG Brüning möchte ich mich insbesondere bei Dr. Bengt Belgardt für seine Betreuung, unermüdlige Geduld und motivierenden Worte, sowie für seine Unterstützung bei den Tierexperimenten bedanken. Brigitte Hampel danke ich für die tollen Färbungen.

Unendlich dankbar bin ich meinen Eltern Horst und Roswitha Reiss, sowie meinem Bruder Thilo, für ihre Liebe, Vertrauen und ihrer bedingungslosen Unterstützung.

Danke auch Chrissy Möller, Michi Kallfass und Nina Taube für die langjährige und tiefe Freundschaft.

9 Erklärung

Ich versichere, daß ich die von mir vorgelegte Dissertation selbständig angefertigt, die benutzten Quellen und Hilfsmittel vollständig angegeben und die Stellen der Arbeit einschließlich Tabellen, Karten und Abbildungen, die anderen Werken im Wortlaut oder dem Sinn nach entnommen sind, in jedem Einzelfall als Entlehnung kenntlich gemacht habe; dass diese Dissertation noch keiner anderen Fakultät oder Universität zur Prüfung vorgelegen hat; dass sie – abgesehen von unten angegebenen Teilpublikationen – noch nicht veröffentlicht worden ist sowie, dass ich eine solche Veröffentlichung vor Abschluß des Promotionsverfahren nicht vornehmen werde. Die Bestimmungen dieser Promotionsordnung sind mir bekannt. Die von mir vorgelegte Dissertation ist von Prof. Dr. Jens C. Brüning betreut worden.

Köln, Oktober 2010

Martina Reiss

10 Curriculum vitae